ELECTROPOLYMERIZATION OF COPPER, COBALT, AND ZINC(II)-TETRAAMINOPHTHALOCYANINE: POTENTIAL RATE MODIFIERS OF LUMINOL CHEMILUMINESCENCE IN THE PRESENCE OF CARBON DIOXIDE

By

KENNETH LIONEL BROWN

Bachelor of Science
Oral Roberts University
Tulsa, Oklahoma
1993

Submitted to the Faculty of the
Graduate College of the
Oklahoma State University
in partial fulfillment of
the requirements for
the Degree of
DOCTOR OF PHILOSOPHY
July, 2000

ELECTROPOLYMERIZATION OF COPPER, COBALT, AND ZINC(II)-TETRAAMINOPHTHALOCYANINE: POTENTIAL RATE MODIFIERS OF LUMINOL CHEMILUMINESCENCE IN THE PRESENCE OF CARBON DIOXIDE

Thesis Approved:

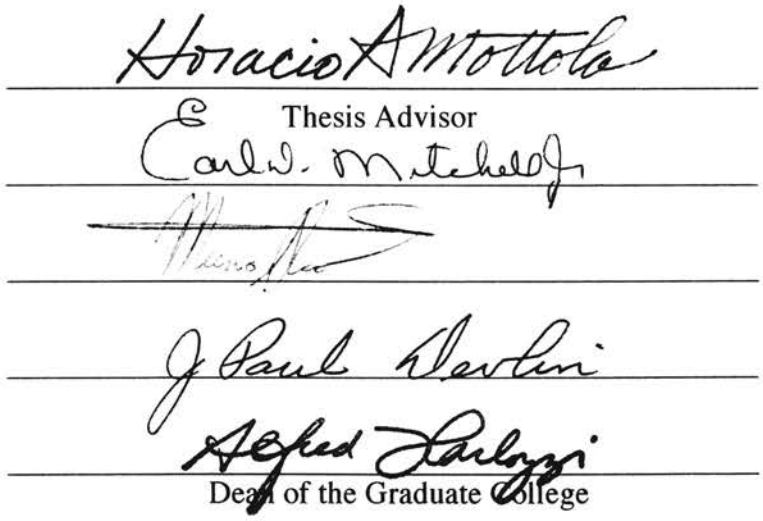

Thesis Advisor

Dean of the Graduate College

ACKNOWLEDGMENTS

I wish to express my sincere and deep appreciation to my advisor, Dr. Horacio A. Mottola, for his on-going guidance, intelligent suggestions, and friendship. The special trips from Florida to Stillwater to attend my seminar, and final examination are greatly appreciated. My appreciation is also extended to my committee members: Dr. J. Paul Devlin, Dr. Mario E. Rivera, and Dr. Earl Mitchell for their support and suggestions for my research and study. In addition, I thank Dr. Rivera and his research group for the use of their equipment which saved nearly three months of research work. Also, a special thanks is given to Dr. E. J. Eisenbraun for the use of his lab and equipment for the synthesis of the compounds used in this research.

My sincere gratitude is extended my colleagues Carlos Rodriguez, and Marc Wirtz for their comments and friendship. A warm thanks is also given to Pastors Harminto Ongko and Grace Ongko, and IFGF for their love, encouragement, and prayers of support. Thanks also goes to Yayee, Da, and Tongchit Tantikul for their trusting love and friendship.

I would like to give my special thanks to my parents, Elax and Helen Brown, and my grandmother, Mary A. Warfield, for their never-ending love and support. A sincere thanks is also given to all family members for their support and encouragement. Most of all, I would like to thank God for giving me the strength to complete these last four years.

Finally, I would like to thank the Department of Chemistry, the Thurgood Marshall Scholarship committee, and the NASA Fellowship committee for financial support during my study at OSU.

TABLE OF CONTENTS

LIST OF TABLES

LIST OF FIGURES

GLOSSARY OF ABBREVIATIONS

Pc: Phthalocyanine ligand moiety

MPc: Metal phthalocyanine

H_2Pc: Metal-free phthalocyanine

MTAPc: Metal tetraminophthalocyanine

CuTAPc: Copper(II)tetraminophthalocyanine

CoTAPc: Cobalt(II)tetraminophthalocyanine

ZnTAPc: Zinc(II)tetraminophthalocyanine

CMEs: Chemically Modified Electrodes

MLCT: Metal to Ligand Charge Transfer

ITO: Indium Tin Oxide

CHAPTER I

INTRODUCTION

Significance of Electrode Modification. The role of chemically modified electrodes (CMEs) to catalyze or modify the rate of chemical reactions has been extensively surveyed for a number of applications [1-4] . The methodology for modifying an electrode surface has a significant impact on its short-term and long-term use in analytical applications. Many of these applications involve the detection and determination of different types of analytes, including transition metal ions, peroxides, anions, and organic species [5-8]. Understanding the properties of materials on electrode surfaces such as mechanisms of charge transfer, electrode stability in different chemical environments such as low and high pH, lays a foundation for developing methods which may be based on certain types of reactions (e.g., luminol chemililuminescence).

Immobilized species on electrode sufaces are normally in the form of a single monolayer or multilayered thin films [1]. The electrode modification procedure is tailored to control charge transfer rates for specific applications. Some of the methods for modifying electrodes include chemisorption, covalent binding, vacuum deposition, and electropolymerization. [9-15]. Applications of CMEs include (1) electrocatalysis, (2) improving electrode stability, (3) development of chemical sensors, (4) directed and controlled mediated charge transfer, and (5) electrochromism for color displays which are potential dependent [16-20]. Such applications are usually based upon the charge-transfer properties of the compound immobilized on the electrode. Presently, many applications involve the use of polymeric multilayered thin films. The polymeric films may be classified as loaded ionomers, redox polymers, or electronically conducting polymers.

Relevance of Metal Phthalocyanines and Derivatives in Electrode Modification. In the area of chemical sensors for the detection and quantitation of the various aforementioned species, limits of detection can be lowered and the linear dynamic range for calibration curves are extended [21]. Sensors based on luminol chemiluminescence reactions are pH dependent and involve complex reaction mechanisms. Transistion metal ions, or organometallic complexes such as metal phthalocyanines (MPc) have been used as catalysts or rate modifiers for these types of reactions [22]. For example, electrodes modified with polymeric thin films of iron(II)-tetraaminophthalocyanine have been used in the determination of hydrogen peroxide and peracetic acid in continuous-flow systems [23]. Without electrode modification, these compounds cannot be detected and determined within the potential range or window utilized. Because interactions and subsequent reactions can occur with the central metal ion or the phthalocyanine (Pc) ligand of metal phthalocyanines, many applications using these compounds can be developed. Electrodes chemically modified with electropolymerized nickel(II) and copper(II)-tetraaminophthalocyanine polymeric thin films have been used as potentiometric pH sensors. Such sensors are based on the protonation-deprotonation of the phthalocyanine ligand [24]. On the other hand, interactions of the central metal ion with species such as carbon dioxide, oxygen, hydrazine allows a pathway for reduction and oxidation reactions [25-26]. For example, cobalt phthalocyanine and cobalt napthalocyanine on glassy carbon electrodes have been used in the reduction of oxygen, and the oxidation of hydrazine [26]. However, due to the napth- substituents on the phthalocyanine ligand, the mechanisms for reduction and oxidation of these compounds are different than when cobalt phthalocyanine is used. This shows the effect of having substituents on the phthalocyanine ligand; different mechanistic pathways are feasible providing greater utility for analytical applications. Tetramethylated-pyridino phthalocyanine immobilized on highly oriented pyrolytic graphite electrodes has been used for the dection of sulfide ions with detection limits as

low as 10^{-6} M [5]. Cobalt phthalocyanine has been used in several cases for the electrocatalytic reduction of carbon dioxide. Yoshida and co-workers incorporated cobalt phthalocyanine in a polyvinylpyridine membrane for the reduction of carbon dioxide [27]. Thin films of copper phthalocyanine have also been used in sensor applications for the detection of NO_2 [28] . However, many of these cases involve the lowering of overpotentials for the reactions to occur .

OBJECTIVES OF RESEARCH

Many types of electrode modifications procedures have been developed to generate thin films with a wide range of applications. These applications are very dependent upon understanding the properties of these films. Although different types of thin films have been extensively studied and used in continuous-flow systems for the detection of various species, more work is specifically needed to be performed for helping in the understanding of the role of electropolymerized-mulitlayered thin films in specific sensor applications. In this research, some pertinent properties of polymeric thin films of metal(II)tetraaminophthalocyanine [M(II)TAPc] are related to the development of a potential sensor for carbon dioxide. The method is based on luminol chemiluminescence in the absence of any added oxidant [29]. Luminol chemiluminescence has been widely used in the determination of various transistion metal ions, peroxides, and gaseous species [30-32]. A large portion of this research has been devoted to the understanding of the redox properties of several monomeric MTAPc compounds and their polymeric thin films. These properties have also been investigated under high pH conditions because the luminol chemiluminescence is dependent upon the pH.

This research has been essentially divided into three parts. The first part was devoted to the synthesis of copper(II), cobalt(II) and zinc(II)-tetraaminophthalocyanine,

since several of the experimental procedures deviated from what is reported in the literature. In addition, observations of changes during the reactions are reported since the literature makes no mention of these changes in the reaction mixture. The second part addressed the electropolymerization of these compounds by cyclic voltammetry, and the electrochemical characterization of these compounds also by cyclic voltammetry and other electrochemical methods. The third part of this research addresses the interaction of the polymeric multlilayered thin films with carbon dioxide. Afterwards, the use of the films as potential rate modifiers in luminol chemiluminescence in the presence of carbon dioxide is presented.

Chapter 2 presents a literature review of CMEs and their analytical applications. The classification of modified electrodes in this research is based upon the type of material on the electrode and the type of modification technique. Modification by electropolymerization is the main focus in this part of chapter 2, since it covers the main work reported here as original research. Several electropolymerization reactions are presented to show the versatility of this type of electrode modification. The ideal properties of modified electrodes are presented in terms as electrochemical properties. The electrochemical properties and electrode stability of CMEs are important because both can affect the catalysis of electrode reactions, and their potential use in chemical sensors.

Chapter 3 gives a brief historical background of metal phthalocyanines and derivatives thereof. The background material presents two reactions: (1) *O*-cyanobenzamide and the (2) phthalic acid reaction. The reactions are presented in terms of autocondensation reactions and cross-condensation reactions. An energy level diagram is shown to describe possible electronic transitions corresponding to various UV-vis absorption bands. These transitions described herein are then related to spectroelectrochemical experiments in chapter 5. A description is made about the bonding in the MPc compounds, and is related to some of the properties of the

compounds. The second part of chapter 3 describes in detail the synthesis of the MTAPc complexes. Spectroscopic characterizations of the compounds made by IR and UV-vis are presented.

Chapter 4 extensively deals with the electropolymerization of the compounds on glassy carbon surfaces by cyclic voltammetry. References are made to the other electrodes surfaces which can be used in electropolymerization. Chapter 4 also includes an examination of the possible mechanisms for electropolymerization of the MTPAc complexes.

Chapter 5 deals with the characterization of the polymeric thin films in aqueous, and nonaqueous systems. Characterization of these films is performed by cyclic voltammetry, square wave voltammetry, chronocoulometry, and spectroelectrochemistry. Cyclic voltammetric, and chronocoulometric measurements are used in conjunction together to evaluate apparent diffusion or charge transfer coefficients. Spectroelectrochemical measurements, facilitated by electropolymerization onto an optically transparent indium tin oxide electrode (ITO), allow the observation of spectral changes as the potential of the ITO is changed. The spectroelectrochemical information is related to the electrochemical characterization of the film on glassy carbon electrodes. One of the unique aspects of characterization by cyclic voltammetry is the capability to determine the amount of material on the electrode surface. The electrode coverage is then used to calculate the apparent number of monolayers. This is related to the idea of having a multilayered-polymeric thin film. This chapter also addresses the use of these films in high pH solutions. The effect of high pH on the films is studied by cyclic votammetry, and square wave voltammetry. Addressing this effect gives information about using these films in applications based on luminol chemilumescence since the reaction conditions require a high pH.

Chapter 6 addressees the electrochemical interaction of carbon dioxide with the CuTAPc, CoTAPc, and ZnTAPc thin films. Metal complexes are known to interact with

carbon dioxide. From cyclic voltammetric, and square wave voltammetric measurements, a possible mechanism for the interaction of carbon dioxide and its subsequent reduction is presented. The last part of chapter 6 describes the flow cell, and some of the instrumentation associated with the luminol chemiluminescence. The flow cell contains the polymeric film on an ITO surface . The ITO surface is placed on the disk, which contains a small magnetic stirring bar, which is rotated by a magnetic stirrer. Immobilization by electropolymerization on the ITO surface is compared to an immobilization procedure in which the monomeric form of metal phthalocyanines is placed on controlled-pore glass. This chapter concludes by describing the luminol chemiluminescence profiles for polymeric MTAPc/luminol/carbon dioxide systems.

CHAPTER II

CHEMICALLY MODIFIED ELECTRODES AND ITS ANALYTICAL APPLICATIONS: A LITERATURE REVEIW

INTRODUCTION

Chemically modified electrodes (CMEs) over the past several years have sparked considerable interest in analytical chemistry with respect to catalysis, electrochemical and chromo-electrochemical detection of organic compounds, and chemical sensor development. Since the pioneering work by Lane and Hubbard, over 20 years ago, involving chemisorbed metals on platinum electrode surfaces, numerous methods have been developed to immobilize species on electrode surfaces [9]. The modification techniques include covalent attachment, spin coating, electropolymerization, and others. In this chapter, the literature review is not comprehensive, but rather focuses on electropolymerizations related to this work. The presence of immobilized species changes the electrochemical behavior of the electrode. These new electrodes possess properties which may be exploited to lay a foundation for new and interesting applications and devices (e.g., electrochromic displays, and sensors) [33].

Immobilized species are considered to be either monolayered or multilayered thin films. Metal oxide surfaces have been functionalized by covalent binding with alkylamines, acid chlorides and silane compounds [34-35]. Covalent binding modification techniques are usually more complicated than other modification techniques, and produce monolayer type coverages. Monolayer coverages may range from 10^{-10}-10^{-11} mol/cm^2 [1]. The electrochemical response of such electrodes is less than electrodes with multilayer coverages.

Multilayered thin films in the form of polymeric layers are classified as ionomers, redox polymers, or electronically conducting polymers. The amount of material attached to the electrode surface varies with the modification procedure and may range from 10^{-9} - 10^{-6} mol/cm^2 [1]. Once the electrode surface has been subjected to one of the aforementioned modification procedures, one needs to ensure that the electrode surface has in fact been modified. Electrochemical methods, such as cyclic voltammetry, are ideal for ensuring that the electrode surface has indeed been modified, and are also useful for investigating the charge transfer within the polymeric film. An ideal cyclic voltammogram for a modified electrode is shown in Figure 2.1 [36]. Both the cathodic and anodic peaks should be symmetrical with no peak separation. Such voltammograms indicate that charge transfer within the film is in Nerstian equilibrium with the applied potential. Oftentimes, information concerning the amount of material on the electrode surface, and spectroscopic studies give useful information which may be combined with information about redox processes to obtain a more complete picture of the electrode surface in terms of charge transfer properties. These properties have a direct impact upon how they can be used to guide the development of chemical sensors.

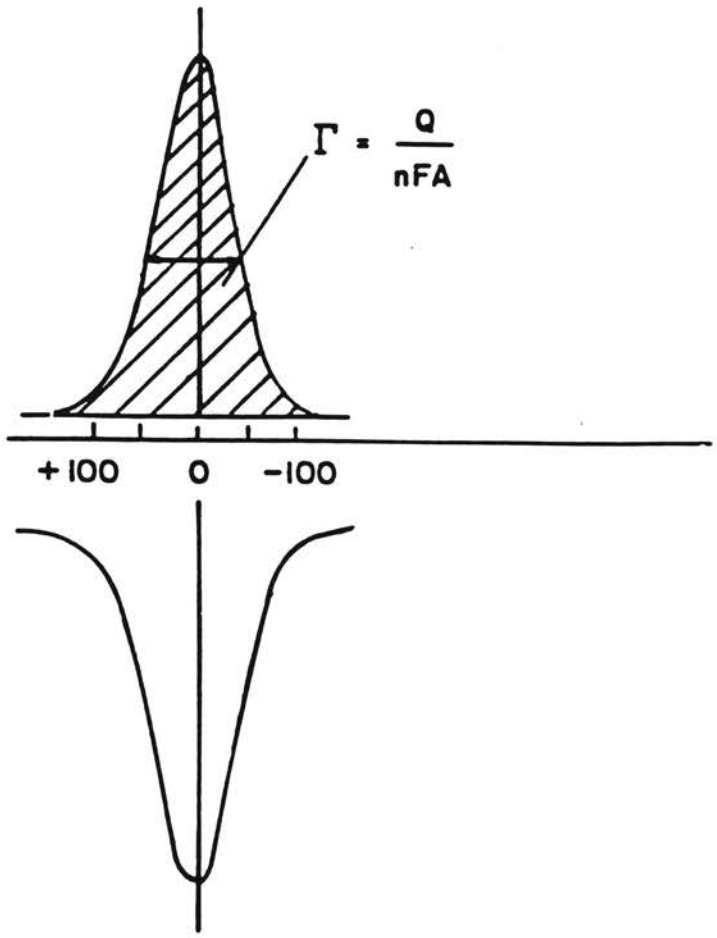

Figure 2.1. Ideal cyclic voltammogram of species immobilized on an electrode surface. The cathodic and anodic peaks are mirror images of each other.

CLASSIFICATION OF POLYMER MODIFIED ELECTRODES

Loaded Ionomers. These polymer coatings are polycation or polyanion ion-exchange polymers which contain electroactive species. The ion-exchange polymer is attached on an electrode via solvent evaporation or spin coating which is then dipped into a solution containing electroactive species. The electroactive species are essentially bound to the ion-exchange polymer through electrostatic forces. One of the most popular and extensively used ion-exchange polymers is Nafion, a perflourosulfonate ion-exchanger [37]. Other ion-exchange polymers which have been investigated are protonated forms of poly(vinylpyridine), and poly-*n*-methylpyrrole with immobilized poly(4-styrenesulfonate) ions as a cation-exchanger [37].

Anson and Oyama utilized protonated forms of poly(4-vinylpyridine) as cation exchange polymers to incorporate $Fe(CN)_6^{3-/4-}$, and hexachloroiridate ($IrCl_6^{2-/3-}$) [38]. Maksymuk, and Doblhofer used poly-N-methylpyrrole as an anion exchanger or poly-N-methylpyrrole with immobilized poly(4-styrenesulfonate) ions as a cation-exchanger to incorparte $Fe(CN)_6^{3-/4-}$, $Ru(NH_3)_6^{3+/4+}$, Eu^{3+}/Eu^{2+}, $Co(en)_3^{3+/2+}$ [en= ethylene diamine], and $Fe(C_2O_4)_3^{3-/4-}$ [39]. The electropolymerization of pyrrole, aniline, or N-methlypyrrole in the presence of polyanions such as poly(vinylsulfate), and poly(stryrenesulfonate) forms an ion-exchanger which is electroactive over a wide potential range [37]. Other workers have several incorporated electroactive inorganic cations such as Co(2,2'-bipyridine)$_3^{2+}$, and Ru(2,2'-bipyridine)$_3^{2+}$ into polystyrene sulfonate [40]. The widely used Nafion has been ultilized by Yagi and co-workers to investigate the charge transfer properties of tris(2,2'-bipyridine)Ru^{2+} [41]. The charge transport parameters are based upon two processes, namely, physical displacement of the electroactive center, and electron hopping or electron self exhange between electroactive centers [37]. Although this method is useful in studying charge transport properties of redox active species within membranes, it suffers from a major disadvantage. The

electroactive species are not irreversible bound to the ion-exchange matrix, and consequently, they can leach out into the solution.

Redox Polymers. These are polymer films with redox-active centers covalently bound to a redox inactive polymer organic moeity. These polymers can be synthesized in large quantities, and then immobilzed onto electrode surfaces by spin coating, or dip coating. One major obstacle associated with using preformed redox polymers is their low solubility in solvents. The solvent must evaporate when using spin coating or dip coating methods in order to leave the preformed polymer on the electrode surface. The mechanism of charge transfer has been exclusively identified as electron hopping or electron self exchange between neighboring redox centers. Such polymers only show conductivity over a limited potential range. Shigehara, and co-workers incorporated $Fe(CN)_5^{3-}$ into poly(4-vinylpyridine) via cooridination, and attached the polymer to graphite electrodes by solvent evaporation [42].

One of the most successful and appealing ways to form redox polymers on electrode surfaces is through electropolymerization. This is simply a method to form polymers by using electrochemical techniques. Electropolymerization is an attractive approach because it allows film thickness to be consistently reproduced, and monitored. In addition, the electrode coverage is normally complete after many scans, and requires multi-layers because polymer may not grow in regular layers. This gives rise to what is commonly called a multilayered polymeric thin film. As mentioned previously, these electrodes show a greater electrochemical response than monolayer coverages. Multilayered films have more electroactive sites in the form of layers. As many as 1000 layers can be formed on a single electrode surface [1, 43]. Iron and ruthenium complexes of 2,2'-bipyridine have been electropolymerized on platinum, glassy carbon, and metal oxide electrodes by Ellis and Meyer to selectively direct charge transfer to redox species in solution [44]. The same research group performed oxidative electropolymerization of

ruthenium complexes of 4-aminopyridine, 3-aminopyridine, and 5-amino-1,10 phenanthroline [45]. Metalloporphyrins have been used in electropolymerization by several research groups. Derivatives of nickel(II) and cobalt(II)-tetraphenylporphyrins with amino-, hydroxy-, and pyrrole-, substituents have been electropolymerized by Murray and co-workers [46]. Such compounds are used because of their rich chemistry in terms of electron transfer properties. These type of compounds can be used as possible catalyst since the central metal ion is capable of axially coordinating with extra ligands. The mechanism(s) for generating polymeric multilayered films are based upon similar principles of either forming radical cations or anions which couple together. This process is looked into further under the discussion of "electropolymerization reactions".

Electronically Conducting Polymers. Conducting polymers are marked by extended π-electron systems which are delocalized. These can be formed in a similar manner as redox polymers. One of the popular methods is again electropolymerization. One of the first compounds to be used in forming these polymers was pyrrole by Diaz and Kanazawa [47]. Later, other research groups explored, aniline, furan, and other heterocyclic aromatic compounds for electropolymerization. The polymerization of these compounds proceeds by a mechanism similar to that of derivatives of metalloporphyrins. For example, pyrrole forms polymeric films via radical cation intermediates. These films usually show good adhesion to the electrode surfaces.

The mechanism of charge transport is attributed to interchain electron hopping. The chain alignment plays a significant role in the kinetics of charge transfer, and in the conductivity of these films. In all cases, electropolyermization is governed by Faraday's Law. Thus, it is easy to monitor film thickness. Film thickness can be an important factor in designing sensors because analytes may penetrante through the film to the electrode surface, partially through the film, or to the film solution interface in order to undergo a charge transfer electrocatalytic reaction [39].

ELECTROPOLYMERIZATION REACTIONS

Introduction. The electropolymerization described in the research presented here was performed using cyclic voltammetry, and this is discussed in detail later on in this dissertation. Worth mentioning in this section is the fact that scanning conditions such as scan rate, number of cycles performed, and the potential window used all affect the overall composition of the polymeric thin film. Electropolymerization reactions are first preceeded by a small amount of adsorption onto the electrode surface. In order for a monomer to be electropolymerized on an electrode surface, it must possess functional groups which can be oxidized or reduced. The most common functional groups noted to initiate eletropolymerizations reactions are amino-, hydroxy-, and vinyl groups. In these instances, there are lone pairs of electrons or a π-electron system available. These functional groups give rise to radical cations or anions depending upon whether oxidation or reduction is the initiating step. These radical species are coupled to the electrode surface, and further undergo redox processes to generate the thin film. The conductivity of the complex on the electrode surface serves to mediate charge transfer at the film-solution interface so that more monomers can be incoporated onto the growing film. It has been statistically verified that increasing the number of aforementioned functional groups on a compound favors the formation of radical species. In addition, multiple functional groups on the monomer, for initiating polymerization reactions, promote the correct orientation for the incorporation of monomer speices. This is significant when one considers how the electrode surface can be fully covered with up to 1000 monolayers.

Oxidative Electropolymerization. Oxidative electropolymerization can be performed when compounds have substituents such as amino-, and hyroxy- groups. It has been well established that with such functional groups electropolymerization proceeds by oxidation involving the lone pair of electrons on a heteroatom as shown in

Figure 2.2 [48]. The electrooxidation of aniline **1**, via the lone pair of electrons of the nitrogen, gives the radical cation **2**. The radical cation **2**, loses a proton to give **3**, and then undergoes radical coupling to form **4**. The dimers are oxidized to form N=N double bonds to give **5**. The benefit of having more than one amine substiuent can be seen from the final product of **5.** With multiple amine sites, the electropolymerization can continue. For compounds such as M(II)TAPc multiple amine sites allow polymerization to continue, and film thickness to increase. As it will be shown later, the mechanism for M(II)TAPc is an oxidative process that proceeds via the amine substituents. The other possible mechanism shown in Figure 2.3 [45] also proceeds via the electroxidation of the amine group to give **2.** The radical cation **2** has a resonance structure **6** and which undergoes C-N coupling to give **7**. Oxidation of **7** gives the product **8** which continues the chain growth process to give **9.** Pathway I (Figure 2.2) presents a self-terminating reaction, while pathway II (Figure 2.3) presents a self-propagting reaction. In Figure 2.2, the product, **5**, does not have amine substituents necessary for continued growth of chain. As a result, the reaction terminates. However, in Figure 2.3, the product shown, **9**, has an amine substituent which can undergo further oxidation and allow the electropolymerization process to continue.

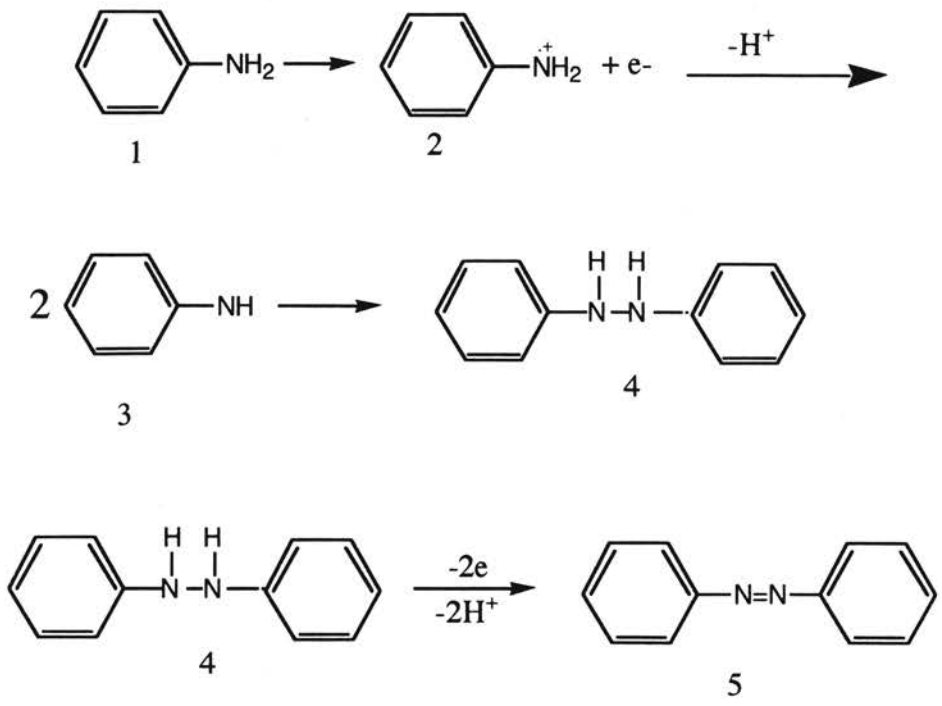

Figure 2.2. Pathway I. Possible mechanism for the electrooxidation of aniline. The process begins by generating a radical cation involving the amine substituent.

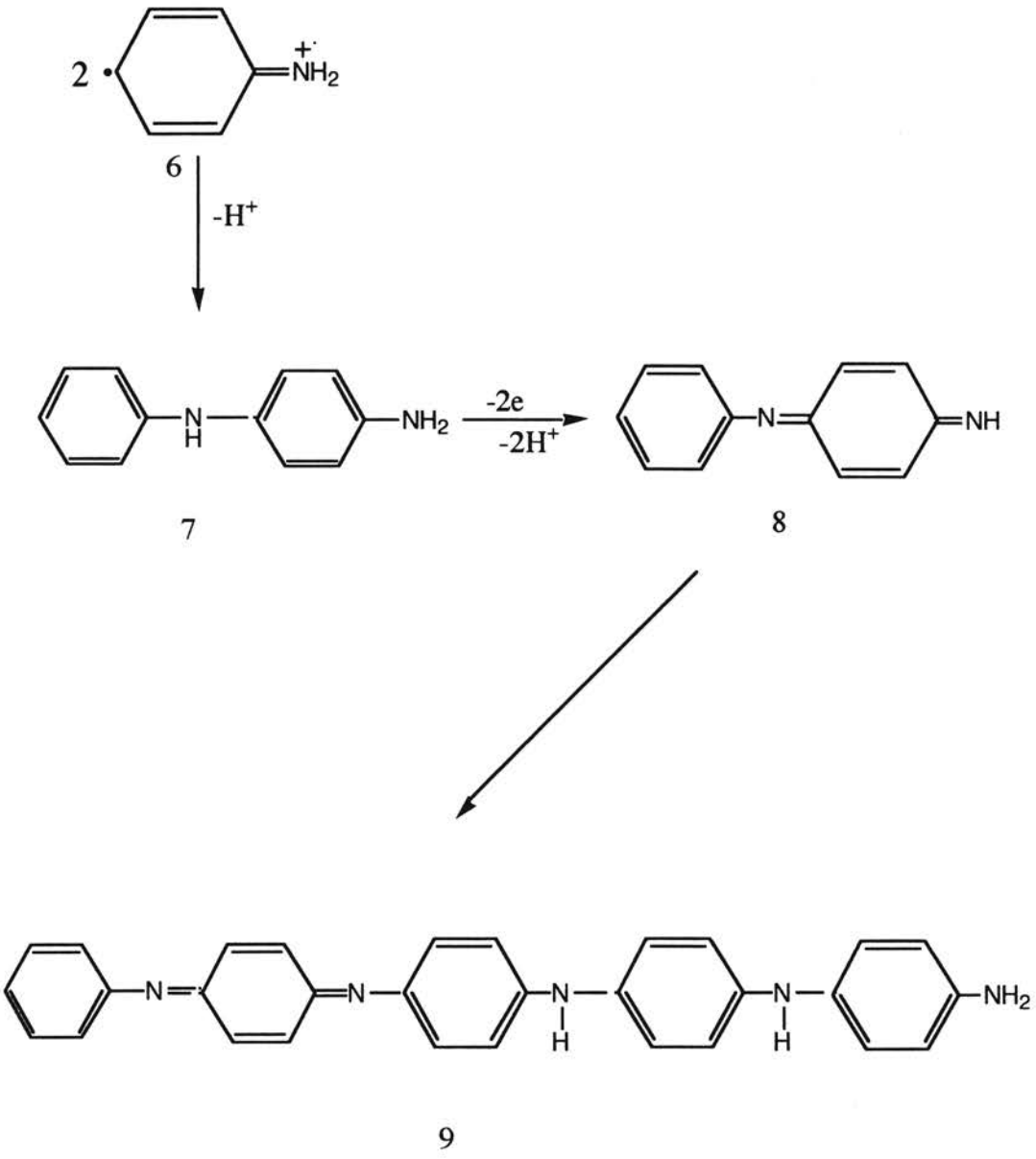

Figure 2.3. Pathway II. Possible mechanism for the electrooxidation of aniline. The process begins by generating a radical cation involving the amine substituent.

PROPERTIES AND APPLICATIONS OF CHEMICALLY MODIFIED ELECTRODES BY ELECTROPOLYMERIZATION

Electropolymerization has many advantages over electrodes modified by spin coating, dip coating, or covalent attachment. In electropolymerization, the electrode surface is more effectively covered, and it is easier to control the thickness of the film. This method is also useful when covering irregular shaped electrodes. By proper choice of electropolymerization conditions such as the potential window, scan rate, number of cycles or scans, solvent choice and concentration of monomer solution, polymeric films can be obtained with different characteristics tailored to meet specific applications. Since Faraday's Law governs electropolymerization, the total amount of charge passed during the polymerization process is an indication of the film thickness. There are several methods to electrochemically immobilize organometallic complexes onto electrode surfaces. One approach is to use cyclic voltammetry, a potential cycling method. The other methods include pulsed potential, and fixed potential approaches. Several research groups have shown that the potential cycling method is better than the fixed potential method in providing information about the catalytic properties for the oxidation or reduction of various compounds [49]. Cycling methods also provide a more covenient approach to elucidate mechanisms, and redox processes associated with forming a polymeric thin film. For these reasons, cyclic voltammetry has been used in this research for the electropolymerization of M(II)TAPc complexes.

Catalysis of Electrode Reactions. Multilayered metal-complex films provide multiple sites for ligand interaction. That is, ligands can coordinate with a metal ion reactive site, and affect the reduction potential of the analyte electroactive species such that the overpotential for an electrochemical reaction is considerably lowered. In many cases, the detection limits for an electroactive species can be lowered or the linear

dynamic calibration range can be extended. For instance, cobalt phthalocyanine has been shown to lower the energy requirements for the electrooxidation of hydrazine, keto-acids, and thiols by several hundred millivolts, in addition to lowering the detection limit of such species up to 1000 times [21]. A biosensor for glucose based on electropolymerized films of CuTAPc, and phenol on glassy carbon with a detection limit of 8 μM has been reported [50]. Nickel(II)tetraminophthalocyanine electropolymerized onto glassy carbon electrodes lowers the oxidation potential of oxalic acid by 400 mV [21]. It is advantageous to have an immobilized compound which shows electroactivity over a wide range of potentials. In addition, the catalytic properties of the polymeric film should mimic the catalytic properties of the monomer in solution. The electrocatalytic activity of many organometallic complexes towards neutral and charged species may be dependent upon the redox activity of the central metal ion and the organic moeity. When the immobilized species behaves as a mediator for charge transfer of an electrocatalytic process, it is desirable to have a fast charge transfer mechanism. The morphology of the film affects how the substrate penetrates the film and undergoes a redox process.

Electrode stability is also of concern when working with CMEs. In the development of chemical sensors, polymeric films are often used to prevent interferences from reaching the electrode surface or to entrap mediators which facilitate charge transfer. In many instances, electrode fouling may take place when a compound comes in direct contact with the electrode surface. When a nonelectroactive species is adsorbed on the electrode surface, passivation occurs. This may cause a decrease in the response time of a sensor. Malitesa and co-workers electropolymerized *o*-phenylenediamine to immobilize glucose oxidase for a biosensor which blocked the interferent ascorbate from reaching the electrode surface [51]. Other compounds such as nitrophenol and, bromo-phenol were also electropolymerized to immobilze glucose oxidase for sensing glucose via hydrogen peroxide [52].

The incorporation of thin films for detection in continuous-flow systems has been performed by different research groups [6, 53]. One of the main concerns when using thin films in continuous-flow systems is the ability of the thin film to withstand sheer and deterioration by the flowing solution. A continuous-flow system for the detection of carbohydrates based on its electrooxidation via cobalt phthalocyanine obtained detection limits as low as 150 pmol [53]. Some detection systems such as one for carbon dioxide based on luminol chemiluminescence is very dependent upon pH. In the research reported here, polymeric films of CuTAPc, CoTAPc, and ZnTAPc are used as rate modifiers in the enhancement of luminol chemiluminescence by carbon dioxide.

CHAPTER III

SYNTHESIS OF METAL PHTHALOCYANINES AND DERIVATIVES

HISTORICAL BACKGROUND

Introduction. Phthalocyanines were discovered by accident in 1907, by heating *o*-cyanobenzamide and dissolving the product in alcohol [54]. Several years later, at the University of Fribourg, copper phthalocyanine was produced from nitriles of benzene. In both cases the solid material was dark in color. Phthalocyanine is derived from the Greek, "naphtha", meaning rock oil, and "cyanine", meaning dark blue [54]. Since the initial synthesis of the phthalocyanine macromolecule, many synthetic pathways for obtaining this compound have been investigated. Currently, more than 40 different metal phthalocyanine compounds have been prepared. Many of these same compounds have been derivatized by placing 4-8 substituents on the phthalocyanine macromolecule. Derivatization with certain substituents such as amine, and sulfonate groups increases the solubility of phthalocyanine compounds and their uses in analytical, and indutstrial applications. Properties of the macromolecule which are changed include redox behavior, and the capability to generate thin films [55].

The synthetic methods are generally divided into two categories: fusion or melt method and solvent method. The fusion method consists of heating the reactants near a temperature of 200 ° C. The heating is continued until the dark blue color formation is complete. In the solvent method, the reactants are normally heated in high boiling inert solvents such as nitrobenzene, *o*-dichlorobenzene, trichlorobenzene, or ethlylene glycol. Product yields, using the solvent method, are nearly 20% higher than with the melt method. Some recent methods, however, employ temperatures near 25°C [55]. The methods of preparation can be further divided into autocondensation or cross-

condensation methods. Autocondesation methods have been used with starting materials such as *o*-cyanobenzamide, and phthalonitrile; cross-condensation methods have been used with starting materials such as phthalic anhydride, phthalimide, and other derviatives of phthalic acid. Cross-condensation methods between 4-nitrophthalonitrile and sterically hindered phenols with temperatures less than 135°C have been used to prepare napthalocyanines [56]. In each type of reaction, the nitrogen coordinates around the central metal ion to form the macromolecule.

<u>*o*- cyanobenzamide Reaction</u> [54]. A common reaction for the synthesis of metal free phthalocyanine (2) is shown below where an autocondensation reaction takes place upon heating o-cyanobenzamide (1) and refluxing in ethanol

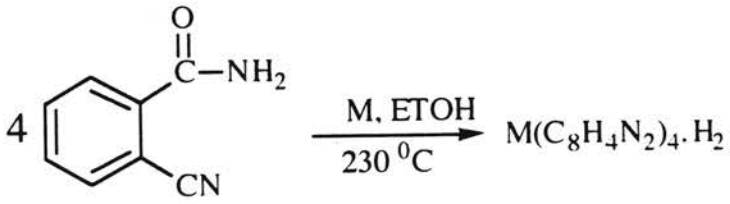

1 2

For sythesizing MPc (3) utilizing the same autocondensation reaction with temperatures greater than 230°C, a metal salt is introduced into the synthesis

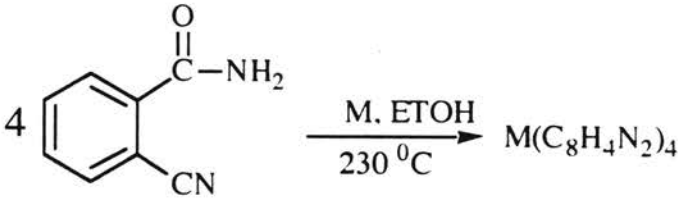

1 3

The yields for such reactions are nearly 40%. These reactions, however, do not give good product yield when tetrasubstitued derivatives of MPc are synthesized. Derivatives are prepared by using an aromatic compoud with the same substituent as the target metal

phthalocyanine or with a substiutent which can be oxidized or reduced to obtain the target metal phthalocyanine.

Phthalic acid Reaction [57]. The phthalic acid (5) reaction is essentially a cross-condensation reaction. When phthalic acid and similar compounds (phthalimide and phthalic anhydride) are used, urea is often used as an aminating reagent. In addition, catalysts such as ammonium molydbate are used. This reaction, briefly shown below, has been used in this research with a slight modification since metal tetraaminophthalocyanines were used in electropolymerizations for electrode modification.

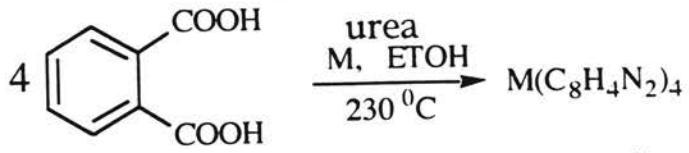

5 3

SYNTHESIS OF Cu(II), Co(II), AND Zn(II)-4, 9, 16, 23-TETRAAMINO-PHTHALOCYANINE

The synthesis of metal (II)-tetraaminophthalocyanine (MTAPc) complexes for this research was necessary because these derivatized metal phthalocyanine complexes are not commericially available. The formation of these compounds is considered to be an autocondensation or polymerization reaction in which the reactants condense and species forms a ring system around the central metal atom [65] thus generating an extended π system. The targeted derivatized metal phthalocyanine determines the type of reactant to use. For example, in the research presented here, since a tetraaminephthalocyanine compound was desired, 4-nitrophthalic acid was used as

starting material. Once the Cu(II), Co(II), and Zn(II)-tetranitro complexes (CuTNPc, CoTNPc, and ZnTNPc) were synthesized, the nitro groups were easily reduced to amine groups.

EXPERIMENTAL PROCEDURE

Reagents and Solutions. Copper(II) sulfate, zinc(II) sulfate, and cobalt(II) sufate were all obtained from Fisher Scientific (Fair Lawn, NJ) and used as the sources for the central metal in the phthalocyanine complexes. Urea obtained from Mallincrockt (St. Louis, MO) and 4-nitrophthalic acid obtained from Sigma (St. Louis, MO) were used as the starting materials agents. The nitrobenzene used to dissolve the 4-nitrophthalic acid was obtained from Eastman Kodak Company (Rochester, NY). The catalyst, ammonium molybdate, was also obtained from Fisher Scientific. Sodium hydroxide and hydrochloric acid were obtained from EM Science (Cherry Hill, NJ). The concentration of sodium hydroxide, and hydrochloric acid were both 1.0 M These solutions were used in the purification steps of the final products. The water used to make all solution preparations was purified by reverse osmosis and further distilled in an all-borosilicate-glass still with a quartz immersion heater. Disks utilizing KBr, were prepared for the characterization of the compounds by IR spectroscopy. Concentrated sulfuric acid (18 M) was obtained from Mallinckrodt, Inc. (Paris, KY) and was used to dissolve all phthalocyanine complexes for spectrophotometric measurements. The concentration of the CuTAPc, CoTAPc, and ZnTAPc for UV-Vis characterization were 1.36×10^{-5} M, 1.32×10^{-5} M, and 1.29×10^{-6} M respectively.

Instrumentation. A Hewlett-Packard Model 8453M single-beam diode-array spectrophotometer was used to record all electronic spectra. The 1.0 cm quartz spectrophotometric cells were obtained from NSG Precision Cells, Inc. (Farmingdale, NY.).

RESULTS AND DISCUSSIONS

Synthesis of CuTNPc. The published procedure [58] was followed with some slight modifications. The modified procedure was based on 0.10 mole of 4-nitrophthalic acid for both the copper and cobalt phthalocyanine complexes, and 0.20 mole of 4-nitrophthalic acid for the zinc phthalocyanine complex. All solid reagents, copper(II) sulfate (6.80 g), ammonium chloride (2.50 g), ammonium molybdate (0.280 g), urea (34.0 g), and 4-nitrophthalic acid (21.0 g) were thouroughly mixed with a mortar and pestle and placed in a three-necked round bottom flask containing 14.3 mL of nitrobenzene. Rather than using a stirring bar, a motor with a rotating shaft which contained a solid glass rod of approximately 12 inches in length equipped with a propeller which could be inserted into the middle neck of the flask was used to mix the contents in the round bottom flask. The rotation speed of the shaft, 100 RPM, was controlled using a variable rheostat. The temperature was monitored for 4.5 hours at 180 °C - 190 °C by placing a thermocouple attached to a small hand-held digital monitor into the right neck of the flask. A condenser was inserted into the left neck of the flask. After 30 minutes of mixing, the material in the flask turned from an off-white color to a green color. Within the next 30 minutes, the material turned blue, and finally dark blue. It was important to note the color change because it was during this time that the material became very viscous. The reaction product was filtered and washed with 95% (v/v) ethanol. This first filtration required 3+ hours to give a filter cake 1 (cake 1). Cake 1 was then added to 286 mL of aqueous 1.0 M HCl and heated for 15 minutes to boiling. This heating continued for 5 minutes. The suspension was filtered while warm. This required only 0.5 hours to give filter cake 2 (cake 2). Cake 2 was then suspended in 286 mL of 1.0 M NaOH (sautrated with NaCl), and was heated at 90° C to drive off the NH_3 (tested with moist Alkacid Paper) which required 3.5 hours. The suspension was filtered to give filter cake 3 (cake 3) and this was suspended in 25 mL of 1.0 M HCl . This new suspension was washed alternately with 1.0 M HCl, and 1.0 M NaOH three times.

Between each wash, the material was centrifuged with a Marathon 10K centrifuge (Fisher Scientific) for 3 minutes at 5000 RPM. Before drying, the material was washed 6 times with distilled water to remove all chloride (tested with 0.10 M $AgNO_3$). The compound was inserted into a sealed drying tube which was then placed into an electrically heated drying apparatus [59]. The material was dried at 125 °C for 3 hours to give 10.4 g of solid copper tetranitrophthalocyanine.

The CuTNPc complex, in the amount of 10.4 g, was placed in 250 mL of distilled water along with 50 g Na_2S. This material was magnetically stirred and heated at 50 °C for 5 hours. This slurry was then mixed with 750 mL of 1.0 M HCl, and became very bulky to produce an aminohydrochloride. The aminohydrochloride was centrifuged at 5000 RPM for 3 minutes. The solid material was then placed in 500 mL of 1.0 M NaOH and magnteically stirred for one hour. The solid material was then washed 9 times with distilled water to free it of hydroxide and chloride. The wet solid CuTAPc was dried in the same manner but at 50 °C. The total amount of the dry product obtained was 7.94 g.

CoTAPc, and ZnTAPc. The cobalt and zinc complexes were synthesized in the same manner using the same amount of starting material except in the case of the zinc complex. For the ZnTAPc complex, the synthesis was based on 0.20 mole of 4-nitrophthalic acid. A scale up of the reaction was performed since the literature value for percent yield of ZnTAPc was much less than the yield for either CuTAPc or CoTAPc [58]. The total amount of dry product obtained for CoTAPc, and ZnTAPc was 4.56 g and 5.01 g respectively.

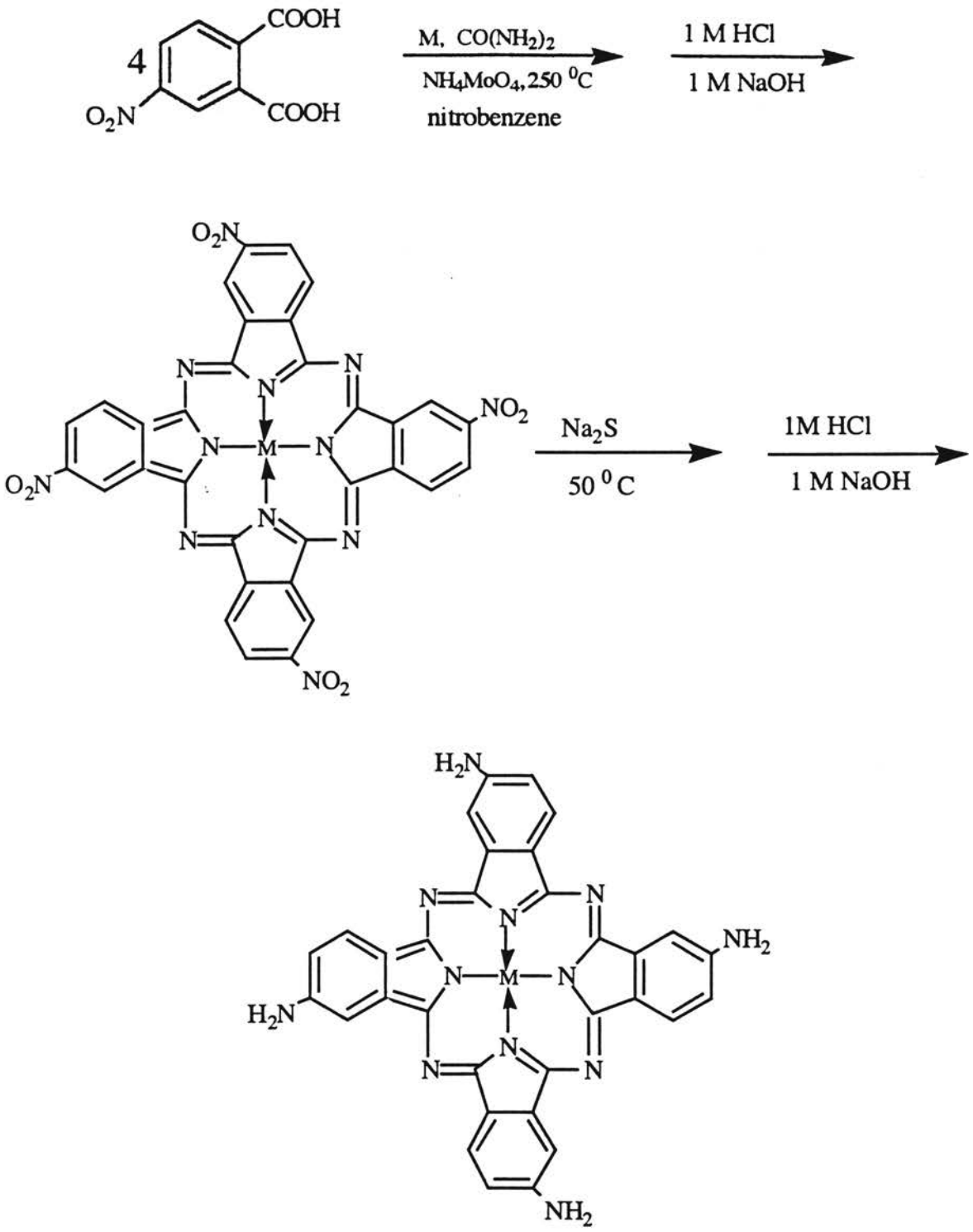

Figure 3.1 Total synthesis of metal (II)-tetraaminophthalocyanine

Spectral Characterization of Copper(II), Cobalt(II), and Zinc(II)-Tetraaminophthalocyanine. Spectrophotometric characterization of CuTAPc, CoTAPc, and ZnTAPc shows similar electronic spectra. Because of the extensive π system in the MPc compounds, intense absorption bands are prevalent in the UV and visible region of the spectrum The three compounds all show significant absorption bands between 200-220 nm, 300-310 nm, and 750-755 nm. Shoulders also appear between 384-390 nm, and 660-700 nm of the complexes. The origin of the small shoulders between 384-390 nm are unknown. The copper complex shows an additional band at 728 nm and two bands are observed between 720-755 nm. The Soret bands between 300 and 400 nm are π--->π^* transistions, and the Q bands (600-750 nm) result from E_g<----A_{1u} transistions. The bands between 200-220 nm are π--->π^* transistions [73]. Table 3.1 gives a summary of the electronic spectra for the three compounds, and Figure 3.2 shows a simplified diagram of the possible electronic transitions [60]. The electronic spectra for CuTAPc, CoTAPc, and ZnTAPc in Figure 3.3 shows the various absorption bands described above.

The 3d metal orbitals lie between the HOMO and LUMO of the ligand. As a result, other charge transfer bands, namely, metal-to-ligand charge transfer (MLCT) bands can be observed. These bands are usually centered between 450-600 nm. In cases where there is more than one charge transfer, the bands are usually split. This is a useful diagnostic tool for evaluating a change in the oxidation state of the central metal ion during redox the processes.

The IR spectra of all compounds are very similar. All M(II)TAPc compounds exhibit N-H, C-N, and C=C stretching. From the spectra, N-H stretching is observed from 3200-3350 cm^{-1}, C-N stretching from 1608-1611 cm^{-1} and C=C vibrational modes near 748, 827, 1099, 1348, and 1497 cm^{-1} [61]. Table 3.2 gives a summary of the IR spectra for the three compounds.

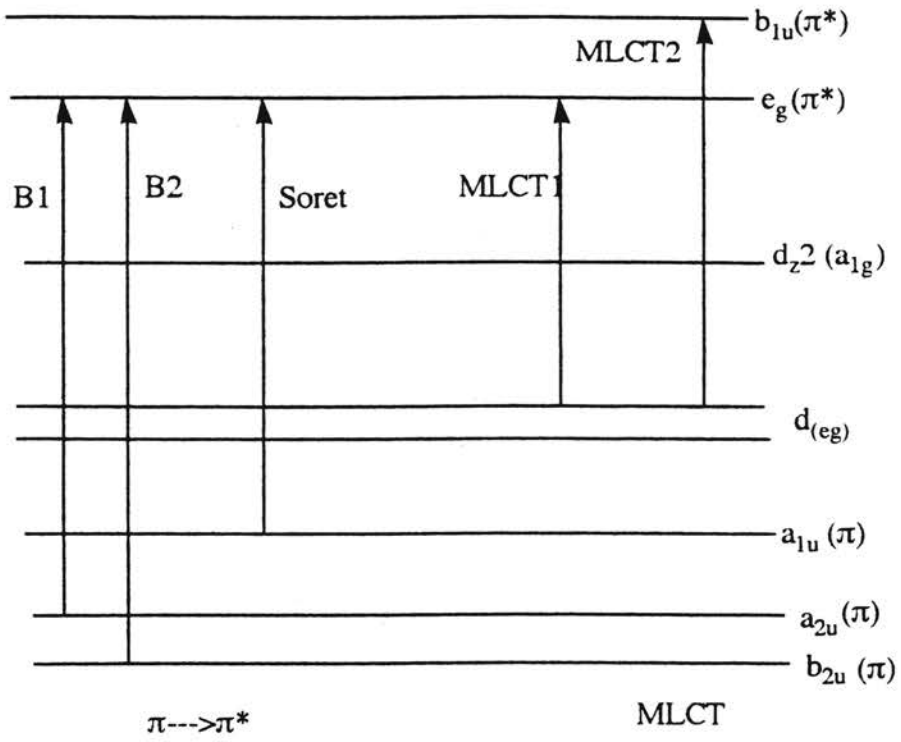

Figure 3.2 Simplified energy level diagram for MTAPc compounds. Electronic transitions are shown for "B" bands, Soret bands, and MLCT bands.

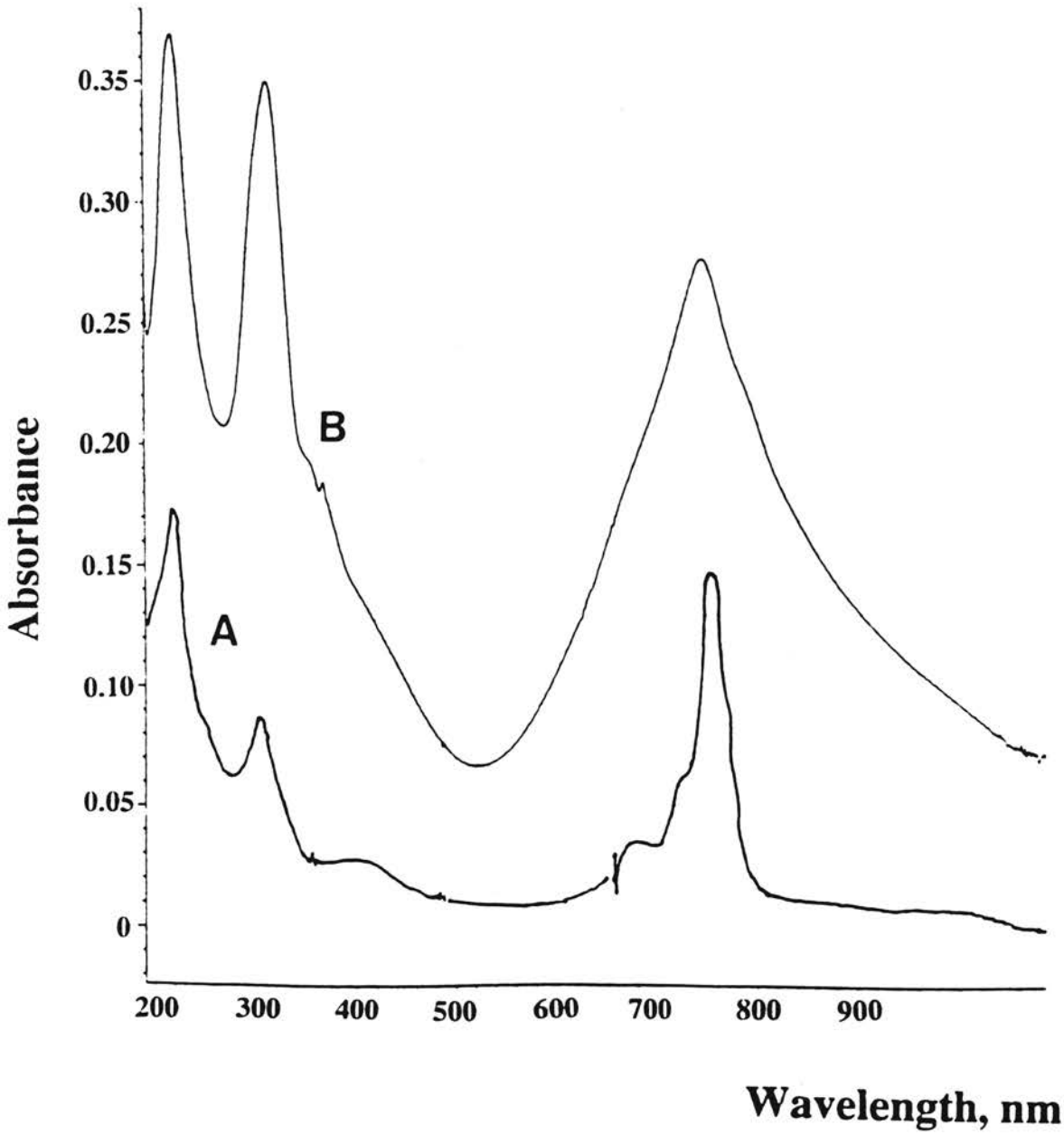

Figure 3.3(A-B) Electronic spectra of: (A) ZnTAPc, (B) CoTAPc, The concentration of ZnTAPc, and CoTAPc, in concentrated sulfuric acid are 1.29 x 10^{-6} M, and 1.32x 10^{-5} M respectively.

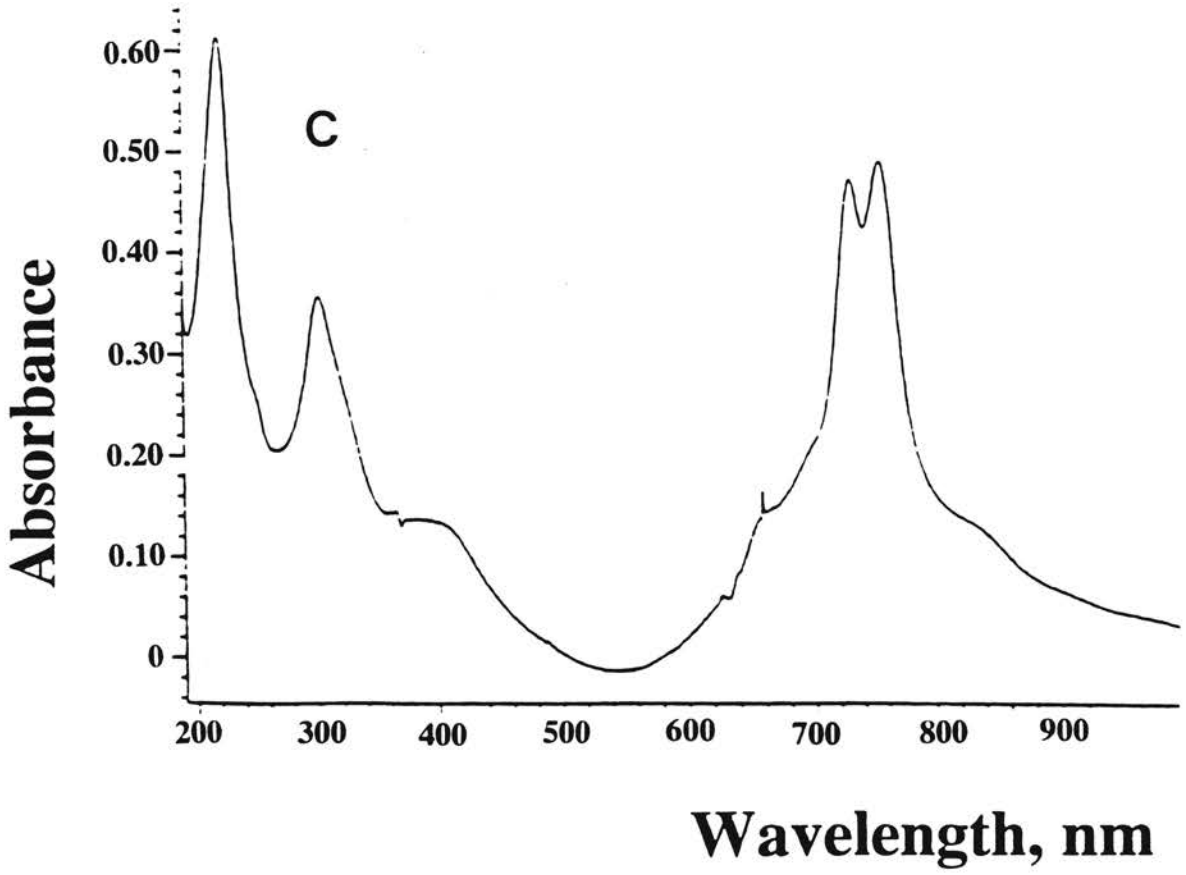

Figure 3.3C Electronic spectra of CuTAPc. The concentration of CuTAPc is 1.36×10^{-5} M respectively.

Table 3.1. Summary of electronic spectra for CuTAPc, CoTAPc, and ZnTAPc. The concentration of CuTAPc, CoTAPc, and ZnTAPc in concentrated sulfuric acid are 1.32×10^{-5} M, 1.36×10^{-5} M and 1.29×10^{-6} M respectively. The values in parenthesis are the log of the molar absorbtivity.

CuTAPc	CoTAPc	ZnTAPc
220 nm (4.65)	220 nm (4.50)	220 nm (5.11)
306 nm (4.42)	299 nm (4.35)	300 nm (4.83)
384 nm (4.01)	390 nm (3.95)	385 nm (4.36)
728 nm (4.54)	740 nm (4.26)	757 nm (5.06)
753 nm (4.56)		

Table 3.2 Summary of IR Spectra for CuTAPc, CoTAPc, and ZnTAPc. Spectra taken from KBr disks. Vibrational modes are given for C=C, C=N, and N-H bonds in cm^{-1}.

	CuTAPc	CoTAPc	ZnTAPc
v(C=C)	748	748	745
v(C=C)	827	823	832
v(C=C)	1090	1099	1099
v(C=C)	1348	1333	1346
v(C=C)	1355	1355	1355
v(C=N)	1608	1611	1611
v(N-H)	3216	3216	3231
v(N-H)	3344	3352	3349

STRUCTURE AND BONDING PROPERTIES OF METAL(II) TETRAAMINOPHTHALOCYANINE

MPc compounds have a planar structure and belong to the D_{4H} symmetry point group while metal free phthalocyanines, also planar belong to the D_{2H} symmetry point group [57]. Because of this difference, there are differences in their electronic spectra. This shows the impact of placing a metal ion in the cavity of the macromolecule ligand. These compounds contain four isoindole groups which form a cyclic-like structure. The central metal atom is bonded to four isoindole nitrogen atoms by two purely covalent bonds and two coordinate covalent bonds. In representing the structure of MPc compounds, the coordinate covalent bonds are shown with arrows or dotted lines. In metal-free phthalocyanine two imino hydrogens are present, but in the metal phthalocyanines, the two imino hydrogens have been replaced by the metal ion. As a result of the displacement of these two hydrogens by the metal (II) ion, the charge on the Pc ligand is -2. Thus, the overall charge on the metal phthalocyanine is zero. This fact is worth mentioning since redox processes can occur with the central metal ion or the Pc ligand. In addition, the metal phthalocyanine compounds may also be considered to be a union of four - six membered chelate rings with the central metal ion.

X-Ray diffraction studies reveal that there exits polymorphism in the MPc compounds in the solid state. The possible forms are the alpha, beta, and gamma forms. These polymorphs are based on the interatomic distances and angles in C--N, C--C, and N-metal bonding. The beta polymorph is the most stable form [54]. The polymorph form in this research was not determined since it was not expected that there would be a change in the MTAPc compounds. The central metal ion has an affect upon the overall dimensions of the MTAPc compounds. This fact is related to the determination of the thickness of thin films for CuTAPc, CoTAPc, and ZnTAPc, discussed later in this dissertation.

Reference was made that MPc compounds and derviatives are essentially composed of 4-six membered chelate rings. The coordination chemistry of these compounds should be addressed since their chemistry is also related to the availibility of the central metal atom to coordinate with various ligands. The optimum coordination numbers of the CoTAPc, and ZnTAPc complexes are 5, and 6 respectively. The CuTAPc complex has a "pseudo" coordination number of 4 [62]. Solvent molecules such as dimethyl sulfoxide and even gaseous species such as carbon dioxide may act as ligands which coordinate axially with the central metal ion. When coordination with electron donor species occurs, the HOMO and/or LUMO energy levels of the phthalocyanine complexes may be affected and hence the redox potentials change. The relevance of the aforementioned ligands is discussed in chapters 5 and 6.

CHAPTER IV

ELECTROPOLYMERIZATION OF COPPER(II), COBALT(II), AND ZINC(II) 4, 9, 16, 23- TETRAAMINOPHTHALOCYANINE

INTRODUCTION

Metal phthalocyanine compounds and derivatives display significant redox activity over a wide range of potentials in a number of different solvent/supporting electrolyte systems [63]. When considering derivatives of metal phthalocyanines there are essentially three possible oxidation and/or reduction processes: (1) the central metal ion, (2) the phthalocyanine (Pc) ligand, and (3) substituents on the Pc ligand. All three of the above processes are important in describing the electropolymerization of MTAPc complexes. That is, in many instances the redox activity of the metal phthalocyanine derivative may be due to the ligand and substituent only, or a combination of the ligand, substituent, and central metal ion [64]. The specific redox activity of either the ligand or central metal ion of the MTAPc over a certain potential range may affect the electrocatalytic mechanism for redox processes of different species in solution. In addition, the central metal ion and ligand redox processes as opposed to only ligand based redox processes may affect the electropolymerization in terms of the film thickness and the rate of electropolymerization [65].

Potential cycling methods such as cyclic voltammetry allows one to determine if a redox process is reversible, quasireversible or totally irreversible. A reversible redox process gives a peak separation near 59 mV for a one-electron transfer process. Under these conditions, the system is under thermodynamic control, and Nerstian equilibrium conditions apply to the redox process. A quasireversible redox process gives a peak

separation greater much greater 59 mV for a one-electron transfer process. The redox couples are, however, within the potential window. An overpotential is present so that one process, either reduction or oxidation, dominates the charge transfer. Under these conditions, the system is under kinetic control. For an irreversible redox process, either the reduction or oxidation process is not present within the potential window. As a result, only one peak, either cathodic or anodic peak is present during the cyclic voltammetric scan. In addition, information concerning specific types of mechanisms can be obtained. For example, some processes are purely electrochemical (E) while other are chemical (C). Plots of the peak currents versus the square root of the scan rates allows one to determine if diffusion controlled conditions are present during the electropolymerization, and to determine diffusion coefficients [66].

EXPERIMENTAL SECTION

Instrumentation. All electropolymerizations were made with a BAS-100 electrochemical analyzer (Bioanalytical Systems, West Lafeyette, IN). A three-electrode system, consisting of glassy carbon (3-mm diameter) or a transparent ITO as working electrode, a Ag/AgCl, 3 M NaCl reference electrode, and a platinum auxiliary electrode was used. The ITO electrode was a glass sheet (7mm x 50 mm x 0.6 mm) coated on both sides. The working electrode area was 3.50 cm^2 (resistance less than 10Ω). The ITO/glass sheets were from Delta Technologies, Ltd. (Stillwater, MN), and the other electrodes were from Bioanalytical Systems.

Reagents and Solutions. All chemicals used were reagent grade unless otherwise noted. The nitrogen used for deoxygenating prior to electropolymerization was from Sooner Airgas Inc., (Shawnee, OK). The dimethyl sulfoxide used as solvent for all solution preparations of monomer complexes was purchased from Sigma (St. Louis, MO). The tetraethylammonium perchlorate (TEAP) used as supporting electrolyte in all

electropolymerizations was from GFS Chemical (Columbus, OH). The concentration of supporting electrolyte was in all cases 0.10 M, and the concentration of all complexes in solution was 1.0×10^{-3} M.

Glassy Carbon Electrode Polishing and ITO Electrode Cleaning. The glassy carbon working electrodes were polished by placing one drop of polishing alumina suspension of 0.05-μm-particle size (Bioanalytical Systems) on a wetted polishing pad. The electrode was moved in a circular motion, both clockwise and counterclockwise across the surface of the pad. A figure-eight motion was also performed. The electrode was rinsed with purified water and the polishing procedure repeated. The approximate time consumed by the polishing procedure amounted to 5 minutes or slightly more. After polishing, the electrode was placed in an ultrasonic cleaner for a minimum of 5 minutes to remove adsorbed alumina particulates from the electrode surface. The electrode was thoroughly washed with purified water and allowed to air-dry. To ensure that a smooth surface was obtained, the electrode surface was inspected under a Stereo Star Zoom (1x to 6x) microscope model AO 580 (AO Scientific Instruments, Buffalo, NY).

The ITO electrode was placed in a 1% aqueous alconox solution (Alconox, Inc., New York, NY) and sonicated for 40 minutes, followed by sonication in purified water for 5 minutes. The electrode was then thoroughly rinsed with purified water and allowed to air-dry.

Electropolymerization Procedures and Conditions for MTAPc Complexes. Prior to each electrochemical experiment, the solutions were deoxygenated with nitrogen gas for 10 minutes, and a nitrogen gas blanket was maintained over all solutions for the duration of the experiment. Once deoxygenating was performed, several minutes were allowed to elapse before commencing the electrochemical run. This was to ensure that the nitrogen blanket did not perturb the surface of the solution. This was to eliminate

possible convective forces which would contribute to mass transport of the monomer material to the electrode surface. It is desirable to have only diffusion controlled conditions so that all calculated currents can be easily related to equations governing the current response. The supporting electrolyte helps to eliminate the effects of migration, and to reduce solution resistance.

For the glassy carbon electrode, the scan rate normally was 50 $mV \cdot sec^{-1}$ or 200 $mV \cdot sec^{-1}$. The potential window for cyclic voltammetric electropolymerization of the CuTAPc complex was +1.000 V to -0.600 V or +1.000 V to -2.000 V. For both the CoTAPc and ZnTAPc complexes, the potential was +1.000 V to -0.200 V or +1.000 V to -2.000 V. The number of electropolymerization cycles was taken as an indication of film thickness. Blank runs were performed prior to all electropolymerizations using an electrolyte solution of DMSO and TEAP only. The concentration of blank solutions in all cases was 0.10 M. Diffusion controlled conditions for the experiments were verified by examining the dependence of the peak current on the square root of the scan rate.

For the ITO electrode, the potential window for cyclic voltammetric electropolymerization of all MTAPc complexes was +1.000 to -0.600 V. In DMSO the useful negative potential window was not extended beyond -0.600 V. A total of 25 cycles were used, and the scan rate was 50 $mV \cdot sec^{-1}$.

RESULTS AND DISSCUSSIONS

Proposed Mechanisms for Oxidative Electropolymerization of MTAPc. The electropolymerization of MTAPc follows a similar mechanistic pathway of aniline [67], and a procedure used previously with ruthenium and iron complexes [68]. This is an efficient way of ensuring multilayer coverage as previously mentioned. A scheme rationalized for the electropolymerization of the MTAPc complexes is shown in Figures 4.1 and 4.2. The amine substituents on the benzene portion of the Pc ligand are ortho-para directing. The pathway for the electrooxidation of aniline occurs by ortho or para

coupling. The final products between ortho and para coupling may give different products with the ortho coupling pathway giving a lower yield . The ortho coupling gives lower yields than para coupling because of steric effects [67]. The pathway for generating the MTAPc polymeric film proceeds by an ortho radical coupling or direct head-to-head coupling because the para position is blocked by the pyrrole unit of the isoindole group of the phthalocyanine ligand. In comparing ortho coupling and direct head-to-head coupling, and in consideration of reaction conditions, direct head-to-head coupling would predominate since ortho coupling would also entail steric effects. For the direct coupling of radicals, N=N bonds are formed, and in ortho radical coupling, C-N bonds are formed. As mentioned in chapter 2, multiple amine sites allows a more favorable orientation so that additional monomer units may be incorporated into the polymer film to continue polymer growth.

Pathway **III** is the direct head-to-head coupling which leads to N=N bonding. As with aniline, the first step is the electrooxidation of the amine substituent to generate the radical cations **11.** The radical cation **11** shown has a resonance structure **12** and loses a proton. The deprotonated radical cation **13** undergoes coupling to give **14**. The R-group represents the rest of the Pc moiety which further allows the growth of the polymer film via the amine substituents. Figure 4.3 shows an ideal structure of the polymeric thin film via pathway **III.**

Pathway **IV** is the ortho radical coupling which leads to C-N bonding. This process continues via the amine substituents on the monomer to form the polymeric film. Structure **15** undergoes an ortho coupling reaction to give **16**. This readily loses 2 protons to neutralize the dication to form **17**. Structure **14** is favored over structure **17** since there is less steric hindrance for the coupling reaction to occur.

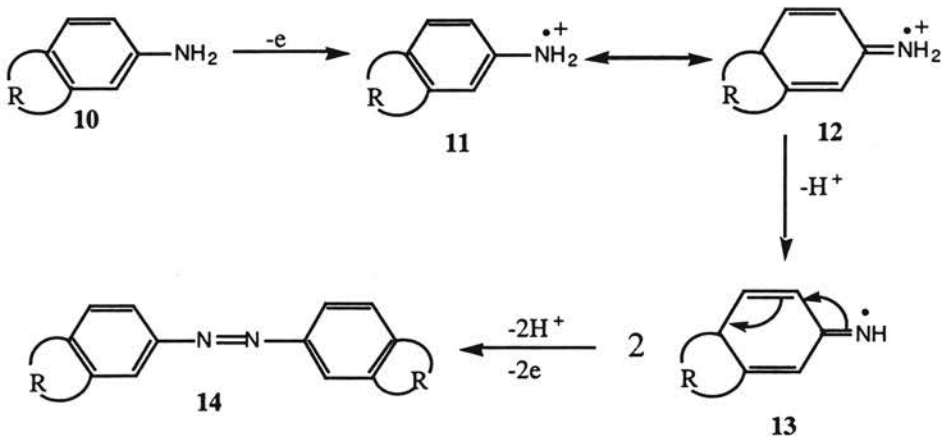

Figure 4.1 Pathway III. Reaction mechanism for the electropolymerization of MTAPc. This results in the formation of N=N bonds.

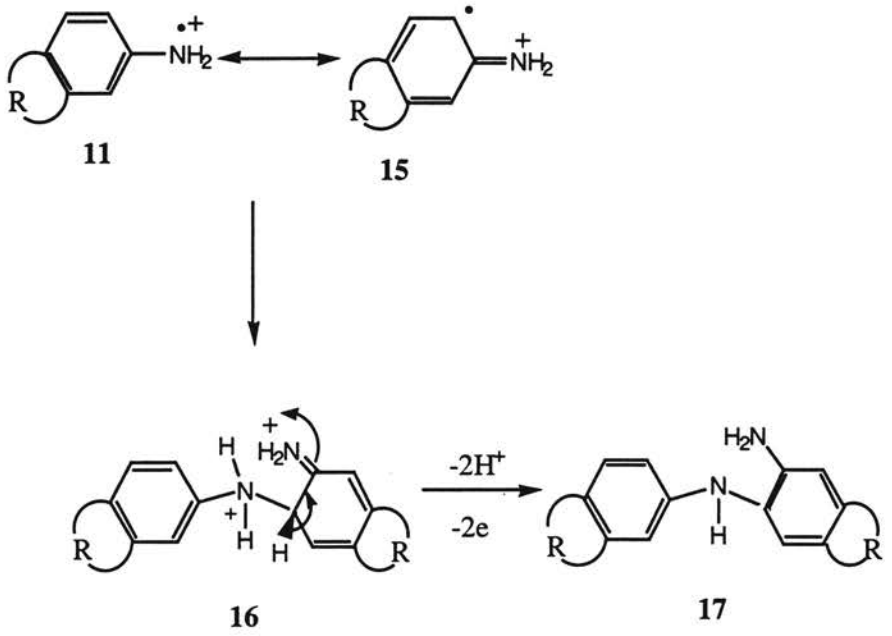

Figure 4.2. Pathway IV. Reaction mechanism for the electropolymerization of MTAPc. This results in the formation of C-N bonds.

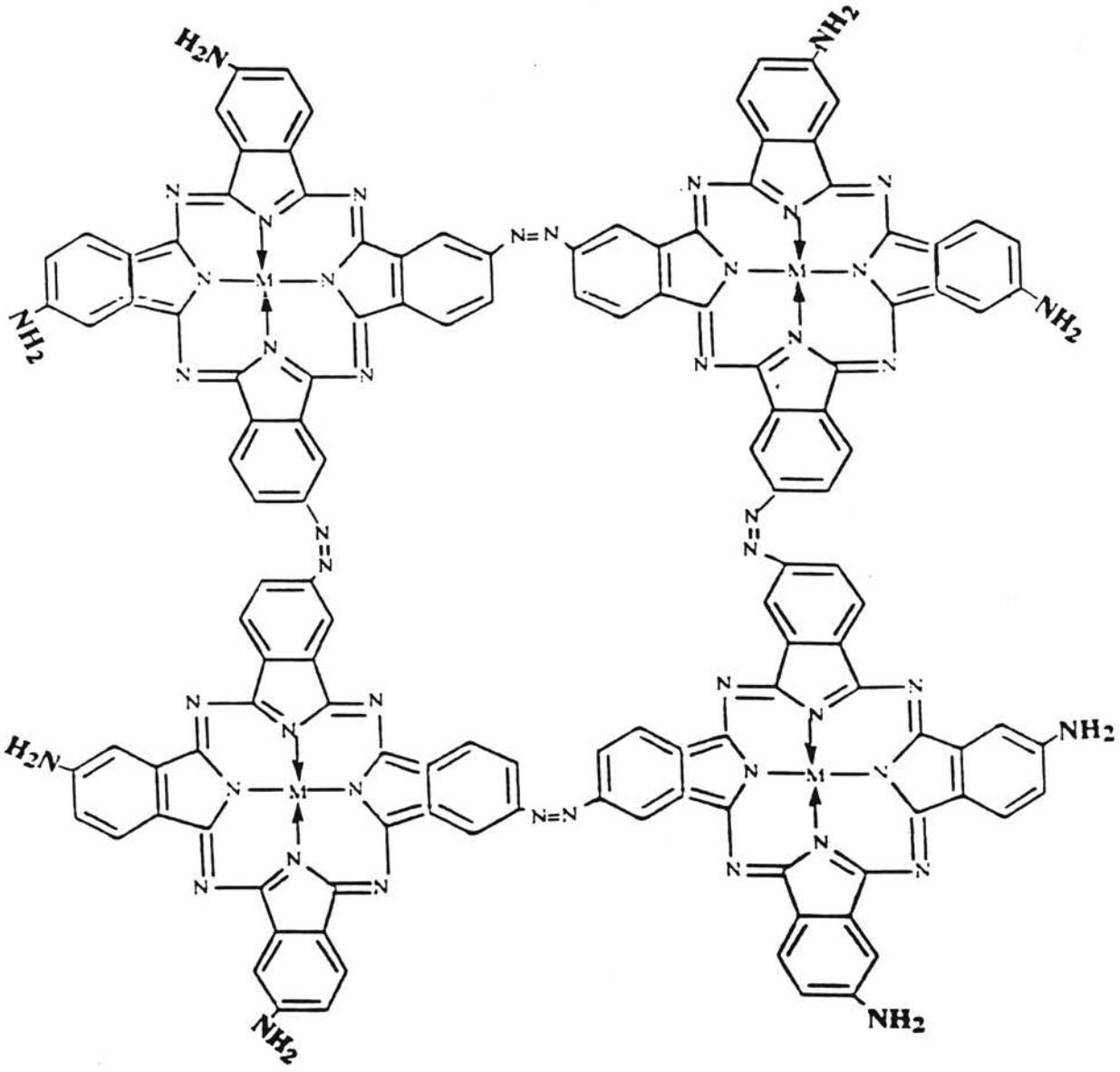

Figure 4.3. Idealized Structure of poly-MTAPc. Polymer formed via pathway III.

Electropolymerization of CuTAPc on Glassy Carbon Electrode. The electropolymerization of CuTAPc was first examined using a full potential window to make full peak assignments for the central metal ion and Pc ligand redox processes. The potential window of +1.000 V to -2.000 V was used as the range to the make assignments. Figure 4.4 are cyclic voltammograms obtained at a scan rate of 50 $mV \cdot sec^{-1}$ and after 10 (Figure 4.4 A) and 20 (Figure 4.4 B) cycles of electropolymerization. Three redox couples are identified; one corresponds to the central metal ion, and the other two correspond to redox processes involving the ligand itself. Peak assignments for the redox processes involving the rings of the ligand are consistent with literature reports involving other MPcs [68]. The proposed assignment is summarized in the equations that follow:

$$[Cu^{2+}, Pc^{2-}] + e^- \underset{2}{\overset{1,3}{\rightleftharpoons}} [Cu^{1+}, Pc^{2-}]^-$$

$$[Cu^{1+}, Pc^{2-}]^- + e^- \underset{5}{\overset{4}{\rightleftharpoons}} [Cu^{1+}, Pc^{3-}]^{2-}$$

$$[Cu^{1+}, Pc^{3-}]^{2-} + e^- \underset{7}{\overset{6}{\rightleftharpoons}} [Cu^{1+}, Pc^{4-}]^{3-}$$

The Pc again represents the organic phthalocyanine moiety and the numbers correspond to the peak numbering in Figure 4.4. The alternative that peaks 4, 5, 6, and 7 involve copper in the +2 oxidation state cannot, however, be ruled out, and consequently, the following is also possible:

$$[Cu^{2+}, Pc^{2-}] + e^- \underset{5}{\overset{4}{\rightleftharpoons}} [Cu^{2+}, Pc^{3-}]^-$$

$$[Cu^{2+}, Pc^{3-}]^- + e^- \underset{7}{\overset{6}{\rightleftharpoons}} [Cu^{2+}, Pc^{4-}]^{2-}$$

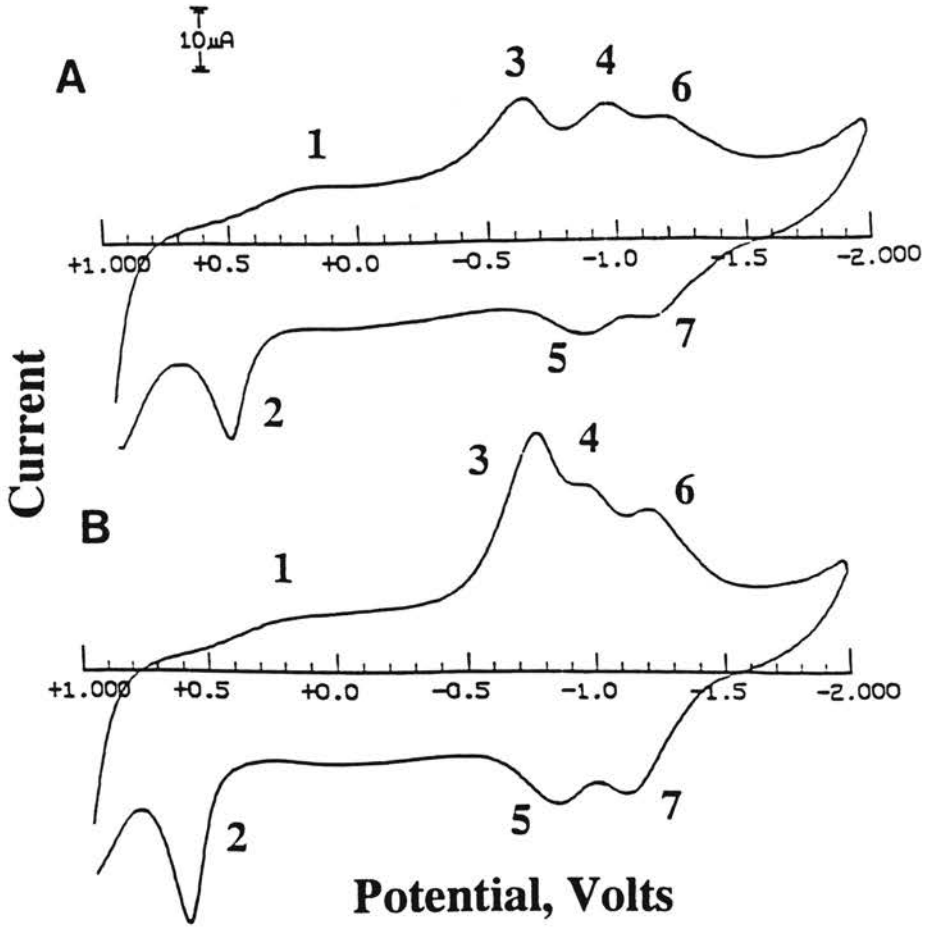

Figure 4.4. Cyclic voltammograms of 1.0 x 10^{-3} M CuTAPc in 0.10 M TEAP in DMSO recorded during electropolymerization. (A) This voltammogram was obtained after 10 cycles, and (B) after 20 cycles. The scan rate was 50 mV·sec^{-1}; initial potential, +1.000 V; working electrode, glassy carbon. Peak assignments are given in the text.

These formulations take into account that the Pc moiety is an aromatic system consisting of 18 π electrons and has a charge of -2. This is due to fact that the central metal ion has replaced the imino hydrogens in the internal cavity of the Pc ligand.

A more detailed look at the redox couples in Figure 4.4(A-B) reveals a peak separation for redox couples involving to Pc^{2-} /Pc^{3-} of 190 mV after 10 cycles of electropolymerization, and 105 mV after 20 cycles of electropolymerization. In addition, peak separation for redox couples involving Pc^{3-}/Pc^{4-} is 50 mV after 10 cycles of electropolymerization and 45 mV after 20 cycles of electropolymerization. The redox process of the central metal ion becomes more quasireversible but, the redox processes for the ligand do not.

To gain a better understanding of the evolution of peaks 1, 2, and 3, and the assignment of these peaks to the same half reaction, the potential window was circumscribed to 1.000 V to -0.600 V (Figure 4.5). Peak 1, clearly seen after one cycle starts decreasing on subsequent scans. Simultaneously, peak 3 increases with increasing cycles. These trends are interpreted as follows: peak 1 and peak 3 are due to the electrochemistry involving Cu^{2+}/Cu^{+}, and this process evolves from almost reversible to quasireversible electrochemical behavior as the electropolymerization proceeds.

Since both peak 1 decreases rapidly and concomitantly peak 3 increases, a correlation [69-70] study was pursued. Since peak heights were found to be more difficult to ascertain, the decrease of peak area of the peak at approximately 0.300 V was correlated with the increase in peak area for the peak at approximately -0.200 V. The correlation plot shown in Figure 4.6, has a regression equation of $y=0.0043 + 1.0093X$ where y is the decrease of peak are at 0.300 V (peak 1) and x is the increase of peak area at -0.200 V (peak 3). The slope of 1.0093 indicates that for every 1 unit of decrease of peak 1 at 0.300 V, there is a corresponding 1 unit of increase in peak 3 at -0.200 V. The corresponding Pearson correlation coefficient of 0.981 indicates a 98.1% degree of

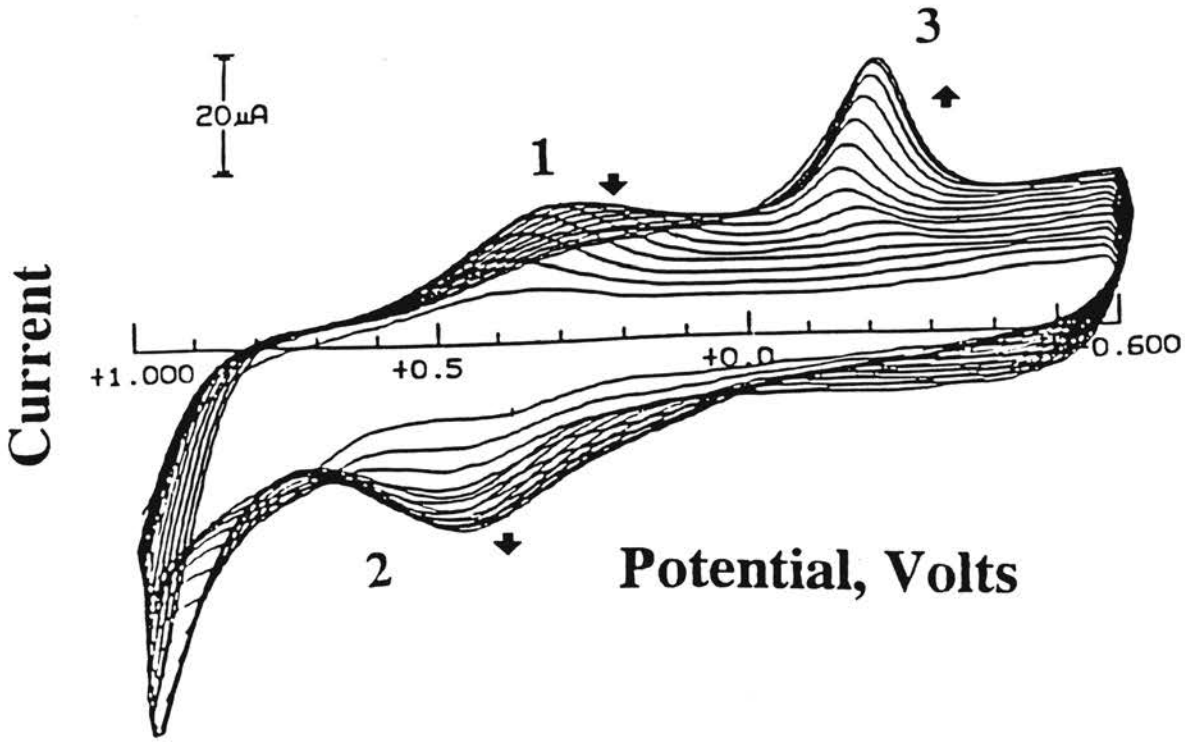

Figure 4.5. Repeated cyclic voltammograms of 1.0 x 10^{-3} M CuTAPc in 0.10 M TEAP in DMSO recorded during the first 15 cycles of electropolymerization, showing the evolution of peaks 1, 2, and 3: scan rate, 50 mV·sec^{-1}; initial potential, +1.000 V; working electrode, glassy carbon. Peak assignments are given in the text.

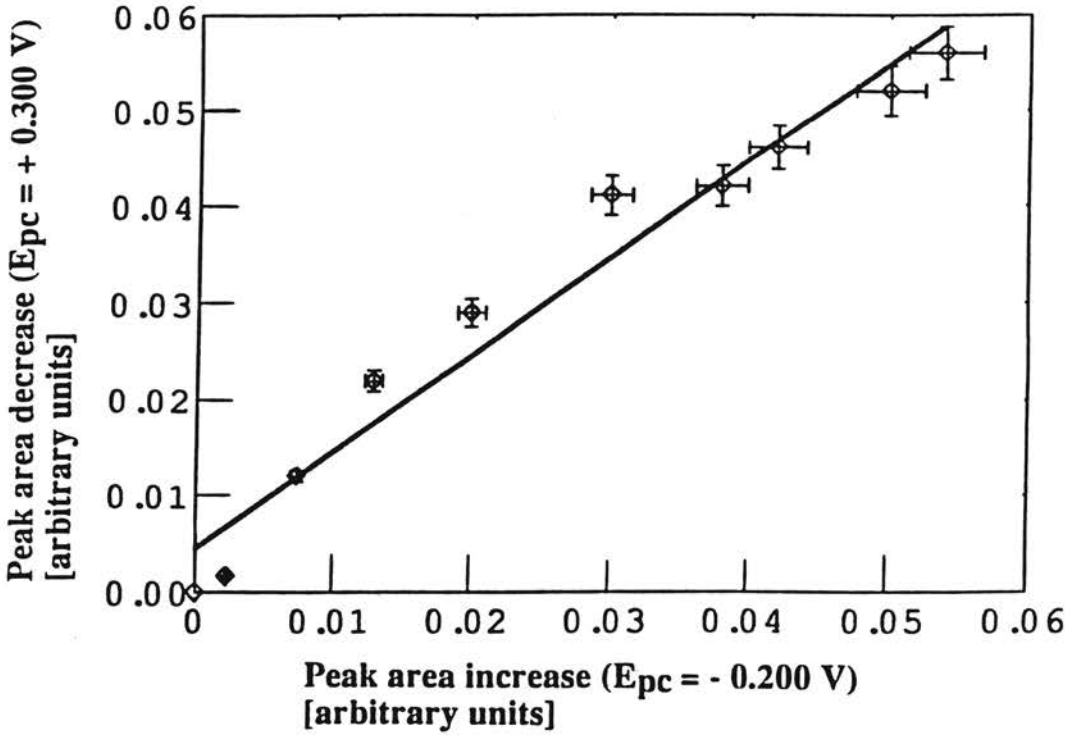

Figure 4.6. Correlation plot of the decrease in peak area for peak 1 and the increase in peak area for peak 3. Both peaks are considered to correspond to $[Cu^{2+}, Pc^{2-}] + e^- \text{----> } [Cu^{+}, Pc^{2-}]^-$.

correlation between the two peaks, and that the deviation from the best fit linear line is very slight. A slope practically close to 1, a very small intercept, and a good correlation coefficient all point to a good correlation. Thus, peaks 1 and 3 are assigned to the same redox process. Further evidence for this assignment is given in chapter 5 dealing with the spectroelectrochemical characterization of CuTAPc thin films.

During the earlier cycles, two anodic peaks appear [Figure 4.7(A)], and the peak at the more positive potential is eventually overlapped by the growth of the anodic peak (peak 2) at the more negative potential due to the electropolymerization process. After five or six cycles [(Figure 4.7(B)] the individuality of the peak is lost. Peak separation for peaks 1 and 2 during the early cycles of electropolymerization (1-2 cycles) is 58 mV, very close the theoretical value of 59 mV for a one-electron redox process. The corresponding cathodic peak of the anodic peak at the more positive potential is absent, and this indicates an irreversible process. This peak is assumed to be due to the extracting of an electron from the $-NH_2$ group and was shown to be absent if the electropolymerization was attempted in acidic medium when protonation of the $-NH_2$ groups is expected. The potential at which this peak appears is +0.700 V to +0.800 V, close to the +0.880 V quoted for the same process using 5-amino-1, 10-phenanthroline [68]. Ellis and co-workers also observed similar results. When $[(bpy)_2\ Ru(5\text{-}phenNH_2)]^{2+}$, and $[(bpy)Ru(5\text{-}phenNH_2)_2]^{2+}$ [bpy=bipyridine] were protonated, the oxidative peaks attributed to the irreversible amine oxidation disappeared [71]. The current increase in all cases is due to additional monomer units being incorporated into the film, resulting in film growth. The film itself mediates charge so that the amine oxidation at the film/solution interface is continued because direct amine oxidation via the electrode surface may not occur [71]. The uniformity of film growth is not known, and in order for the electrode surface to be fully covered multiple layers should accumulate onto the electrode surface.

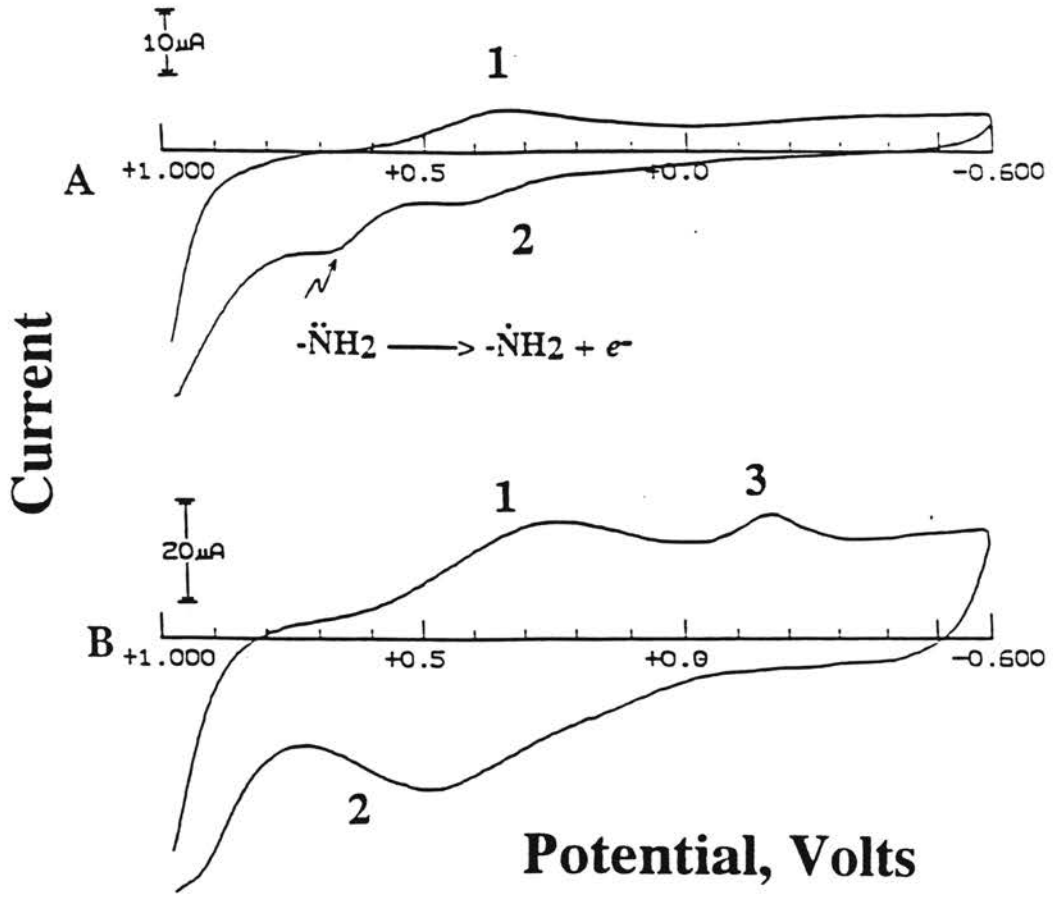

Figure 4.7. Cyclic voltammograms of 1.0 x 10^{-3} M CuTAPc in 0.10 M TEAP in DMSO recorded after (A) two cycles of electropolymerization, and (B) after 15 cycles of electropolymerization, showing the appearance and overlapping of the peak assigned to the electron subtraction from the amino group that initiates the electropolymerization process. Numbers for the other peaks correspond to the assignment given in Figures 4.4 and 4.5.

The cathodic peak potential for peak 3, E_{pc3}, depends on the age and light exposure of the solution of monomer in DMSO. Figure 4.9 shows the trend exhibited by the shift toward more negative potential values for E_{pc3} with solutions kept in the dark between measurements and solutions exposed to room illumination. A relatively constant value for E_{pc3} is obtained after more than 150 hours of solution preparation. Regression analysis using residual plots [70] confirms the presence of two different models describing the movement of peak 3 with time and light exposure. One model corresponds to the solution in dark and the other model in room illumination. This explains why in Figure 4.4, E_{pc3} appears at about -0.620 V and in Figure 4.5 it is close to -0.200 V.

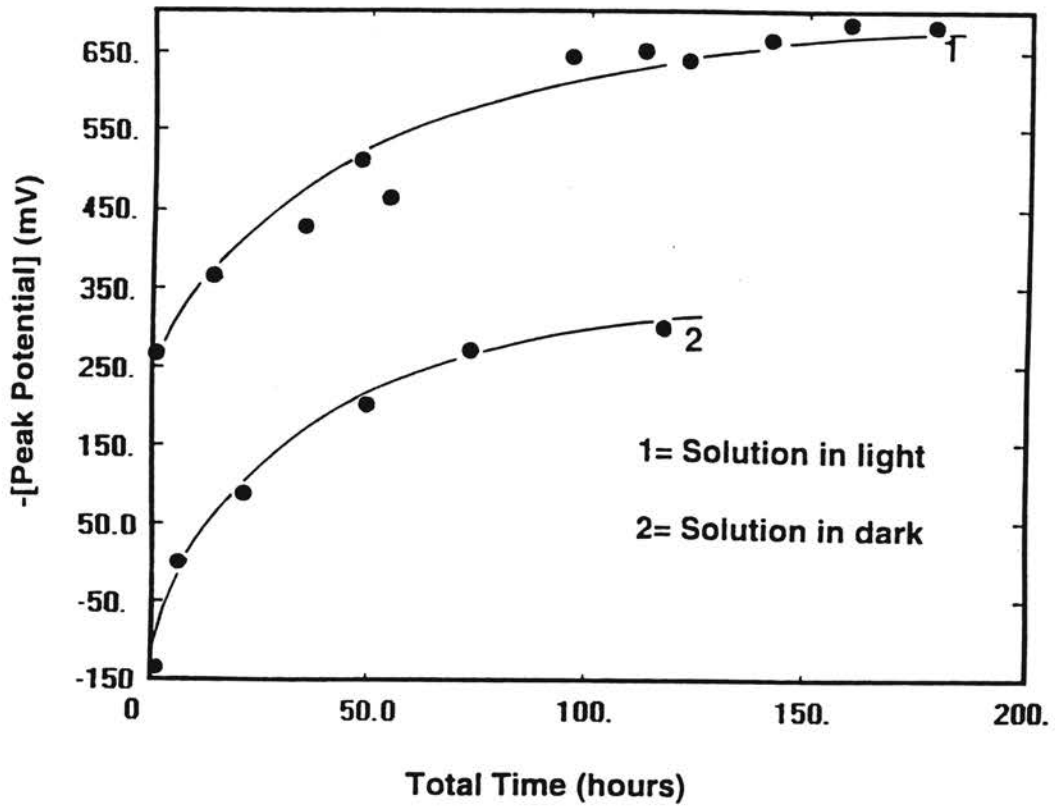

Figure 4.8. Shift of the cathodic peak potential for peak 3, with the age of the solution of monomer in DMSO. The smooth solid curve represent the best trend describing the evolution to higher overpotentials for the half reaction $[Cu^{2+}, Pc^{2-}] + e^{-} \text{----> } [Cu^{+}, Pc^{2-}]^{-}$ with the age of solution. Profile 1 corresponds to solution exposed to room light; profile 2 corresponds to solution kept in dark between measurements.

Electropolymerization of CoTAPc on Glassy Carbon. Figure 4.9 shows cyclic voltammograms corresponding to twelve cycles of electropolymerization (Figure 4.9A) and to one cycle of electropolymerization (Figure 4.9B). Three redox couples are identified after twelve cycles and are represented by the following equations:

$$\left[Co^{3+}, Pc^{2-}\right]^{+} + e^{-} \underset{9}{\overset{8}{\rightleftharpoons}} \left[Co^{2+}, Pc^{2-}\right]$$

$$\left[Co^{2+}, Pc^{2-}\right] + e^{-} \underset{11}{\overset{10}{\rightleftharpoons}} \left[Co^{+}, Pc^{2-}\right]^{-}$$

$$\left[Co^{+}, Pc^{2-}\right]^{-} + e^{-} \underset{13}{\overset{12}{\rightleftharpoons}} \left[Co^{+}, Pc^{3-}\right]^{2-}$$

Peak separation for the three redox couples are 51 mV, 122 mV, and 133 mV respectively. These peak assignments are consistent with what is known about the electrochemical behavior of metal-phthalocyanine complexes and films derived from them [72].

Figure 4.9B, depicting the first cycle of electropolymerization, shows two anodic peaks and one cathodic peak The anodic peak at about 0.625 V, without a corresponding cathodic peak, is due to the oxidation of the amino groups in the ligand moiety. This peak can be seen during the first 2 or 3 cycles, but is overlapped by the growth of the anodic peak labeled as peak 9 in Figure 4.9B. The other two peaks in this figure correspond to the redox processes identified as involving the Co(III)/Co(II) redox couple. The oxidation of the $-NH_2$ group is considered to be the initial step in the electro-polymerization process. This oxidation occurs at a more negative potential than the one

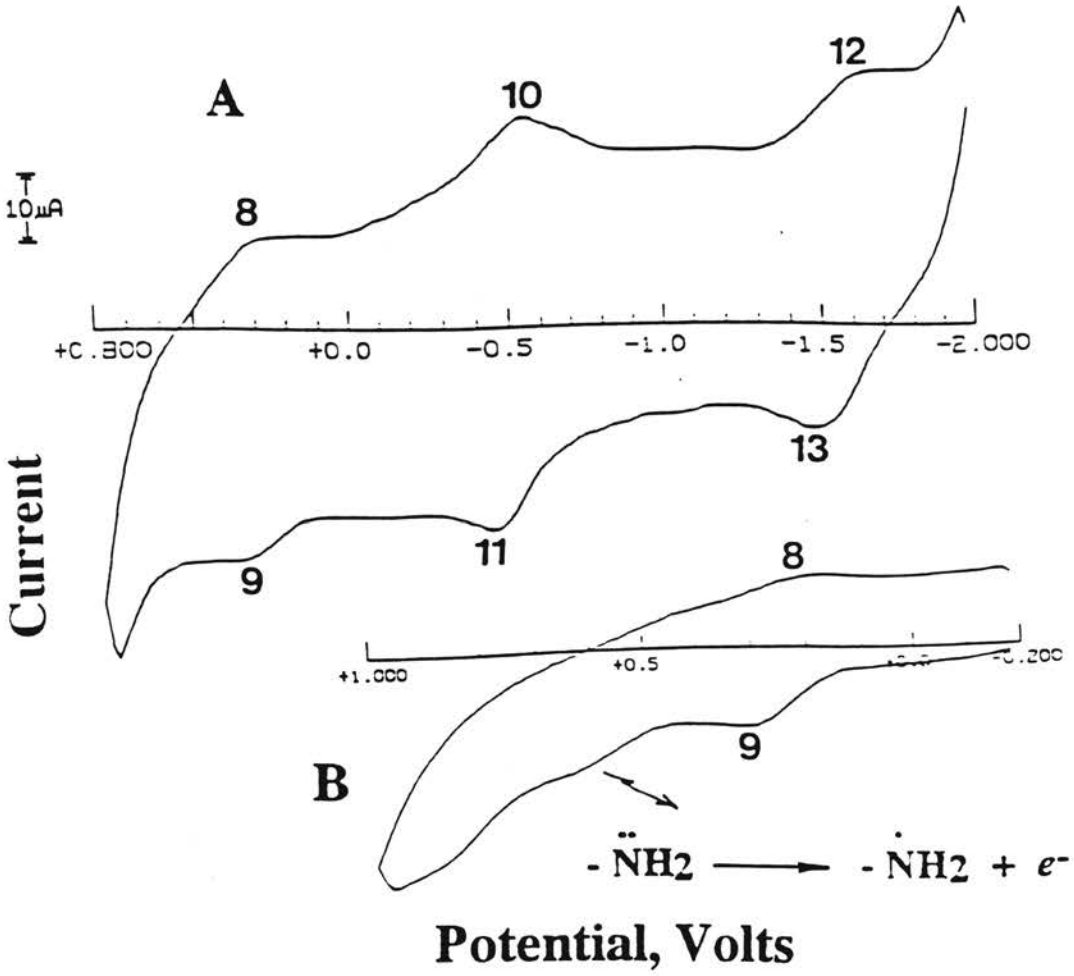

Figure 4.9 Cyclic voltammograms of 1.0 x 10^{-3} M CoTAPc in 0.10 M TEAP in DMSO. Scan Rate: 200 mV·sec^{-1}. (A) Cycle number 12 using the +0.800 V to -2.000 V potential window; peak numbering follows the assignment indicated in the text. (B) Cycle number one using the +1.000 V to -0.200 V potential window, and indicating the oxidation peak responsible for the start of electropolymerization.

observed for the same process in the electropolymerization of CuTAPc. A slight increase in the separation of these peaks is observed with increasing cycles. This insinuates increasing sluggishness in the charge transfer process involving the electrode and the monomer in solution due to the increased thickness of the film as the electropolymerization progresses. In Figure 4.10, plots of anodic (plot A) and cathodic (plot B) peak currents as a function of the number of electropolymerization cycles are linear, up to at least 45 cycles. The slopes of these linear plots (with regression coefficients of 0.987, and 0.997) indicate a slightly faster rate of oxidation since the slope of the line corresponding to the anodic process is 0.053 μA/cycle while the slope of the line for the cathodic process is 0.0464 μA/cycle.

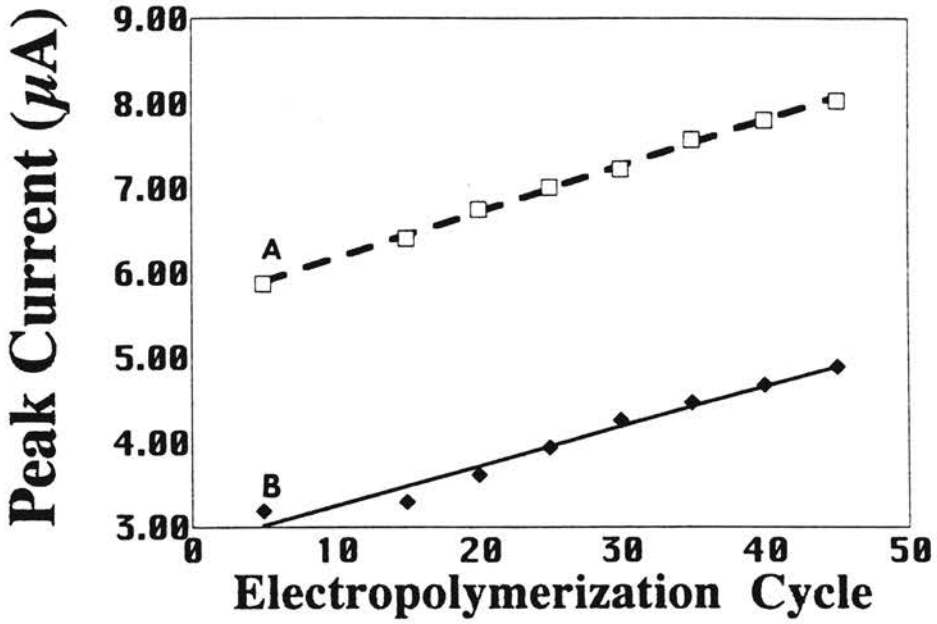

Figure 4.10 Plot of (A) anodic peak current and (B) cathodic peak current vs number of electropolymerization cycles for 1.0 x 10^{-3} CoTAPc in 0.10 M TEAP in DMSO. Regression equation for the oxidation: y=5.66 + 0.0531x, and the reduction: y=2.80 + 0.0464x.

Electropolymerization of ZnTAPc on Glassy Carbon. Three redox couples can be identified from the cyclic voltammograms obtained during electropolymerization of the zinc complex (Figure 4.11). The redox couples are all ligand based, without the metal center undergoing a redox process [55]. This was verified by spectroelectrochemical experiments which are discussed in chapter 5. The processes occurring during electropolymerization can then be illustrated as follows:

$$\left[Zn^{2+}, Pc^{2-}\right] + e^- \underset{15}{\overset{14}{\rightleftharpoons}} \left[Zn^{2+}, Pc^{3-}\right]^-$$

$$\left[Zn^{2+}, Pc^{3-}\right]^- + e^- \underset{17}{\overset{16}{\rightleftharpoons}} \left[Zn^{2+}, Pc^{4-}\right]^{2-}$$

$$\left[Zn^{2+}, Pc^{4-}\right]^{2-} + e^- \underset{19}{\overset{18}{\rightleftharpoons}} \left[Zn^{2+}, Pc^{5-}\right]^{3-}$$

In Figure 4.11 A, the peak separation for the three redox couples are 127 mV, 73, mV, and 55 mV. Using the short potential window, +1.000 V to -0.200 V (Figure 4.11B), the peak due to the amine oxidation appears close to +0.750 V, and the peak separation for peaks 14-15 is about 69 mV in the first cycle, and decreases close to the theoretical value for a one electron transfer when the scan rate is decreased to 50 $mV \cdot sec^{-1}$. The separation, however, increases as the number of electropolymerization cycles increase. This is particularly noticeable after 20 cycles of electropolymerization and using the +1.000 V to -2.000 V window. Undoubtedly, with increasing film thickness the electrochemistry evolves from reversible to quasireversible due to the more sluggish charge transfer across the film. The voltammograms in Figure 4.12(A-B) show the current profiles of repetitive cycling between the potential limits of +1.000 V to -0.200 V

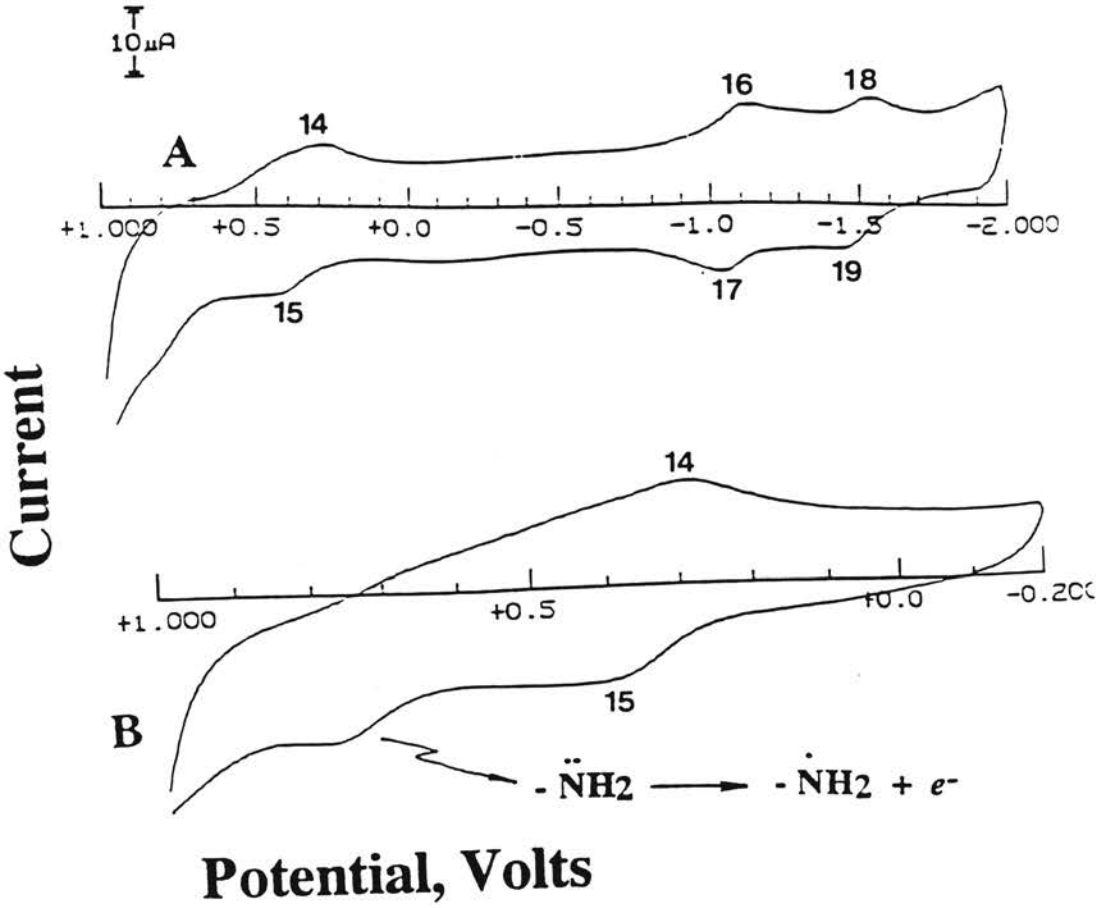

Figure 4.11. Cyclic voltammograms of 1.0 x 10^{-3} M ZnTAPc in 0.10 M TEAP in DMSO. Scan Rate: 200 mV·sec^{-1}; working electrode, glassy carbon (A) Cycle number 10 using the +1.000 V to -2.000 V potential window; peak numbering follows the assignment indicated in the text. (B) Cycle number 5 using the +1.000 V to -0.200 V potential window, and indicating the oxidation peak responsible for the start of electropolymerization.

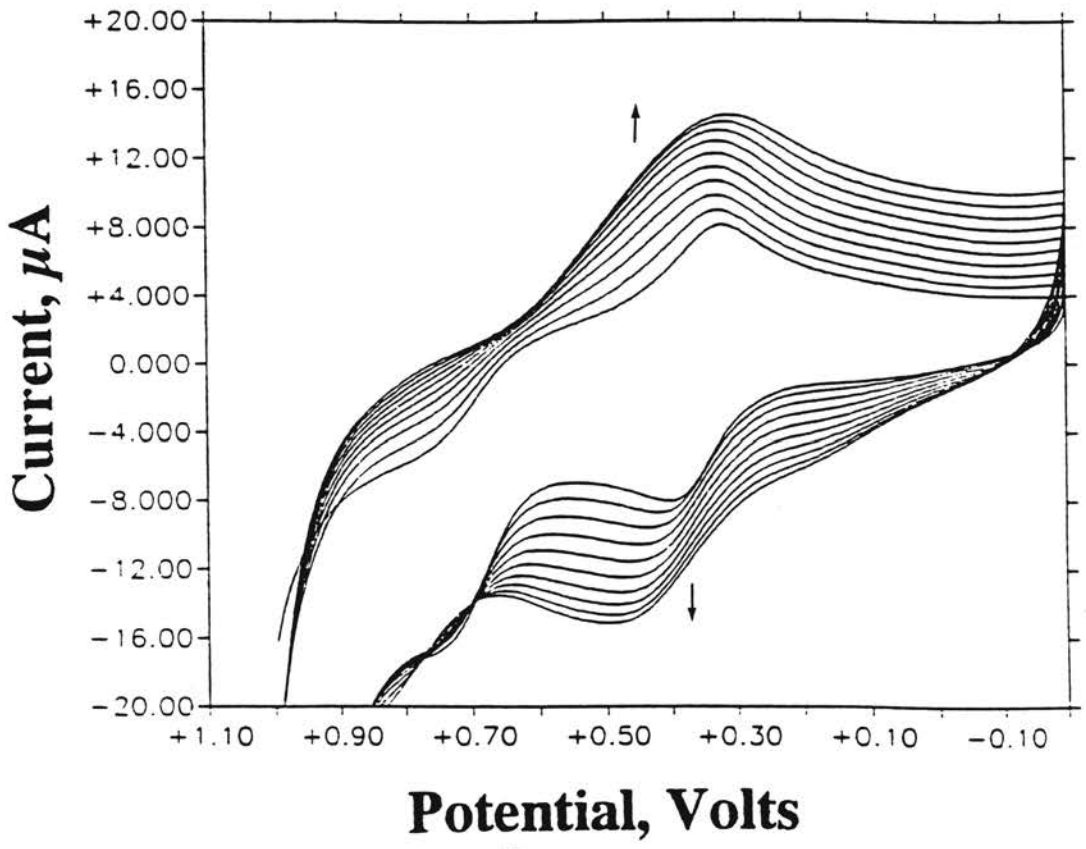

Figure 4.12 A. Repeated cyclic voltammograms of 1.0 x 10^{-3} M ZnTAPc in 0.10 M TEAP in DMSO recorded during the first 10 cycles of electropolymerization, scan rate: 200 mV·sec^{-1}; working electrode: glassy carbon; potential window, +1.000 V to -0.200 V. Peak assignments are given in the text. Arrows indicate an increase in current.

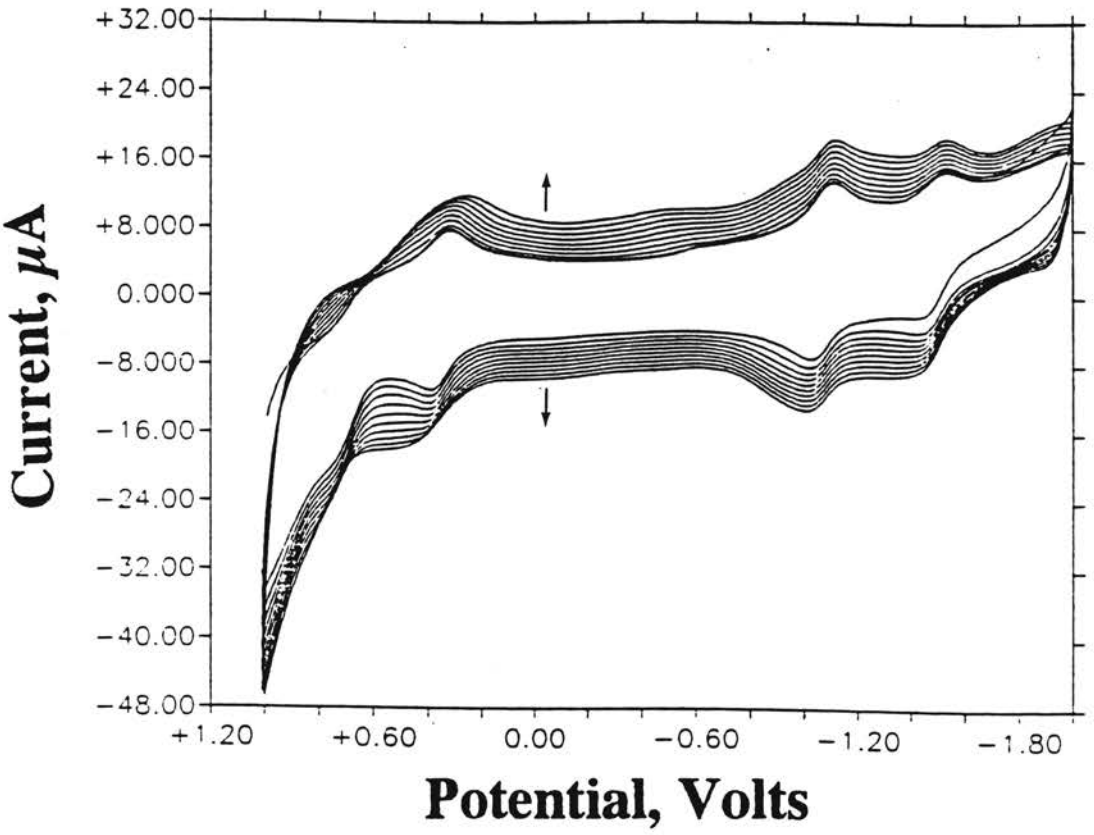

Figure 4.12 B. Repeated cyclic voltammograms of 1.0 x 10^{-3} M ZnTAPc in 0.10 M TEAP in DMSO recorded during the first 10 cycles of electropolymerization, scan rate: 200 mV·sec^{-1}; working electrode: glassy carbon; potential window +1.000 V to -2.000 V Peak assignments are given in the text. Arrows indicate an increase in current.

and +1.000 V to -2.000 V. The peaks correspond to the numbering system in Figure 4.11. Similar growth patterns are observed for CoTAPc. Plots of the peak current versus the number of electropolymerization cycles shown in Figure 4.13 indicate a much larger rate of oxidation than reduction. The slopes of such plots for the reduction and oxidation processes are 0.908 μA/cycle and 1.55 μA/cycle respectively. These values are larger than those for CoTAPc. One possible reason is that within the same potential window of +1.000 V to -0.200 V, redox processes for CoTAPc are ascribed to the metal ion, while for ZnTAPc redox processes are ascribed to the Pc ligand. As the applied potential is made more negative, electrons are placed into the $E_g(\pi^*)$ LUMO orbitals which are ligand based. The $d_{x^2-y^2}$ metal orbital of zinc is higher in energy than the $E_g(\pi^*)$. The other metal d orbitals are filled. In addition, the zinc metal ion is not polarizable. The negative charge is better stabilized on the Pc ligand by the conjugated π-system rather than on the central metal ion. In comparison to the delocalized charge on the Pc ring system, the charge on the central metal ion, as a result of a reduction process, may be considered as a point charge.

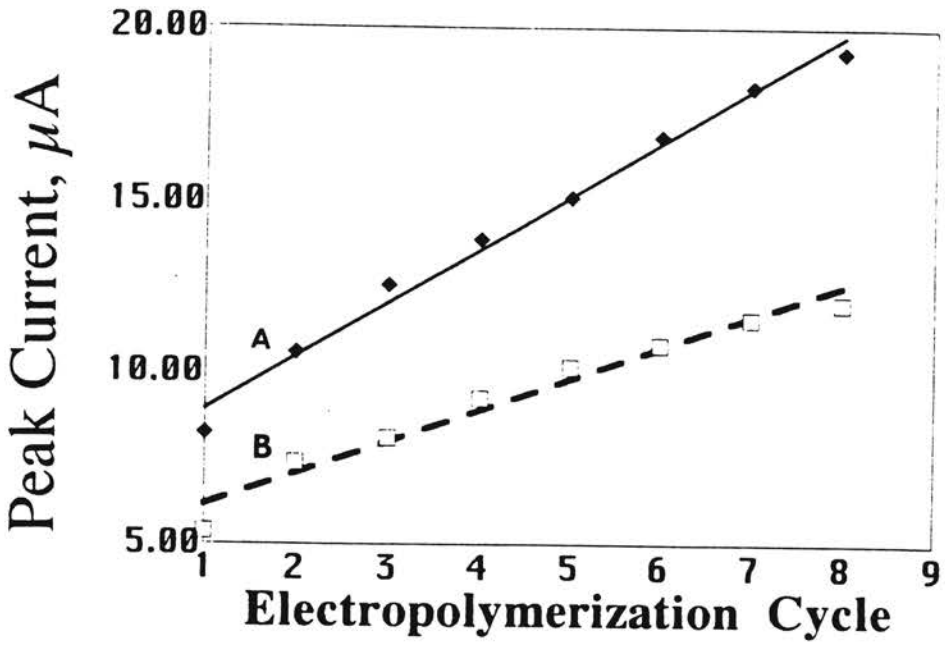

Figure 4.13. Plot of (A) anodic peak current and (B) cathodic peak current vs. number of electropolymerization cycles for 1.0 x 10^{-3} ZnTAPc in 0.10 M TEAP in DMSO. Regression equation for the oxidation: y= 1.55x + 7.43; and, the reduction: y = 0.909x + 5.22

Electropolymerization on ITO Surfaces. CuTAPc. The thin films on ITO surfaces are of blue-green color, becoming more intense as the number of electropolymerization cycles increased. Although, in principle, the potential window could be extended to -0.600 V, in practice it was limited to -0.200 V because the cyclic voltammograms for the electropolymerization of the complex yielded currents off scale. Consequently, the larger potential window provided by glassy carbon is unavailable using ITO and as such, the only visualized processes are those assigned to peaks 1-3. The electropolymerization on ITO surfaces (Figure 4.14) shows some differences as well as some similarities when compared with electropolymerization on glassy carbon. On the first cycle, the anodic peak for the oxidation of the amine group appears near 0.726 V, close to the anodic peak for the same oxidation of glassy carbon. Also, on the first cycle, the separation between peaks 1 and 2 is 74 mV, which is larger than when electropolymerization is performed on glassy carbon. As the number of cycles increases, the evolution of peak 3 follows the same pattern as when glassy carbon was used as the working electrode.

Electropolymerization on ITO Surfaces. CoTAPc, and ZnTAPc. Figure 4.15(A-B) are traces for the 2nd cycle for both the CoTAPc complex [Figure 4.15 (A)] and ZnTAPc complex [Figure 4.15(B)]. Peak separation for the Co(III)/Co(II) redox couple is over 300 mV, and the peaks are very broad. As a result, it is noted that electropolymerization is better facilitated for ZnTAPc for which peak separation of the redox couple Pc^{2-}/Pc^{3-} is about 100 mV and the peaks are more clearly defined. The peak potential for the amine oxidation for the zinc complex is near 0.700 V. However, for the CoTAPc complex, the amine oxidation is unnoticeable due to the aforementioned reasons.

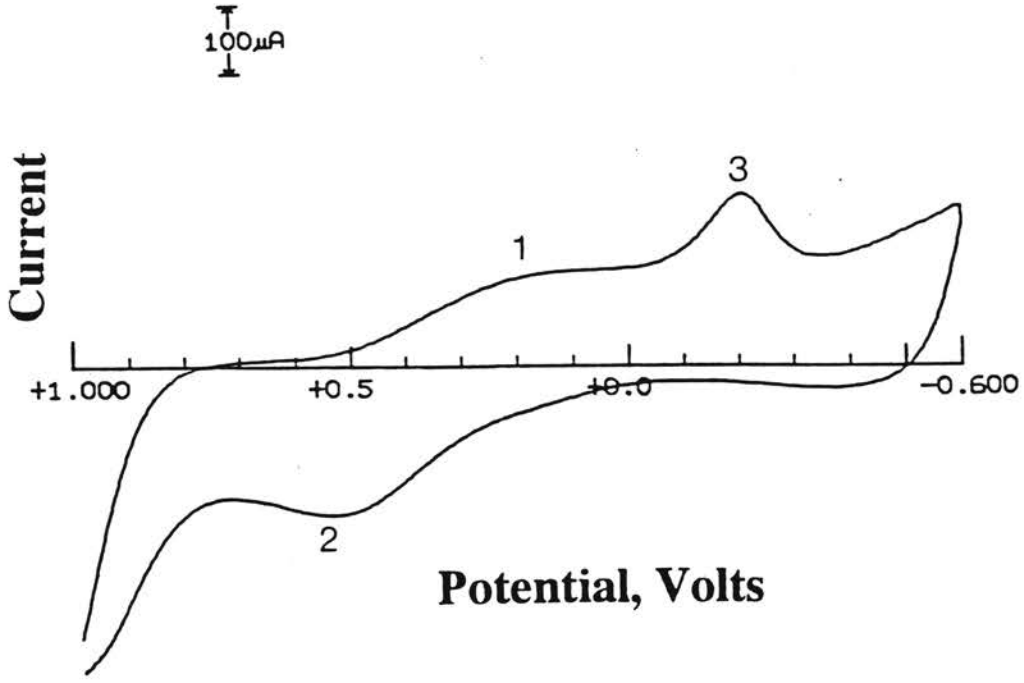

Figure 4.14. Cyclic voltammogram of 1.0 x 10^{-3} M CuTAPc in 0.10 M TEAP in DMSO on ITO working electrode. Peaks 1-3 correspond to the same numbering in Figure 4.5. Scan rate, 50 mV·sec^{-1}. Voltammogram corresponds to cycle number 12.

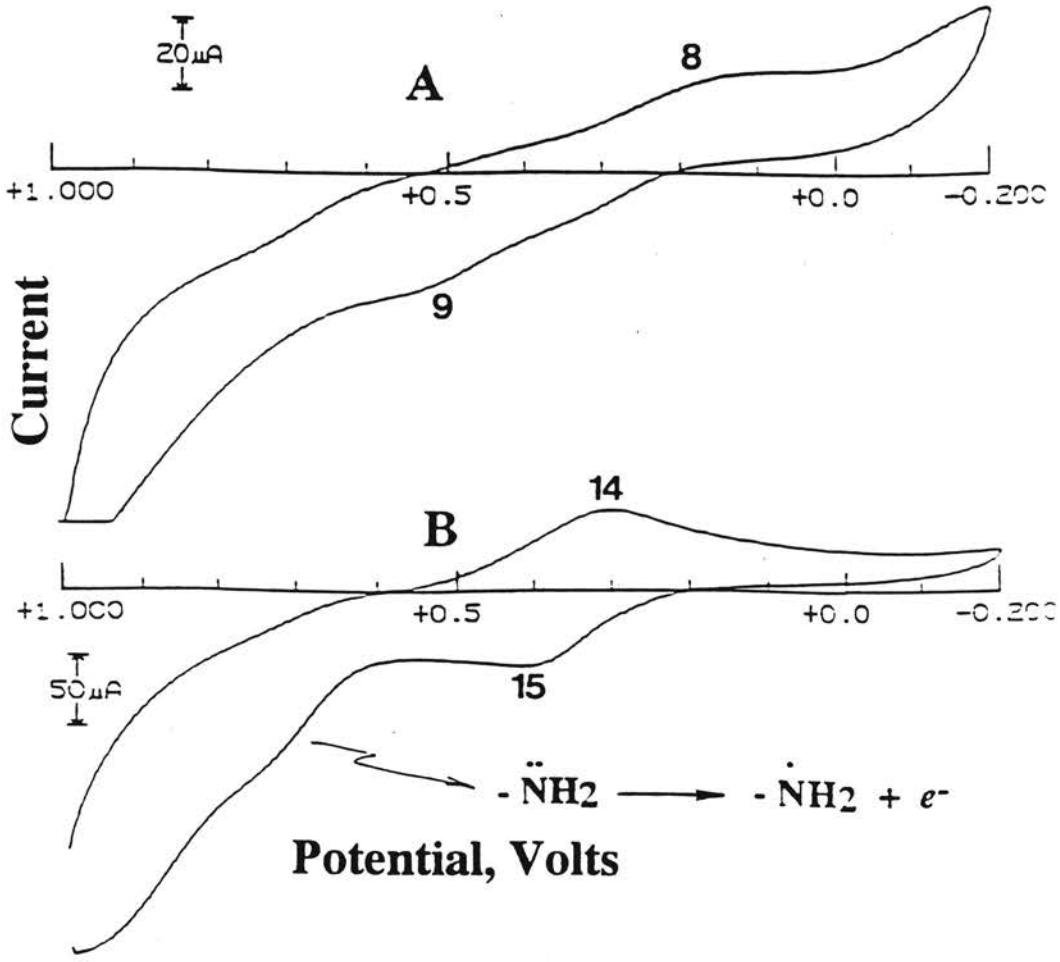

Figure 4.15. Cyclic voltammograms of (A) 1.0 x 10^{-3} M CoTAPc, and (B) 1.0 x 10^{-3} M ZnTAPc in 0.10 M TEAP in DMSO on ITO working electrode. Scan rate: 50 mV·sec^{-1}. Both cyclic voltammograms correspond to the second cycle of electropolymerization. Peak numbering follows assignments given in the text.

A plot of the peak current versus the square root of the scan rate is a diagnostic tool to verify that mass transport to the electrode surface is under diffusion controlled conditions. From the Randles-Sevcik equation [73]:

$$i_p = (2.69 \times 10^5) n^{3/2} A D^{1/2} v^{1/2} C \qquad (4.1)$$

where **n**=number of electrons transferred in the redox process, **A**= area of electrode surface, **D**= diffusion coefficient, and **C**=concentration of solution, the peak current is shown to be proportional to the square root of the scan rate, **v**. Figure 4.16 (A-C) are diagnostic plots for CuTAPc, CoTAPc, and ZnTAPc. The peak currents were calculated using Nicholson's formulation [74] shown in Equation 4.2

$$(i_{pa})/(i_{cp}) = (ipa)_o/(i_{cp}) + 0.485(i_{sp})_o/i_{cp} + 0.086 \qquad (4.2)$$

where $(i_{sp})_o$ is the measured peak current at the switching potential, while (ipa) and (i_{cp}) are the measured peaks currents for anodic and cathodic peaks. All peak currents are measured from the zero current line.

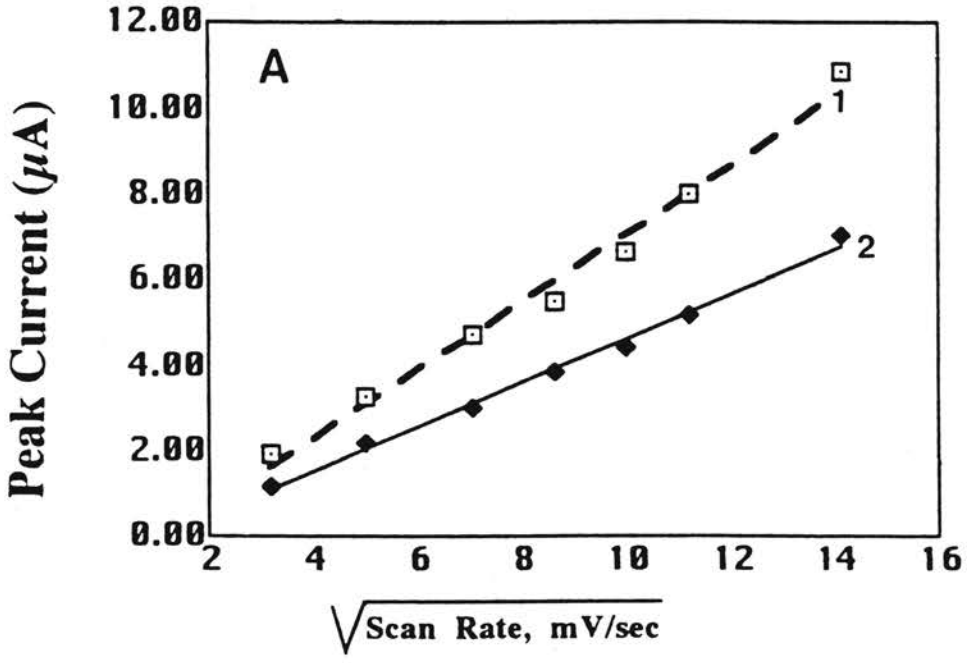

Figure 4.16 A. Plots of peak current vs square root of the scan rate for CuTAPc. In all cases, line 1 refers to the oxidation, and line 2 refers to the reduction. All concentrations are 1.0 x 10^{-3} M in 0.10 M TEAP in DMSO.

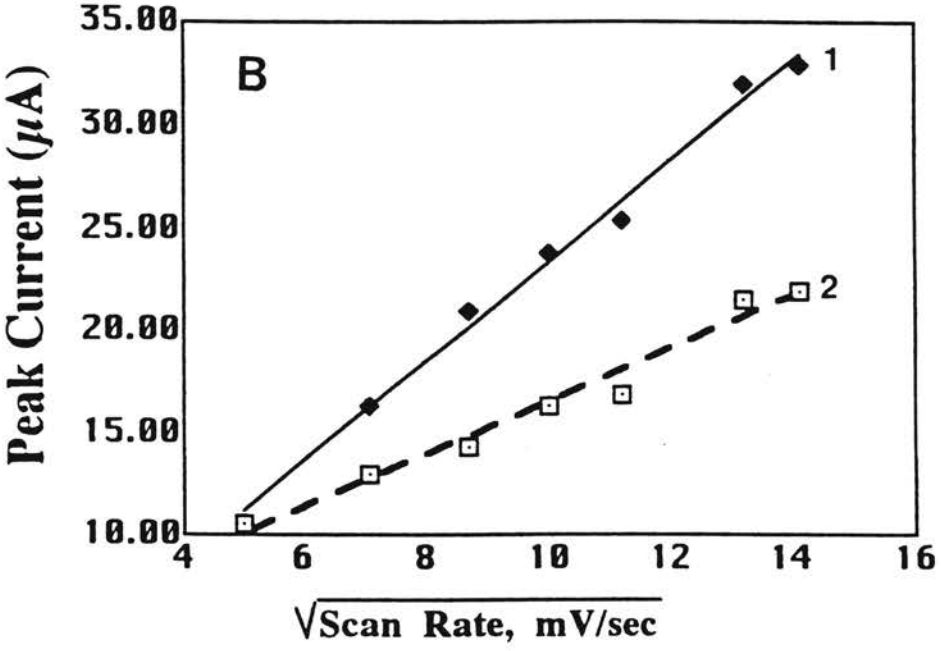

Figure 4.16 B. Plots of peak current vs square root of the scan rate for CoTAPc.

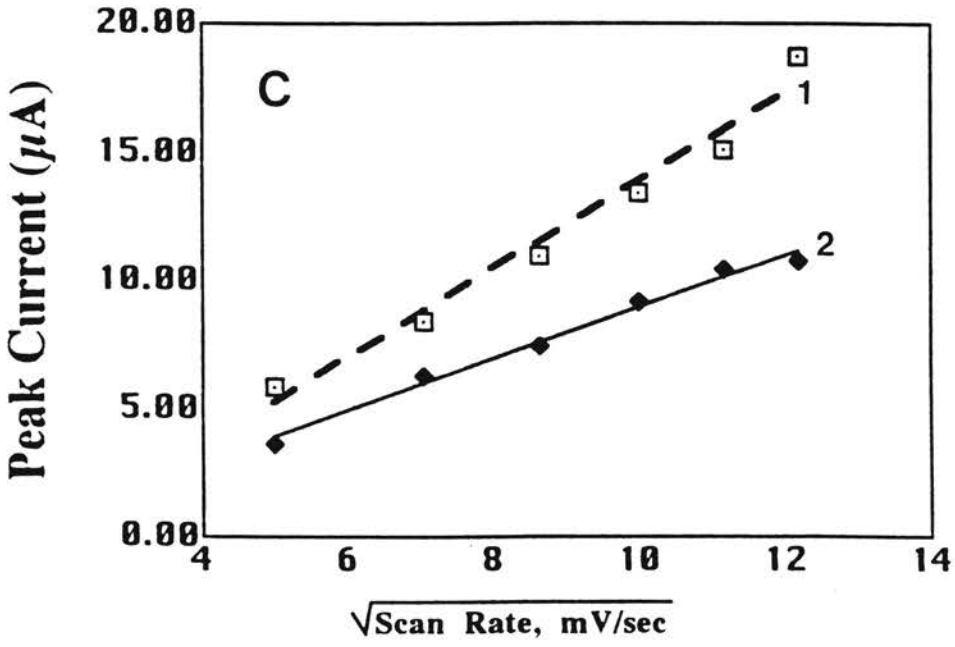

Figure 4.16 C. Plots of peak current vs square root of the scan rate for ZnTAPc.

CHAPTER V

VOLTAMMETRIC, CHRONOCOULOMETRIC, AND SPECTROELECTROCHEMICAL CHARACTERIZATION OF ELECTROPOLYMERIZED THIN FILMS OF COPPER, COBALT, AND ZINC-TETRAAMINOPHTHALOCYANINE

INTRODUCTION

Characterization of thin films is performed to verify that an electrtode surface has been modified. Some specific methods used to characterize thin films include cyclic voltammetry, chronocoulometry [75-84], and spectroelectrochemistry [85-86] (i.e., a combination of spectroscopic and electrochemical methods). A wealth of information can obatined from the above methods. The redox potentials of immobilized species can be ascertained using cyclic voltammetry, and spectroelelectrochemical methods. In addition, the amount of material immobilized on the electrode surface can be determined with the aid of cyclic voltammetry. Chronocoulometry is often used to investigate the charge transfer properties of the immobilized species, and to determine the amount of absorded material on the electrode surface [87].

In spectroelectrochemistry, spectroscopic methods such as UV-vis spectroscopy are combined with electrochemical methods, and have been proven to be extremely versatile in studying the redox chemistry of organometallic compounds. One of the most frequent designs in spectroelectrochemistry uses a thin layer of solution confined next to a transparent electrode. The spectral properties of this layer of solution adjacent to the electrode, is monitored while the potential of the electrode is changed to cause a redox reaction. In other cases, the redox species is immobilized on the electrode surface. Spectral changes such as the shift in wavelength of an absorption band or the apperance of a new band is often the result of a charge transfer process [88]. For example, MLCT

bands can be observed between Soret and Q bands when the charge on the central metal ion increases as a result of its reduction.

In chronocoluometry, the potenial is stepped from a value at which there is no redox reaction to a potential where, for all practical purposes, all of the species on the electrode surface are reduced or oxidized. This provides an avenue to determine ratios the apparent charge-transfer diffusion coefficient for the reduction and oxidation of the redox species of the thin film, the electrode suface area, and the amount of a material immobilized on an electrode surface. In this reaserch, chronocoulometry has been used to evaluate the ratios of the apparent charge-transfer diffusion coefficients .

EXPERIMENTAL SECTION

Instrumentation. The three-electrode system, potentiostat, and UV-vis spectrophotometer described in Chapter 4 was also used in the voltammetric, and chronocoulometric, and spectroelectrochemical characterization of polymeric films of MTAPc. An ITO electrode was used for all spectroelectrochemical measurements. For the spectroelectrochemical measurements, the opening of the 1.0 cm quartz cell was covered with a modified septum to hold the reference and platinum wire auxiliary electrodes in place. The ITO electrode was placed on the internal front side of the cell.

All pH measurements were performed with an Orion Research (Cambridge, MA, USA) model 601A, digital pH-meter, equipped with an epoxy-body combination electrode (Sensorex, Stanton, CA, USA).

Reagents and Solutions. The water used for solution preparations is described in chapter 4. The KOH used for high pH adjustment was obtained from EM Science (Cherry Hill, N.J . , USA). The $KClO_4$ solution, used as supporting electrolyte, was in all cases 0.10 M and the resulting solutions exhibited a pH of 5.75. Potassium salts were

used because of the much smaller alkaline error of the glass electrode towards K^+ rather than Na^+.

Procedure for Cyclic Voltammetric Characterization of CuTAPc Films on Glassy Carbon and ITO Surfaces. The dependence of peak currents on scan rate was studied with films of thckness corresponding to five cycles of electropolymerzation, and measurements were performed in aqueous 0.10 M $NaClO_4$ or 0.10 M TEAP in DMSO. Five cycles of electropolymerization generates a film which is multilayered, covers the electrode surface, and is relatively thin. The third cycle of cyclic voltammetric characterization was chosen for all measurments to ensure that the anodic and cathodic currents and peak potentials remained practically constant. Unless otherwise stated the scan rate used for characterization was 50 $mV \cdot sec^{-1}$. The potential window was +1.000 V to -0.600 V or +1.000 V to -2.000 V.

Procedure for Chronocoulometric Measurements with CuTAPc Films on Glassy Carbon Surfaces. Chronocoulometric measurements were performed to obtain an estimation of the apparent ratio of charge-transfer diffusion coefficients for the oxidation and reduction steps. The initial and final potentials were chosen from the cyclic voltammogram corresponding to the third cycle of characterization. The pulse was initiated from a potential at which the electroactive centers on the film were all-oxidized and terminated at a potential at which they were totally reduced. Table 5.1 gives a summary of the pulse potentials applied after the different number of electropolymerization cycles were completed. The pulse duration amounted to 0.500 s. It is important to note that after each set of data was obtained, the electrode was thoroughly polished to remove the thin film, and a fresh electropolymerized film was deposited. After each thin film was deposited on the electrode surface, the electrode was washed with purified water and allowed to air dry. The supporting electrolyte used was

aqueous 0.10 M $NaClO_4$. The information obtained from chronocoulometric measurements is related to the observations of the electropolymerization of CuTAPc.

Procedure for Voltammetric Characterization of CoTAPc, and ZnTAPc Films on Glassy Carbon and ITO Surfaces. The dependence of peak currents on the scan rate for electropolymerized films was studied using scan rates ranging from 25 $mV \cdot sec^{-1}$ to 200 $mV \cdot sec^{-1}$. A 60 $mV \cdot sec^{-1}$ scan rate was used in studies involving square wave voltammetry. The potential window normally used was +1.000 V to -0.200 V or +1.000 V to -2.000 V for both cyclic voltammetry and square wave voltammetry. This allows the characterization of one redox couple or all three redox couples.

Procedure for Chronocoulometric Measurements with CoTAPc, and ZnTAPc Films on Glassy Carbon Surfaces. Chronocoulometric measurements were performed in order to obtain an estimation of the apparent charge transfer diffusion coefficients. For both CoTAPc, and ZnTAPc, chronocoulometry was performed on thin films corresponding to thicknesses of 10, 20, 30, and 40, and 50 electropolymerization cycles conducted at scan rates of 200 $mV \cdot sec^{-1}$. This gives a range of multilayers on the electrode surface which can be used to ascertain the effects of film thickness on the charge transfer within the films. As with CuTAPc, after each set of chronocoulometric data were obtained the electrode was thoroughly polished. A pulse duration of 0.500 s was utilized. The pulse was initiated from a potential at which the electroactive centers on the film were all-oxidized and terminated at a potential at whch they were totally reduced. Table 5.2 gives a summary of the pulse potentials applied after the different number of electropolymerization cycles completed. These potentials were again selected from the third cycle of characterization using the cyclic voltammograms. All measurements were performed in aqueous 0.10 M $KClO_4$ or in 0.10 M TEAP in DMSO.

Table 5.1 Summary of the Initial and Final Potentials for the Pulses Applied at Different Film Thicknesses of CuTAPc (Proportional to the Number of Electropolymerization Cycles) in Chronocoulometric Studies.

	anodic peak		cathodic peak	
no. of cycles	E_i (V)	E_f (V)	E_i (V)	E_f (V)
5	0.100	0.550	0.700	0.350
10	0.200	0.547	0.750	0.266
15	0.151	0.531	0.700	0.153
20	0.195	0.574	0.700	0.100
25	0.200	0.584	0.700	0.068

The dependence of the peak currents on scan rate was studied with films of thickness corresponding to five cycles of electropolymerization, and measurements were performed in aqueous 0.10 M $NaClO_4$ or 0.10 M TEAP in DMSO. The number of electropolymerization cycles was taken as an indication of the thickness of the polymeric film. Peak currents were measured at the third cycle of the characterization cyclic voltammogram.

Procedure for Spectroelectrochemical Studies of CuTAPc on ITO Surfaces. The modified ITO surface was placed on the internal front side of the 1.0-cm quartz cell containing the supporting electrolyte. For the initial spectroelectrochemical measurements, the applied potentials were +0.700 V, +0.500 V, +0.300 V, +0.100 V, -0.200 V, and -0.400 V, and were held for 5 minutes before the spectrum was obtained. Difference spectra were obtained with respect at these potentials with respect to open circuit conditions.

Procedure for Spectroelectrochemical Studies of CoTAPc, and ZnTAPc on ITO Surfaces. The ITO electrode was modified according to the procedures described in Chapter 4. After 20 cycles were used in depositing the thin film, the ITO electrode was washed with purified water and allowed to air dry. For spectroelectrochemical studies, the applied potentials were +1.000 V, +0.800 V, +0.500 V, +0.000 V, -0.500 V, and -1.000 V. Difference spectra were obtained with respect to the corresponding polymeric film on the ITO in an open circuit.

RESULTS AND DISCUSSIONS

Cyclic Voltammetric Characterization of Electropolymerized CuTAPc Flims on Glassy Carbon Surfaces. Examination of the glassy carbon surfaces after

electropolymerization revealed a dark purple color. Thin films (few cycles of electropolymerization) required the aid of an optical microscope for observation of the deposited film. However, films on electrodes with a large number of deposited layers (high number of electropolymerization cycles) can be directly observed without microscopic help. After a given number of electropolymerization cycles wereperformed, the modified surface was thoroughly washed with purified water and then immersed in an aqueous solution of 0.10 M $NaClO_4$ or 0.10 M TEAP in DMSO, and the corresponding CV was recorded. Figure 5.1 shows CVs obtained after 5, 15, and 25 cycles of electropolymerization cycles. Shown in equation 5.1 is the redox couple of Cu^{2+}/Cu^{+} involved in the charge transfer process

$$[Cu^{2+}, Pc^{2-}] + e^{-} \underset{2}{\overset{1}{\rightleftharpoons}} [Cu^{1+}, Pc^{2-}]^{-}Na^{+} \quad (5.1)$$

The thin-layer electrochemistry illustrated in these, and in other typical voltammograms obtained at different film thicknesses, indicates sluggish charge transfer, since after five cycles of electropolymerization there is a separation between the cathodic and anodic peaks of about 100 mV. This separation, illustrated in Figure 5.2, increases with increasing film thickness (e.g., about 150 mV after 10 cycles, 230 mV after 15 cycles, and 350 mV after 25 cycles). The system becomes more quasireversible toward with the overpotential contribution affecting the reduction process more than the oxidation process (the E_{pa} remains practically constant at +0.500 V). A plot of ΔE_p as a function of film thickness (represented by the number of cycles of electropolymerization) given in Figure 5.2. The plot is linear with a correlation of 0.997. All these considerations are valid for scan rates of 50 $mV \cdot sec^{-1}$. Decreasing the scan rate when obtaining the cyclic voltammogram for electrodes bearing these thin films shows a decrease in the value of ΔE_p. Peak separations of about 70 mV at scan rates of 20-30 $mV \cdot sec^{-1}$ are decreased to about 13 mV at scan rates of 10 $mV \cdot sec^{-1}$. Peak separation approaches the expected ideal behavior ($\Delta E_p = 0$ mV) as more time is allowed for the charge-transfer process to

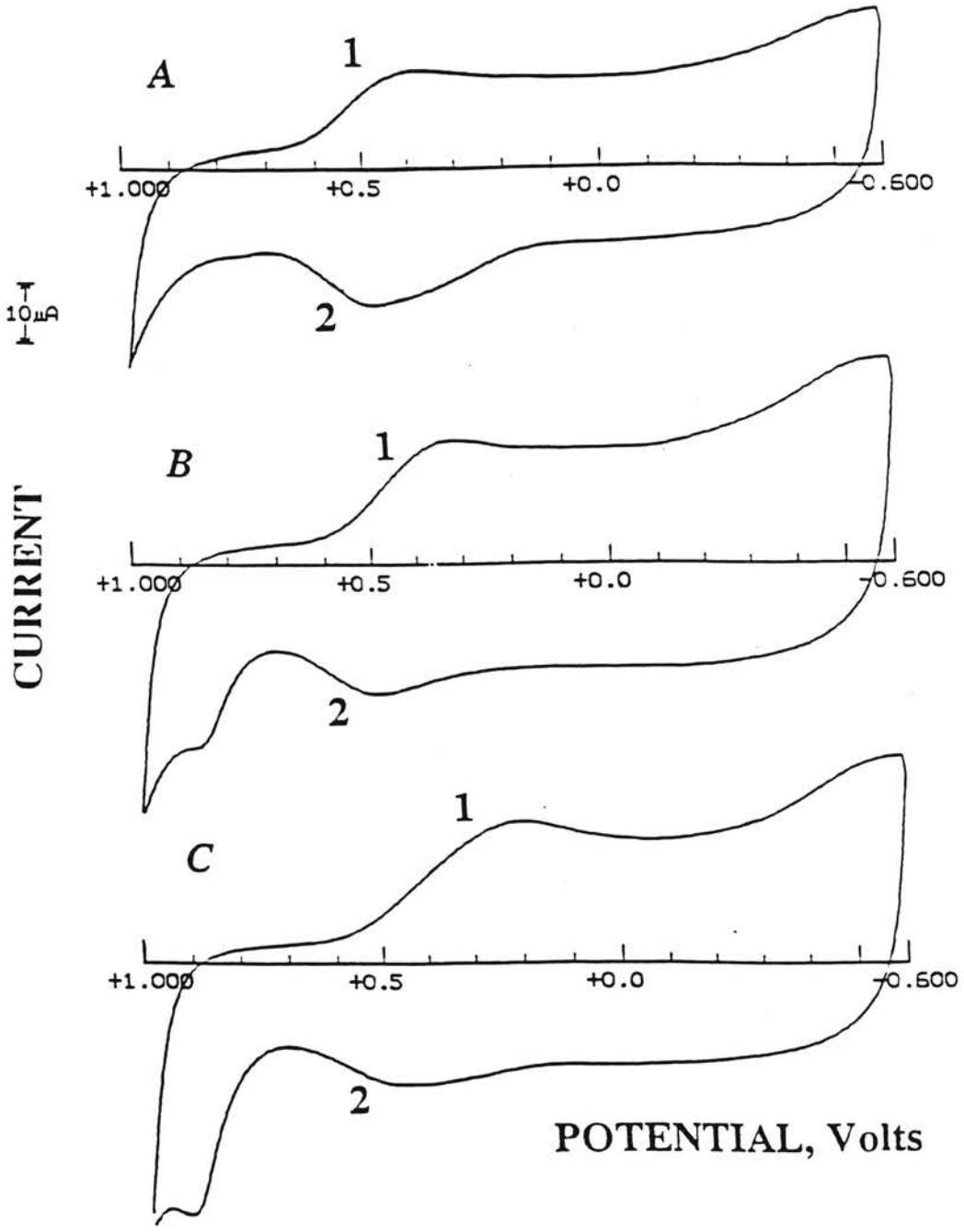

Figure 5.1. Cyclic voltammograms of glassy carbon electrodes modified with CuTAPc films of different thicknesses: scan rate, 50 mV·sec-1; supporting electrolyte, 0.10 M aqueous $NaClO_4$. Cycles of electropolymerization: (A) 5; (B) 10; (C) 15. Numbers for the peaks correspond to the assignment given in previous figures.

take place when the scan rate is lower than 10 $mV \cdot sec^{-1}$. Further evidence that the films do exhibit thin-layer electrochemistry is given by the fact that both anodic and cathodic peak currents give better linear plots as a function of scan rate [89] than with the square root of the scan rate (Figure 5.4). Correlation coefficients for the square root plots were in the 0.899-0.913 range, while those for the scan rate plots were typically equal to 0.978-0.983. A ΔE_p= 0 mV was observed with IR compensation (the resistance measured at +0.850 V or at -0.400 V was used to compensate for the IR drop in the whole potential window used). Uncompensated IR drop results in a loss of potential control [90-91]. The result is that the applied potential is not the potential experienced at the working electrode. Resistance in films may be due to low ion population or low ion mobility [92]. The rate of charge-transfer is a combined process of electron "hopping" between redox sites, solvent motion, and counterion movement [92]. This process is driven by the electrochemical potential. The charge transport process within the film affects the peak potenial. If the charge transfer is slow, on the time scale of the experiment, the peak separation will be greater than 0 mV [92]. The charge transfer is not in Nerstian equilibrium with the applied potential. The peak currents were measured using Nicholson's proposition [74]. It should be mentioned that IR compensation during electropolymerization runs does not alter the general trends discussed above under peak assignments and general electrochemical characterization of the thin films. Plots of anodic peak current (I_{pa}) versus scan rate in Figure 5.3 show a larger current /scan rate ratio than similar plots for cathodic peak current (I_{pc}); this points to a more facilitated oxidation than reduction. If the voltammetric characterization is performed in 0.10 M TEAP in DMSO, the oxidation (peak 2) shifts to more positive potentials (an increase in quasireversible-to-irreversible behavior) than when aqueous $NaClO_4$ is used as supporting electrolyte solution. The Na^+ cation is shown in the reaction 5.1 because charge electroneutrality must be maintained in the film throughout the redox process [94]. Since the reduced polymeric unit has a charge of -1 it is compensated by the counterion,

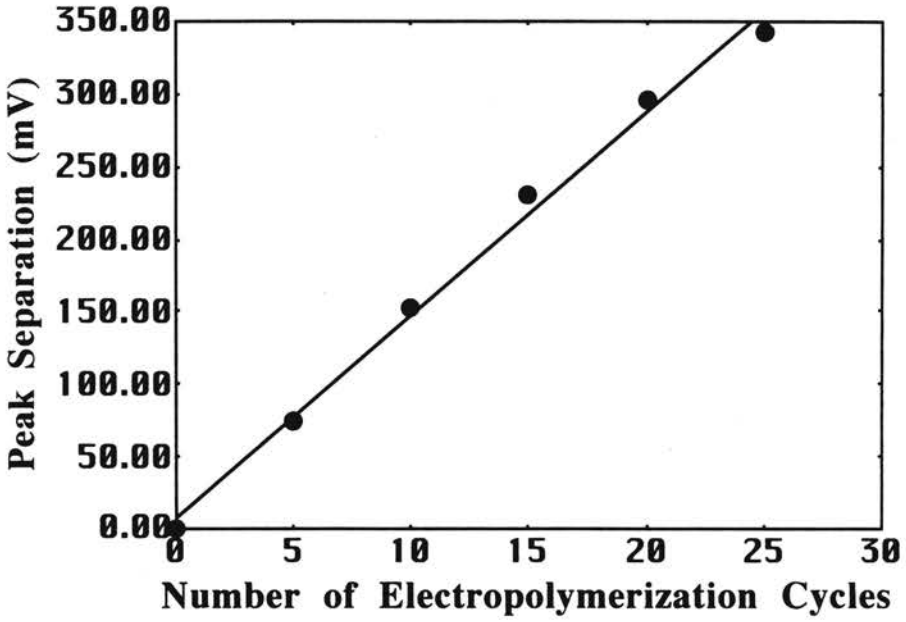

Figure 5.2. Plot of peak separation versus the number of electropolymerization cycles of CuTAPc. Electropolymerization cycles is taken as an indication of film thickness.

Na^+. The result is a polymeric unit with a net charge of zero. The hydration of the counterion, and its entry into the film may cause some film swelling to occur and thus form interstitial pockets [95]. The interstitial solvent pockets, randomly distributed within the polymeric network, increase in number with surface coverage. These pockets contain solvent alone when the films are totally oxidized because the net charge on the polymer is zero [e.g., the predominant unit is (Cu^{2+}, Pc^{2-})]. When the predominant unit is $[Cu^+, Pc^{2-}]^-$, the negative charge on the polymeric unit needs to be compensated by cations entering from the supporting electrolyte solution. These cations are released back to the solution when the applied potential is such that $Cu^+ + e^- \text{------} > Cu^{2+}$. At high surface coverage (i.e., many cycles of electropolymerization), the charge mobility should be facilitated by the cations incorporated into the solvent pockets, and at low surface coverage such incorporation may have little, if any, significance on charge mobility.

The foregoing discussion seems to agree with several observations. At low surface coverage the oxidation and reduction processes for the central metal ion seem to pose comparable energy barriers. This is seen in the fact that there is little shift in peak 1 (peak 3 is not evident during the first several cycles). The peak separation between peaks 1 and 2 is quite close to 59 mV. As surface coverage increases, the reduction step becomes more and more sluggish, and this is seen by the increasing overpotential for the reduction (shift to more negative potentials: e.g., peak 1-----> peak 3). As the overpotenial increases, the oxidation process dominates, and the process evolves from reversible to quasireversible. The peak separation is much greater than 59 mV. There is no shift in the peak potential corresponding to $Cu^+ \text{-----} > Cu^{2+}$ (in this case, probably the ionic content in the solvent pockets helps in facilitating charge transfer). As the film thickness increases, it is more difficult to realize the reduction of the central metal ion. This is seen in the evolution of peak 3; the solvent pockets in going from Cu^{2+} to Cu^+ are devoid of cationic charges, and there is no extra contribution to charge transfer. The uncompensated resistance of films with predominantly Cu^+ centers remains practically

constant with increasing thickness; meanwhile, for films with predominantly Cu^{2+} centers, it increases with increasing film thickness since the net charge on the polymeric unit is zero. The charge, ion mobility, and ion size should all be considered in reducing film or solution resistance.

Chronocoulometry: Charge-Transfer Diffusion Rates in CuTAPc Films Deposited on Glassy Carbon Surfaces. Chronocoulometry used in conjunction with the integrated form of the Cottrell equation permits an estimate of the ratio of charge transfer diffusion coefficients, and should allow to confirm that thick, totally oxidized films permit charge movement across the film faster than totally reduced films. Figure 5.4 (A-D) shows the result of stepping the potential so that all species on the electrode surface are reduced. In all cases, the current varies with $\mathbf{t^{-1/2}}$ shown by equation 5.2 (corresponding to Figure 5.4 B),

$$i= [nFA(D_{ct}^{1/2})C]\pi^{1/2}t^{-1/2} \qquad (5.2)$$

Integration of equation 5.2 with respect to time gives equation 5.3, and shows that the total charge, $\mathbf{Q_c}$ is proportional to $\mathbf{t^{1/2}}$,

$$Q_c= [2nFA(D_{ct})^{1/2}C]\pi^{1/2}t^{1/2} \qquad (5.3)$$

This is the integrated charge over the time interval (Figure 5.4 C) when the material on the electrode surface becomes all-reduced or all-oxidized. Linear plots of $\mathbf{Q_c}$ (charge) versus the square root of time (Figure 5.4 D) should have slopes equal to $[2nFA(D_{ct})^{1/2}C]\pi^{1/2}$, and the ratio of slopes obtained for the oxidation and reduction steps of the same film, assuming that the concentration **C** is the same for an all-oxidized

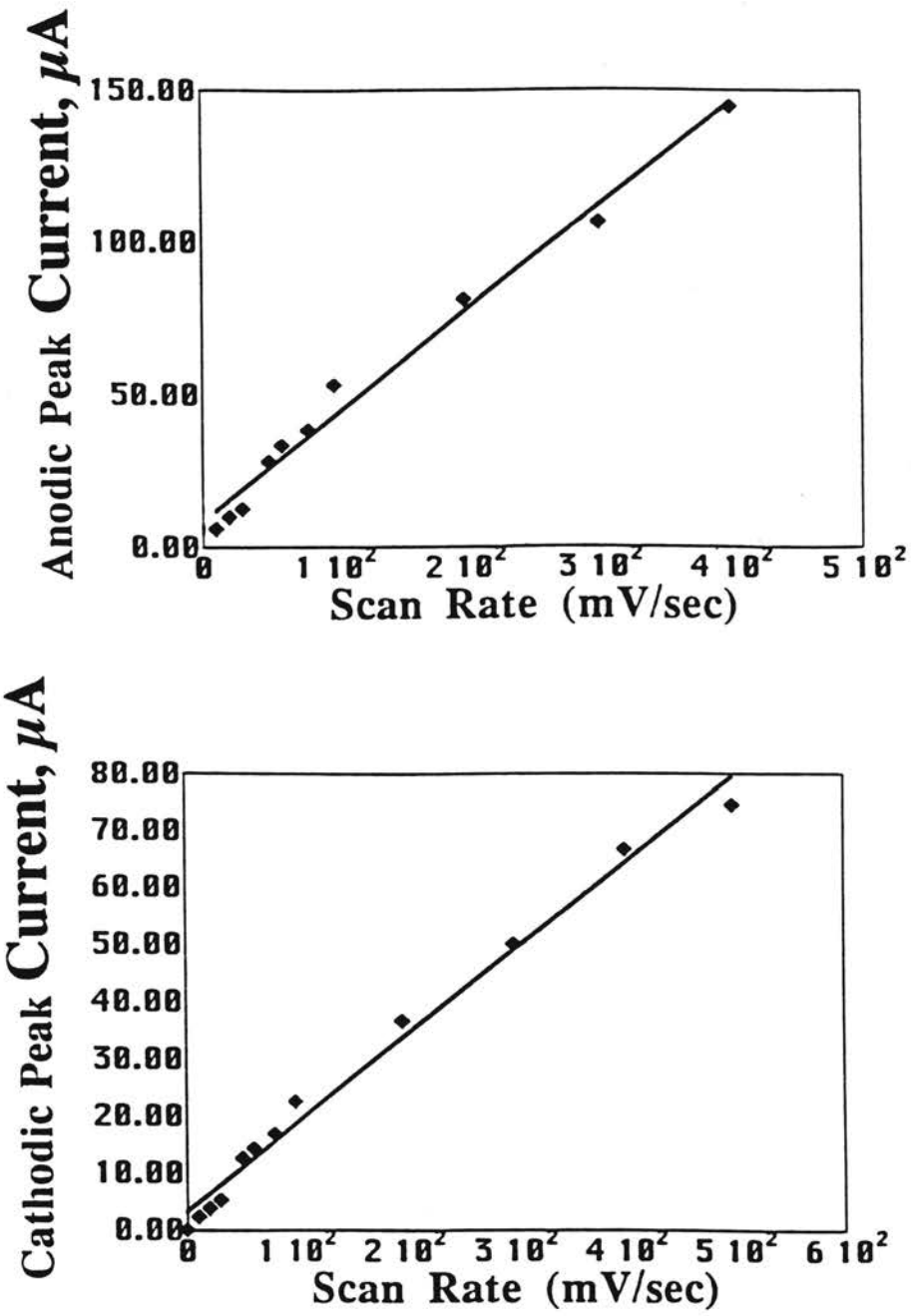

Figure 5.4. Plot of peak current versus scan rate. Thin film of CuTAPc immersed in 0.10 M $NaClO_4$. Scan rate ranges from 10 to 600 $mV \cdot sec^{-1}$. Thickness of film corresponds to 5 cycles of electropolymerization; (A) anodic peak current versus scan rate, (B) cathodic peak current versus scan rate.

and for an all-reduced film (the number of redox center does not change in the film), should give an estimate of $(\mathbf{D_{ct}})^{1/2}_{oxidation}/ (\mathbf{D_{ct}})^{1/2}_{reduction}$. The value of $\mathbf{D_{ct}}$ is the value of an apparent charge-transfer diffusion coefficient. Plots of these ratios, shown in Figure 5.5, as a function of film thickness (number of electropolymerization cycles), were all linear (correlation coefficients: 0.992-0.990), and if the number of cycles was below 10, reduction appears to be faster than oxidation. Films obtained with 10 or so electropolymerization cycles show ratios close to 1, but as the thicknes of the film increases, the fully oxidized films have larger $\mathbf{D_{ct}}$ than fully reduced ones. These observations are in agreeement with the evolution of cyclic voltammograms observed both during electropolymerization and during electrochemical characterization of films in solutions with supporting electrolyte only. For example, during electropolymerization, the cathodic peak shifts to more negative potentials as the film thickness increases; the anodic peak, on the other hand, practically does not change position, or its shift is at most modest.

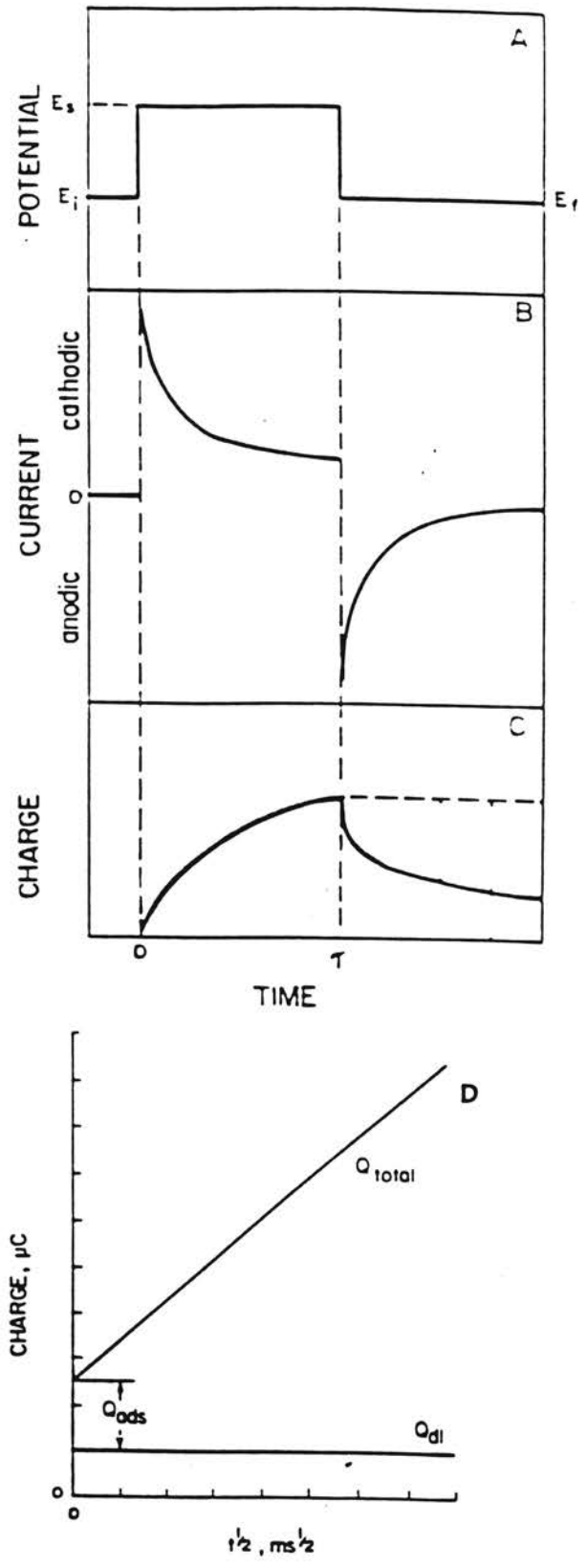

Figure 5.4. (A) Potential step from E_i to E_f; corresponding (B) current versus time profile, (C) charge versus time and (D) charge versus (time)$^{1/2}$ profiles.

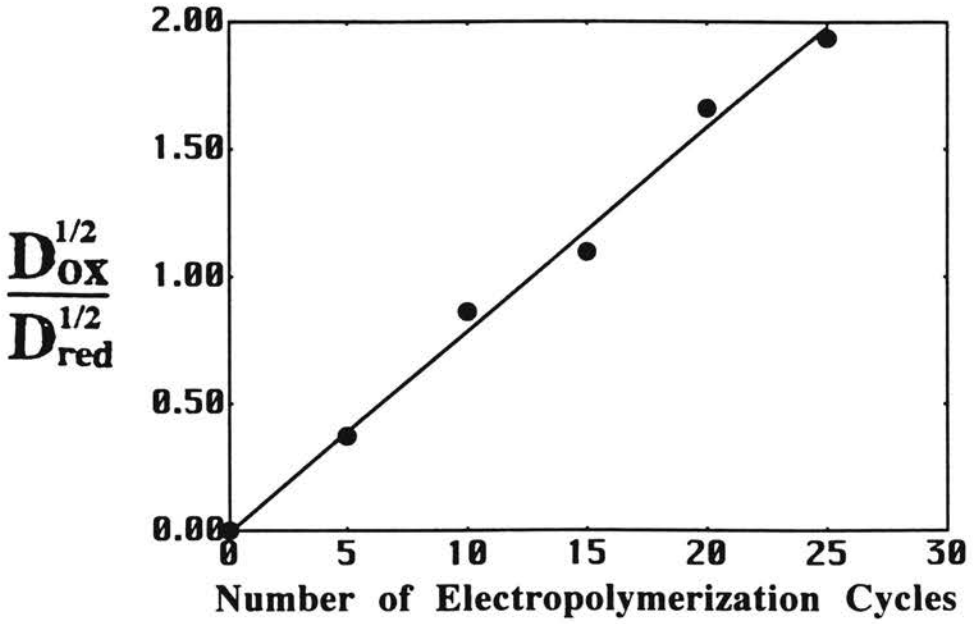

Figure 5.6. Plot of $(D_{ct})^{1/2}_{oxidation}/(D_{ct})^{1/2}_{reduction}$ versus number of electropolymerization cycles for CuTAPc.

Surface Coverage: Relationship between Monolayers of CuTAPc Deposited on Glassy Carbon Surfaces and Electropolymerization Cycles. The larger the number of electropolymerization cycles, the thicker the film. An approximate idea of the number of monolayers accumulated per cycle can be obtained by calculation of the surface coverage ($\Gamma = Q_c/nFA$, where n is the number of electrons transferred per molecule, F is the Faraday constant, A is the electrode area in cm^2, and Q_c is the charge (proportional to the area under the reduction or oxidation peak in the cyclic voltammogram for characterizing the films) and is evaluated by the cut and weigh technique [96]. The value of A was estimated to be 0.0706 ± 0.0004 cm^2 after measuring the diameter of the electrode with the help of the Stero Star Zoom microscope and a ruler with an uncertainty of ±0.02 cm. The apparent number of monoloayers can be calculated assuming a prism-like model for the metal-phthalocyanine complex molecule. From X-ray diffraction data the area for the base of the prism (considered to be a rectangle of 15.21 Å x 15.40 Å) was estimated as 2.34×10^{-14} cm^2 [97]. The height of the molecule was taken as the diameter of the central metal atom, Cu, which is equal to 2.6 Å [98]. On the basis of this model, the typical monolayer coverage corresponds to 7.08×10^{-11} $mol \cdot cm^2$, and the concentration of material after five cycles of electropolymerization was found to be 5.78×10^{-5} $mol \cdot cm^{-3}$. Via integration, the amount of material on the electrode surface can be estimated after a given number of cycles. Dividing this by the typical monolayer coverage gives an estimate of the accumulated number of layers.

Some difficulties were experienced in the calculation of Q_c because, depending on the scan rate, the anodic and/or cathodic peak became difficult to distinguish after a given number of cycles. Considering the uncertainties associated with the model and assumptions made, as well as in the measurement of Q_c, after 5 cycles of electropolymerization, the number of accumulated monolayers is 110 ± 40, after 10 cycles it is 134 ± 45, and after 15 cycles it is 164 ± 60. Above 15 cycles of electropolymerization, estimation of Q_c for the cathodic peak was difficult to ascertain.

The Appendix gives more information concerning the estimation of the accumulated number of layers.

Spectroelectrochemical Studies of Electropolymerized CuTAPc on ITO Surfaces. The spectrum in Figure 5.6B of the thin polymeric film shows two peaks: one intense peak near 300 nm and a small, broad peak near 740 nm. The peak at 384 nm of Figure 3.3A appears as a small broad shoulder in Figure 5.6B. The absence of bands near 200 nm in Figure 5.6B is because the glass substrate is not transparent in the UV region (Figure 5.6A). The large peak centered at 300 nm results from having a highly conjugated system. The broadness of the peak at 740 nm may be due to the polymeric film exhibiting more resonance and electron density surrounding the central metal atom in comparison to the monomeric unit. Worth mentioning is the fact that this broad peak is symmetrically positioned at the same wavelength as the two peak centered at 740 nm in Figure 3.3A . This may again be attributed to the high conjugation in the polymeric film. The comparatively lower intensity of the peak may be the result of "optical paralysis" [57]. As the polymeric thin film increases in thickness and length, it is likely that not all chromophores responsible for the absorption band are simultaneously excited. Other metallophthalocyanines exhibit similar behavior. Figure 5.7 shows difference spectra at 0.700, 0.500, 0.300, 0.100, -0.200, and -0.400 V obtained wtih respect to a thin film of the polymer on ITO in an open circuit. As the applied potential becomes more negative, the Soret band near 360 nm increases and undergoes a slight red shift. On the other hand, the Q band undergoes a slight blue shift. This suggest that the ground levels of the CuTAPc complex are both affected, but in opposite directions, since each has a common excited state [97]. The MLCT band between the Soret band and the Q band (about 500 nm) shows no split; this suggests that the central metal-ion ligand units in the polymer framework are energetically equivalent and that the band corresponds to transistions from the same energy level. Similar films involving cobalt as the central metal atom were

observed to show a split of the MLCT band between 500 and 600 nm [97]. This was interpreted as involving two transistions from different energy levels in more than one kind of metal ion or ligand [97]. The decrease in absorbance with increasing negative potential suggest an increasingly more difficult reduction, and this is in accordance with the increase in overpotential as peak 1 evolves to peak 3. Difference spectra at potentials more negative than 0.300 V are flat baselines (with respect to the specturm at 0.300 V) but different from those at potentials more positive than 0.300 V. This suggests that a different oxidation state predominates at the potentials above and below 0.300 V.

CoTAPc Films on Glassy Carbon: Cyclic Voltammetric Characterization.

Glassy carbon surfaces covered with films of CoTAPc take on a blue color, particularly dark when the film is thick. When these surfaces are used as working electrodes, and immersed in solutions of supporting electrolyte, characterization via cyclic voltammetry yields similar information collected during electropolymerization. The same redox couples illustrated in Fig. 4.9 are observed, but values for the $E^{o'}$ are slightly changed. For peaks 8/9, $E^{o'}$ is +0.368 V, for peaks 10/11 $E^{o'}$ is -0.459 V, and for peaks 12/13, $E^{o'}$ is -1.541 V. The anodic peak due to the $-NH_2$ oxidation, seen during the first cycles of electropolymerization, could be seen in characterization runs of relatively thicker films, indicating that some $-NH_2$ groups where left unreacted during electropolymerization. The peak potential for this anodic process was close to +0.700 V. In all cases, the peaks are broad and the peak width at half hight is greater than the theoretical value of 90.6 mV [100] for a one electron exchange. This is probably due to repulsive or attractive forces within the film as well as nonequivalent redox centers [100]. At higher scan rates the peaks are more asymmetrical and peak separation increases with peak thickness since, as expected, the charge transfer process becomes increasingly sluggish.

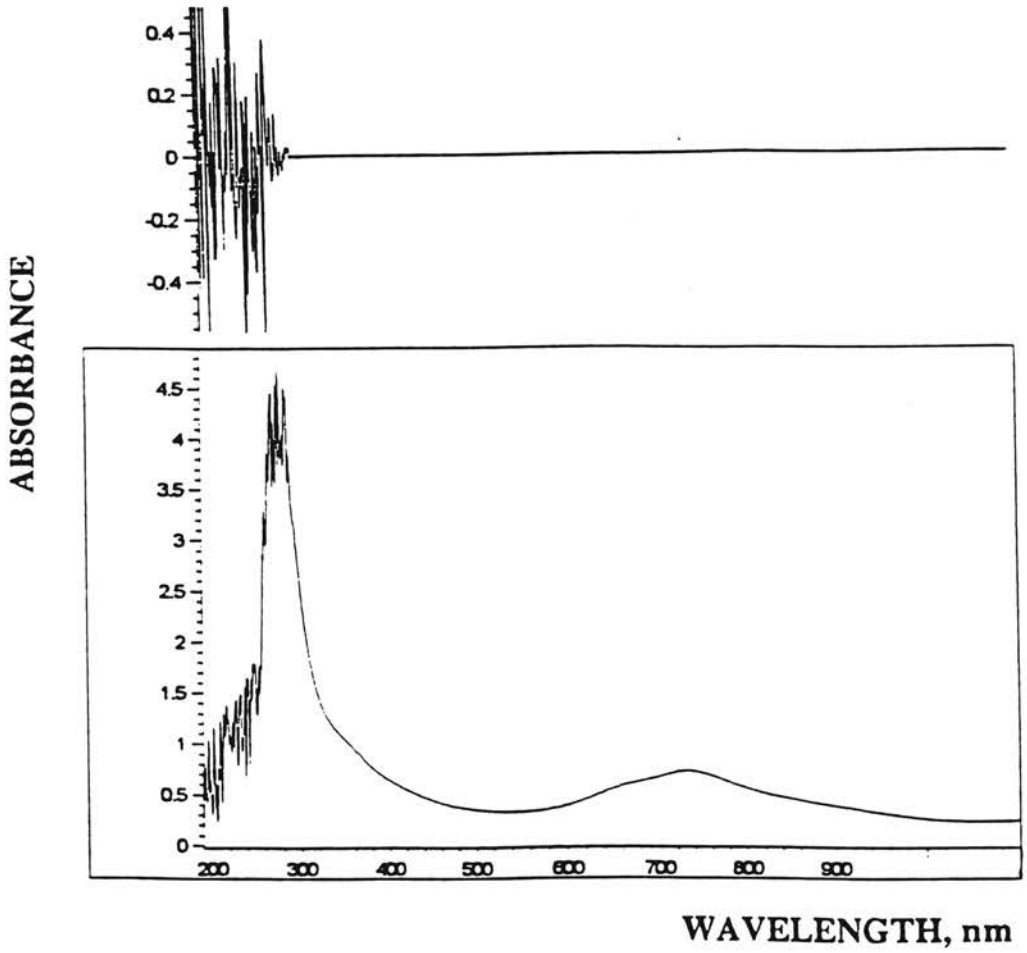

Figure 5.6. (A) An ITO blank electrode immersed in DMSO containing 0.10 M TEAP, and (B) an ITO electrode covered with a thin film of electropolymerized CuTAPc.

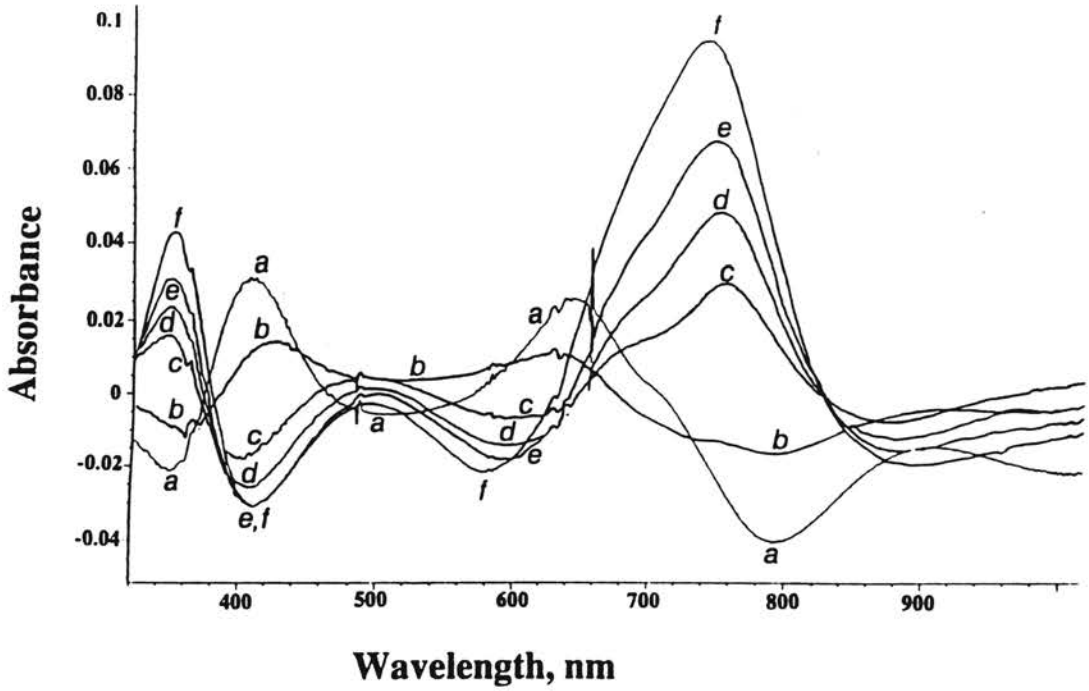

Figure 5.7. Absorbance spectra recorded at different applied potentials for a thin film of electropolymerized CuTAPc immersed in a solution of 0.10 M TEAP in DMSO. Applied potentials are: (a) 0.700 V; (b) 0.500 V; (c) 0.300 V; (d) 0.100 V; (e) -0.200 V; and, (f) -0.400 V. These are difference spectra with respect to the spectrum at open circuit.

When using the short potential window (+1.000 to -0.200 V) the only process observed corresponds to peaks 8 and 9. The oxidation process yields a film with a predominantly positively charged surfaces and ClO_4^- plays the role of the counterion to satisfy electroneutrality. On the other hand, a totally reduced film should have no net charge on its surface and no counterions are needed in its vicinity. The slopes of the plots of peak current as a function of scan rate indicate a more facilitated oxidation process than reduction process. Such plots show a linear relationship (thin-layer electrochemistry) with regression coefficients of 0.990-0.989 and slopes of 0.0219 μA·s/mV for the oxidation process and 0.0125 μA·s/mV for the reduction process. Peak separation increases linearly with scan rate until 0.800 $V \cdot s^{-1}$ after which a constant ΔE_p of 174 mV was observed. When the thickness of the film is increased, the peak separation also increased. For example, with 15, 20, and 25 cycles of electropolymerization the peak separations are 64 mV, 100 mV, and 108 mV, respectively (Figure 5.9 A-C). As the film thickness increases, the formal redox potential becomes less positive. These values correspond to scan rates of 50 $mV \cdot sec^{-1}$ with thin films in 0.10 M TEAP in DMSO. Similar trends are observed when the supporting electrolyte is 0.10 M $NaClO_4$ in purified water.

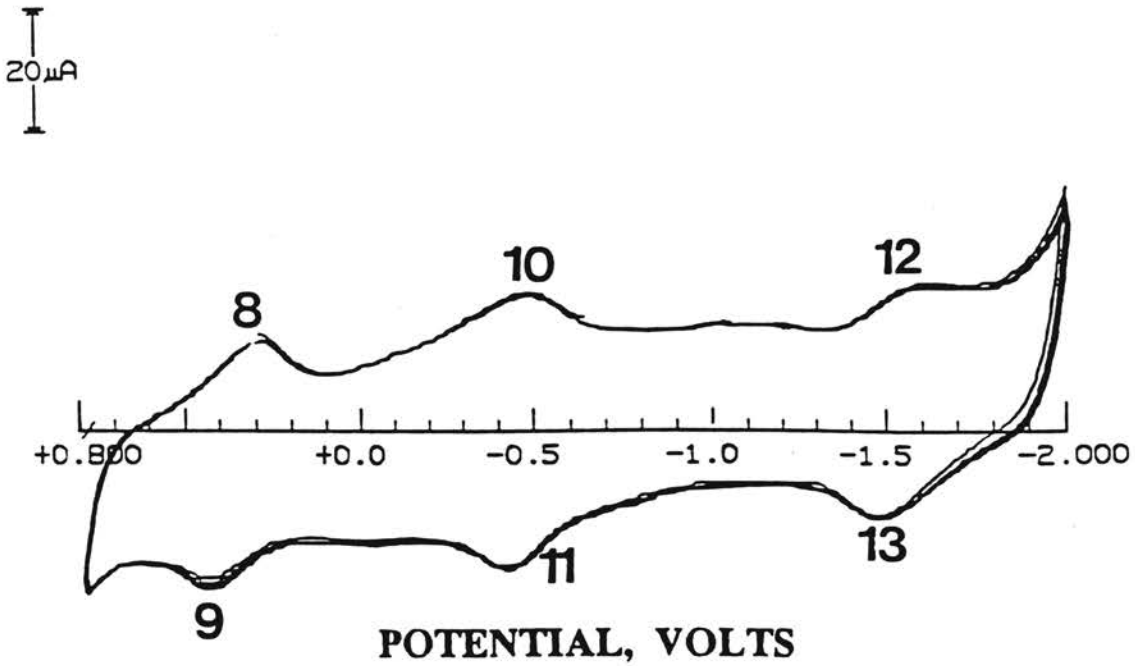

Figure 5.8. Cyclic voltammetric characterizaiton of electropolymerized CoTAPc on glassy carbon. Thickness corresponds to 12 cycles of electropolymerization; scan rate for characterization is 200 mV·sec^{-1}. Supporting electrolyte: 0.10 M TEAP in DMSO.

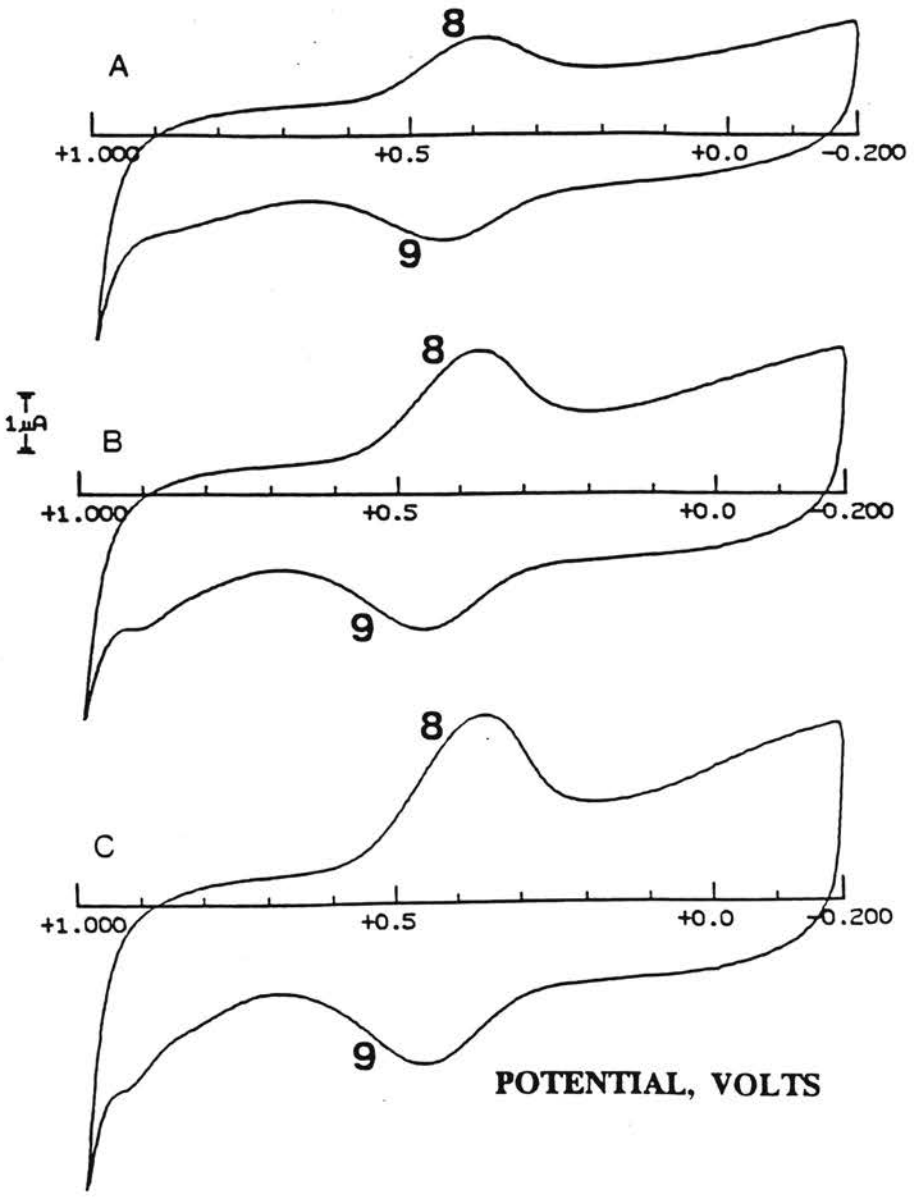

Figure 5.9. Cyclic voltammograms for glassy carbon electrodes modified with CoTAPC films of different thicknesses: scan rate, 50 $mV \cdot sec^{-1}$; supporting electrolyte, 0.10 M TEAP in DMSO. Cycles of electropolymerization: (A) 15; (B) 20; (C) 25. Numbering for the peaks correspond to the assignment in Figure 4.9.

ZnTAPc Films on Glassy Carbon: Cyclic Voltammetric Characterization. As with CoTAPc, glassy carbon surfaces covered with films of ZnTAPc take on a blue color. The characterization cyclic voltammograms with the +1.000 V to -2.000 V potential window (Figure 5.10), however, are not as distinctive as those obtained with CoTAPc films. The peaks are much broader and difficult to distinguish. On the other hand, the shorter potential window of +1.000 V to -0.200 V in Figure 5.11 clearly shows the peaks identified as 14 and 15 in Figure 4.12. As the thickness of the film increases (obtained via increasing cycles of electropolymerization), the ΔEp slightly increases since charge transfer becomes slower.

CoTAPc and ZnTAPc Films on ITO Surfaces: Cyclic Voltammetric Characterization. The cyclic voltammetric characterization of electropolymerized films on ITO surfaces paralleled the observations mentioned above for films on glassy carbon surfaces.

CoTAPc and ZnTAPc Films on Glassy Carbon Surfaces: Chronocoulometric Measurements. The value of D_{ct} is the value of an apparent charge transfer diffusion coefficient, and chronocoulometric measurements gave values of $[(D_{ct})^{1/2}]_{oxidation}/[(D_{ct})^{1/2}]_{reduction}$, for the redox process involving the Co(III)/Co(II) couple, ranging between 1.40 to 1.01 (Table 5.2). In thin films of CuTAPc, the charge transfer for oxidation is favored, but as the thickness of the film increases, the rate of charge transfer for oxidation and reduction become comparable since the ratio of the corresponding D_{ct} values approaches 1 and remains at this value even with films thicker than that corresponding to 25 cycles of electropolymerization. This would seem to indicate that although the film thickness increases, the distance between the cobalt redox centers does not change much and such redox centers are in very close proximity of each other. This trend is the opposite of what was observed for

the CuTAPc complex. As can be seen in Table 5.3, reduction is faster in thinner films, but as film thickness increase the rate of oxidation increases and at relatively thicker films oxidation is faster than reduction.

In films of electropolymerized ZnTAPc, the central metal ion does not undergo any redox process; all redox couples observed involve the organic moiety. If the process involving the Pc^{2-}/Pc^{3-} couple is considered, the ratio of the rates of charge transfer for oxidation and reduction remains, for all practical purposes, constant with $[(D_{ct})^{1/2}]_{oxidation}/[(D\ ct)^{1/2}]_{reduction}$ =2.27 ± 0.19, and with oxidation exhibiting a rate of charge transfer about twice the same rate for reduction. Interestingly, for the redox couple involving Pc^{2-}/Pc^{3-} in the complex with Co^{+} as metal central ion, the same ratio is also fairly constant (1.07 ± 0.18). Oxidation, however, is more facilitated in the ZnTAPc than in the CuTAPc or CoTAPc complexes.

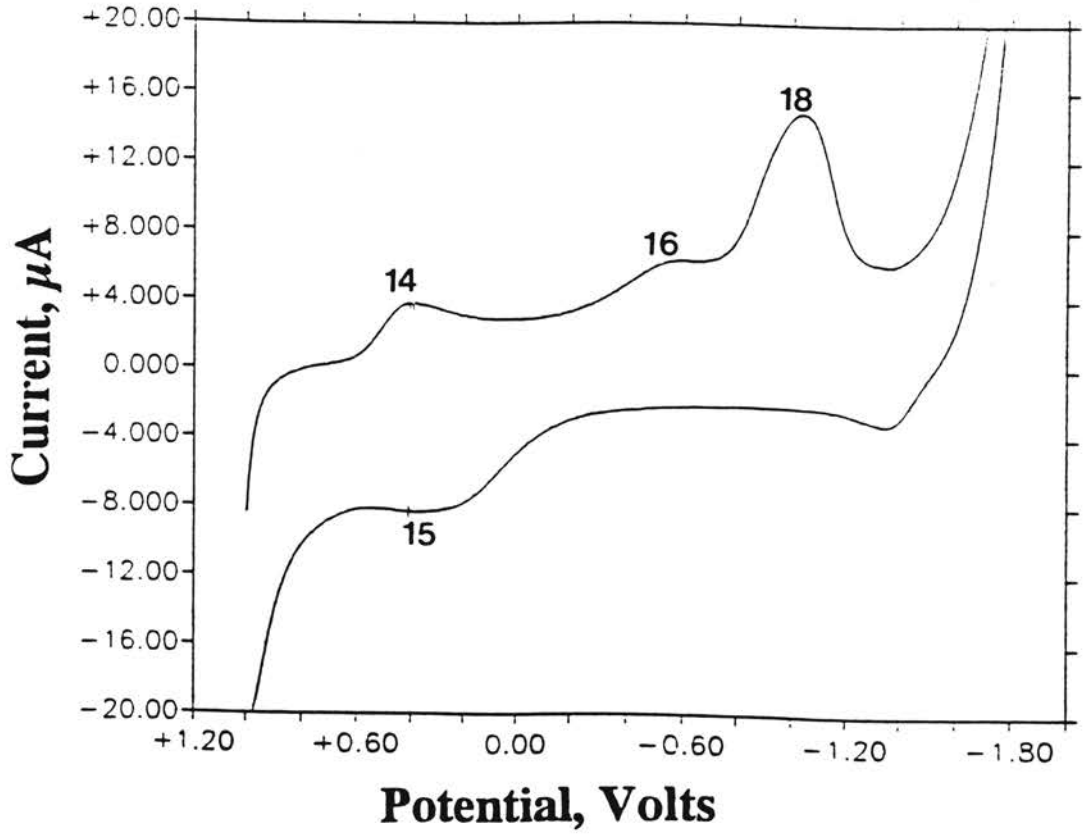

Figure 5.10. Cyclic voltammogram of ZnTAPc film on glassy carbon electrode in aqueous 0.10 M KClO4. Scan rate, 50 mV·sec^{-1}. Potential window, +1.000 to -2.000 V.

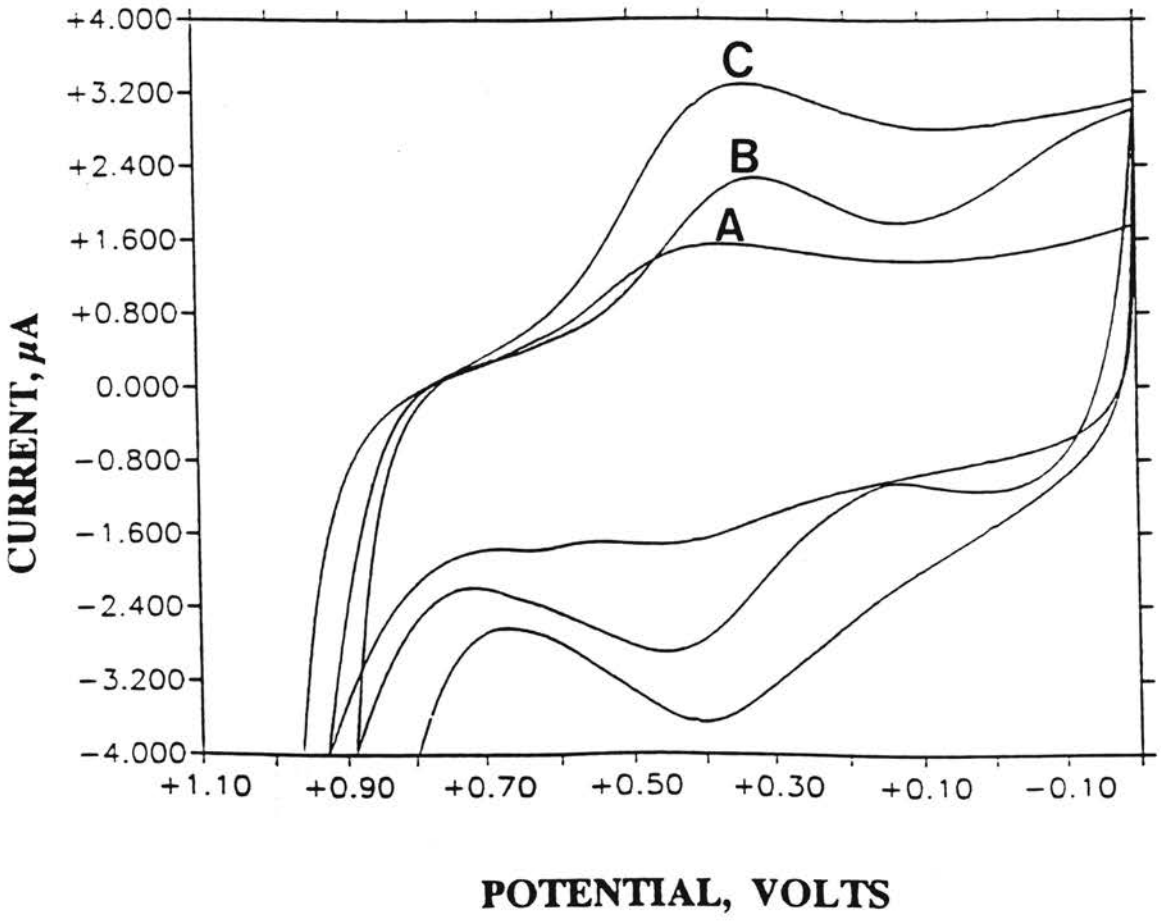

Figure 5.11. Cyclic voltammogram of ZnTAPc film on glassy carbon electrode immersed in aqueous 0.10 M KClO4. Scan rate, 50 mV·sec^{-1}. Potential window, +1.000 to -0.200 V. Cycles of electropolymerization: (A) 5, (B) 10, and (C) 15.

Table 5.2. Summary of the initial and final potentials for the pulses applied at different film thicknesses (proportional to the number of electropolymerization cycles) in chronocoulometric studies. Data for the [Cu(II/I)]TAPc system are given in reference [4].

	[Co(III/II)]TAPc	
Number of cycles	Cathodic Peak	
	E_i(V)	E_f(V)
5	0.700	0.350
10	0.700	0.310
15	0.750	0.325
20	0.750	0.325
25	0.700	0.300
	ZnTAPc	
5	0.700	0.350
10	0.700	0.300
15	0.700	0.300
20	0.650	0.250
25	0.700	0.250
	[Co(II/I)]TAPc	
5	-0.594	-0.732
10	-0.575	-0.725
15	-0.533	-0.760
20	-0.500	-0.750
25	-0.500	-0.800
	[Co(I)]TAPc	
5	-1.319	-1.475
10	-1.295	-1.517
15	-1.349	-1.450
20	-1.250	-1.450

E_i: initial potential; E_f: final potential

TABLE 5.3. Summary of $[(D_{ct})^{1/2}]_{oxidation}/[(D_{ct})^{1/2}]_{reduction}$ ratios for the (Co^{3+}/Co^{2+})TAPc and the $[Zn^{2+}, Pc^{2-}]/[Zn^{2+}, Pc^{3-}]^-$ redox couples.

Number of electro-polymerization cycles[a]	[Co(III/II)]TAPc[a]	ZnTAPc[c]	[Cu(II/I)]TAPc[b]
5	1.40	2.36	0.37
10	1.23	2.38	0.86
15	1.10	2.45	1.01
20	1.12	2.00	1.66
25	1.01	2.15	1.94

	[Co(II/I)]TAPc[b]	[Co(I)]TAPc[c]
5	0.23	1.01
10	0.21	0.85
15	0.37	1.28
20	0.45	1.14
25	0.36	

[a] increasing number of cycles implies thicker films.

[b] the redox process involves only the metal center.

[c] the redox process involves the couple Pc^{2-}/Pc^{3-}.

Surface Coverage: Relationship between Monolayers of CoTAPc, and ZnTAPc Deposited on Glassy Carbon Surfaces and the Number of Electropolymerization Cycles. An approximate idea of the number of monolayers accumulated per cycle can be obtained as described for the copper complexes. This calculation assumes a prism-like model for the metal-phthalocyanine complex with a height limited by the diameter of the central metal atom. These diameters for Zn and Co are very close to each other (2.68 Å for Zn and 2.50 Å for Co [96]). The zinc complex, however, is postulated as a 5-coordinate square pyramidal involving a molecule of solvent in the coordination sphere, while the cobalt complex is 6-coordinate octahedral involving two molecules of solvent in the coordination sphere of the unit moiety [102]. Consequently, the cobalt complex is less compact than the zinc one, and when the solvent (DMSO) contribution is taken into consideration, the number of layers in the zinc-containing film is more than 4 times higher than the equivalent cobalt-containing film. For example, after 15 cycles of electropolymerization, 22 layers (corresponding to a thickness of 1.90×10^{-6} cm) have accumulated using the cobalt complex, but 96 layers (corresponding to a thickness of 5.53×10^{-6} cm) have accumulated when using the zinc complex.

Electronic Spectra and Spectroelectrochemical Studies (at High and Relatively Low pH) Using CoTAPc and ZnTAPc Films on ITO Surfaces. Electropolymerized films of CoTAPc and ZnTAPc on ITO surfaces show only one peak and a small broad band (Figure 5.12). These spectra have the same general characteristics as those observed with CuTAPc. The peak with greater absorbance appears ca. 340 nm with the cobalt complex and ca. 400 nm with the zinc complex. The broad peak in the 750-780 nm region may be due to the polymeric film exhibiting more resonance and electron density surrounding the central metal ion in comparison with the

monomeric unit. The comparatively lower absorbance value for peaks in the 750-780 nm range may again be the result of "optical paralysis". Spectroelectrochemical studies were conducted by obtaining the difference spectra of electropolymerized films with respect to a thin film of the polymer in an open circuit. The applied potentials used were +1.000 V, +0.800 V, +0.500 V, 0.000 V, -0.500 V, and -1.000 V. The difference spectra for the CoTAPc in solutions of pH = 5.75 shows two MLCT bands (Figure 5.13). The MLCT2 [104] band evolves in the vicinity of 400 nm when the film is kept at potentials from +1.000 V to 0.000 V, and a blue shift of about 50 nm is observed as the potential becomes less positive. This is assumed to be the result of a $b_{1u}\pi^* \leftarrow\!\!- d_{(eg)}$ transition. When the potential becomes negative, the MLCT1 band is observed about 500 nm and red shifted about 80 nm from the MLCT2 band at -0.500 V. The MLCT1 band is assigned to an $E_g^* \leftarrow\!\!- d_{(eg)}$ transition, since both charge transfer bands originate from the same doubly degenerate E_g level. The large absorbance increase for the MLCT1 bands points to an increase in charge density on the cobalt metal ion center as the reduction process occurs. The smaller bands that appear near 700 nm are assigned to the $E_g \leftarrow\!\!- A_{1u}$ transition. In solutions of high pH (10.60), the difference spectra for CoTAPc films show the same features observed at the lower pH (5.75).

The difference spectra for electropolymerized films of ZnTAPc on ITO surfaces immersed in 0.10 M $KClO_4$ of pH 5.75 do not show MLCT bands (Figure 5.14). Only the Soret and Q bands are recorded, and this may result from a lack of charge increase on the central metal ion. When the pH of the solution is raised to 10.60, significant changes are observed (Figure 5.15). Bands appear in the vicinity of 550 nm for spectra identified as *a*, *b*, and *c*, which then shift to lower wavelengths and and show an increase in absorbance as the applied potential becomes more negative. Such Soret bands, ca. 440 nm, exhibit a slight blue shift, and are assigned to π ------> π^* transitions. Between 600 and 800 nm Q bands are observed clearly when the applied potential is -0.500 and -1.000 V. These two bands (appearing in the spectra identified as *e* and *f*) are

assigned to E_g <---------- A_{1u} transitions. Undoubtedly, the increase in [OH^-] (or concomitantly [H_3O^+] decrease) significantly affect the available electronic transitions in the ZnTAPc film, and the photon absorption behavior of these films at a pH of 10.60 get closer to the one exhibited by CoTAPc films.

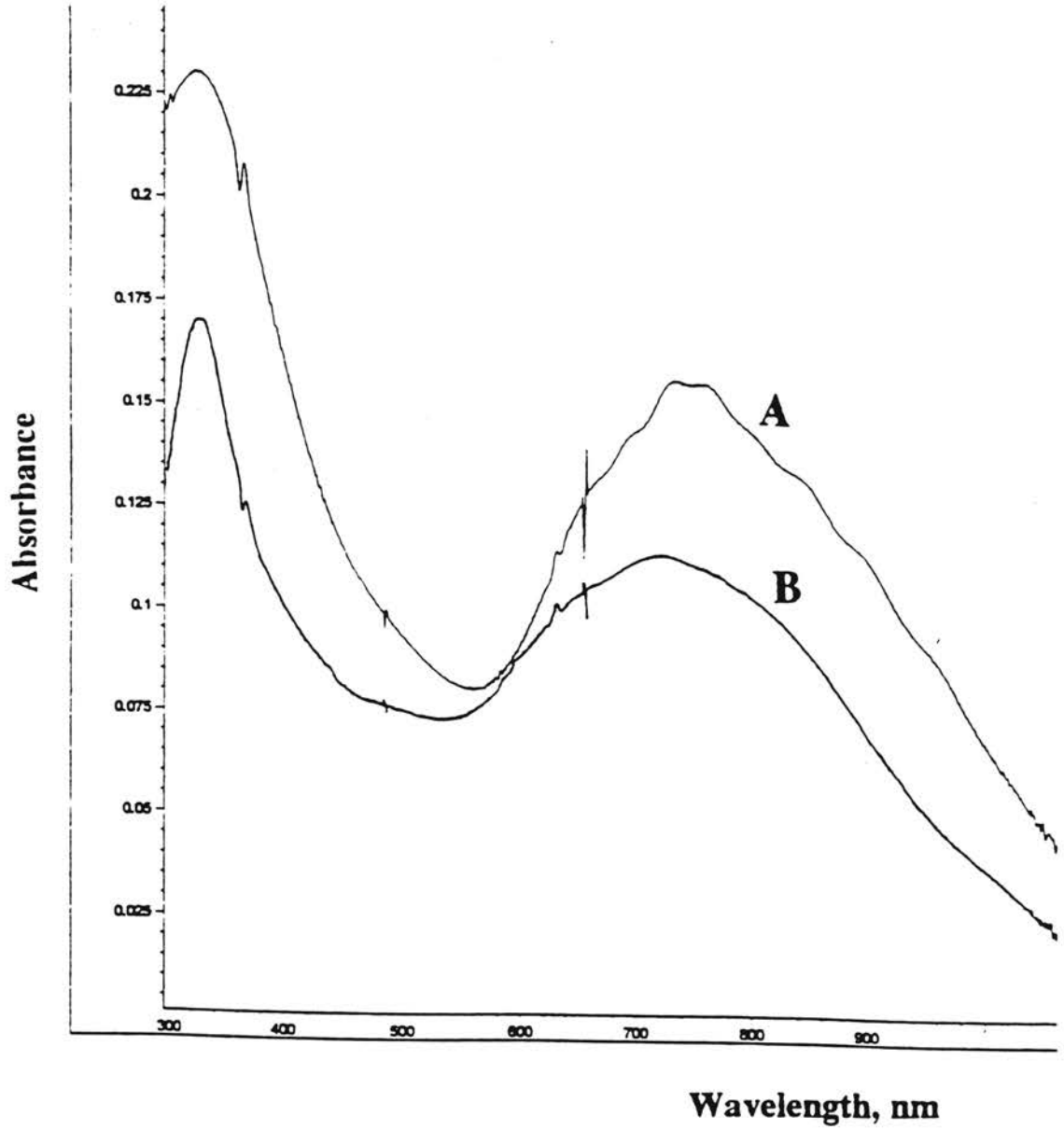

Figure 5.12. Absorption spectra of electropolymerized films on ITO Surfaces: (A) CoTAPc. (B) ZnTAPc. Films immersed in 0.10 M $KClO_4$.

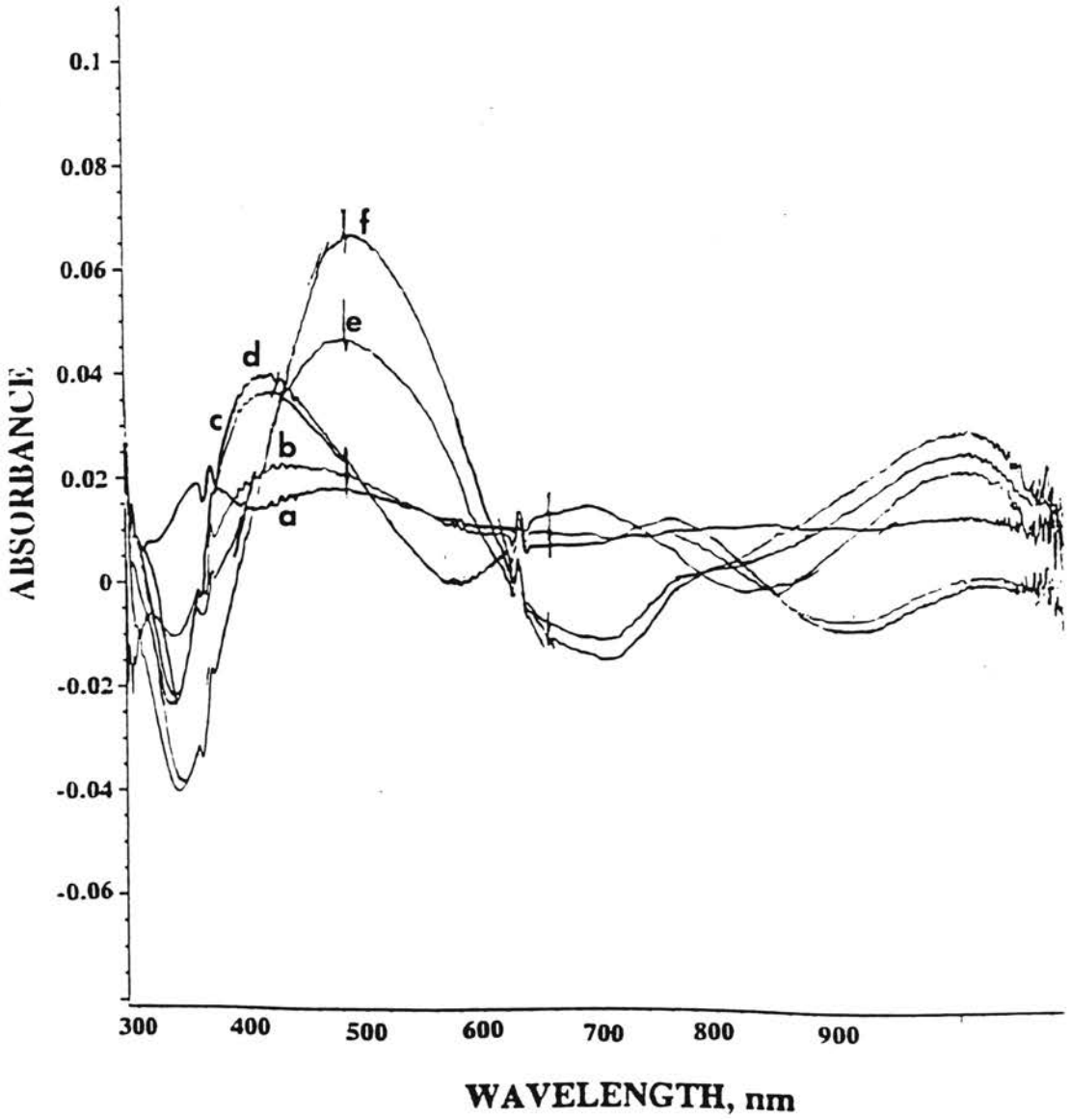

Figure 5.13. Difference spectra (with respect to open circuit conditions) of electropolymerized films of CoTAPc on ITO surfaces immersed in 0.10 M $KClO_4$ of pH=5.75. Applied potentials: (a): 1.000 V, (b): +0.800 V, (c): +0.500 V, (d): 0.000 V, (e): -0.500 V, and (f): -1.000 V.

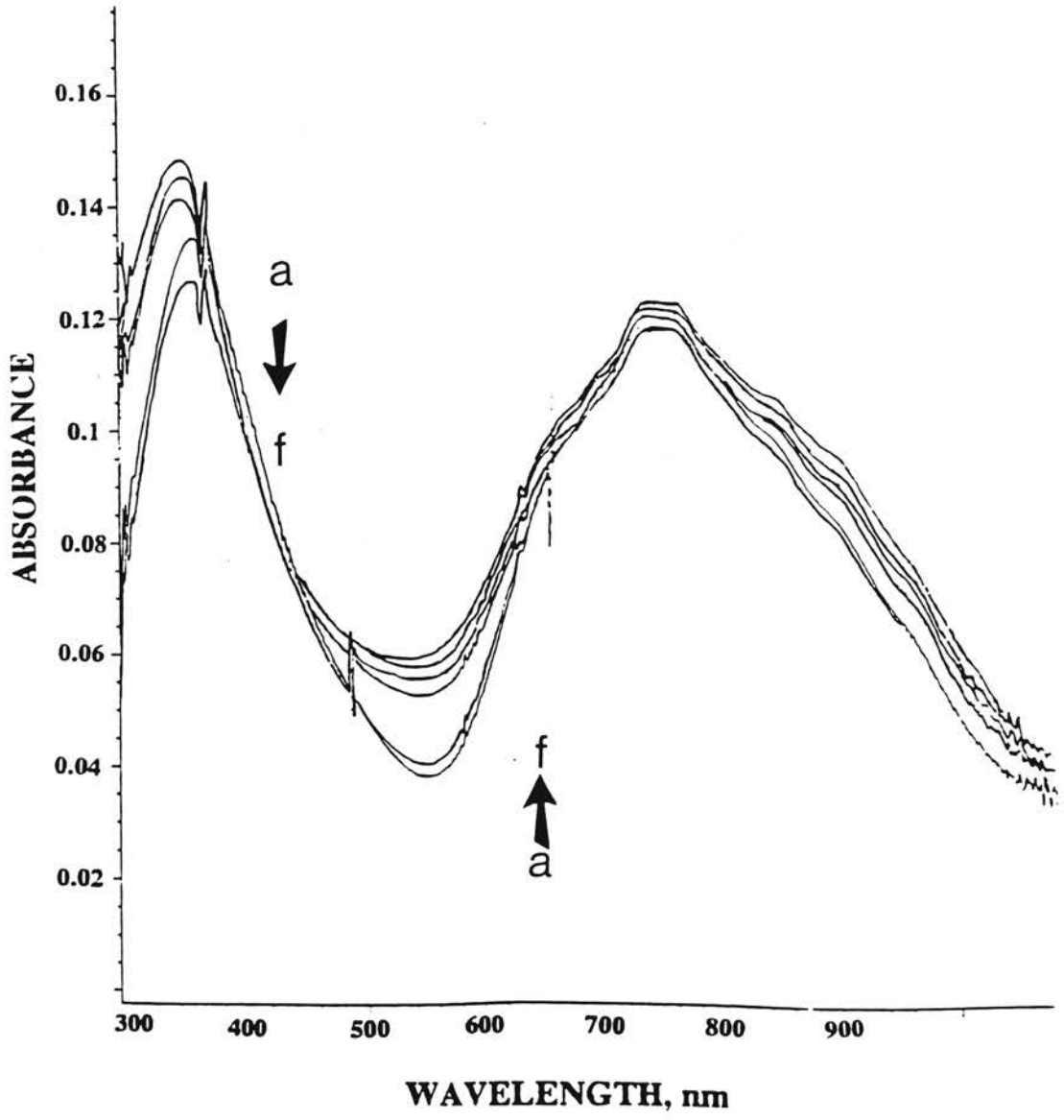

Figure 5.14. Difference spectra (with respect to open circuit conditions) of electropolymerized films of ZnTAPc on ITO surfaces immersed in 0.10 M $KClO_4$ of pH=5.75. Applied potentials: (a): 1.000 V, (b): +0.800 V, (c): +0.500 V, (d): 0.000 V, (e): -0.500 V, and (f): -1.000 V.

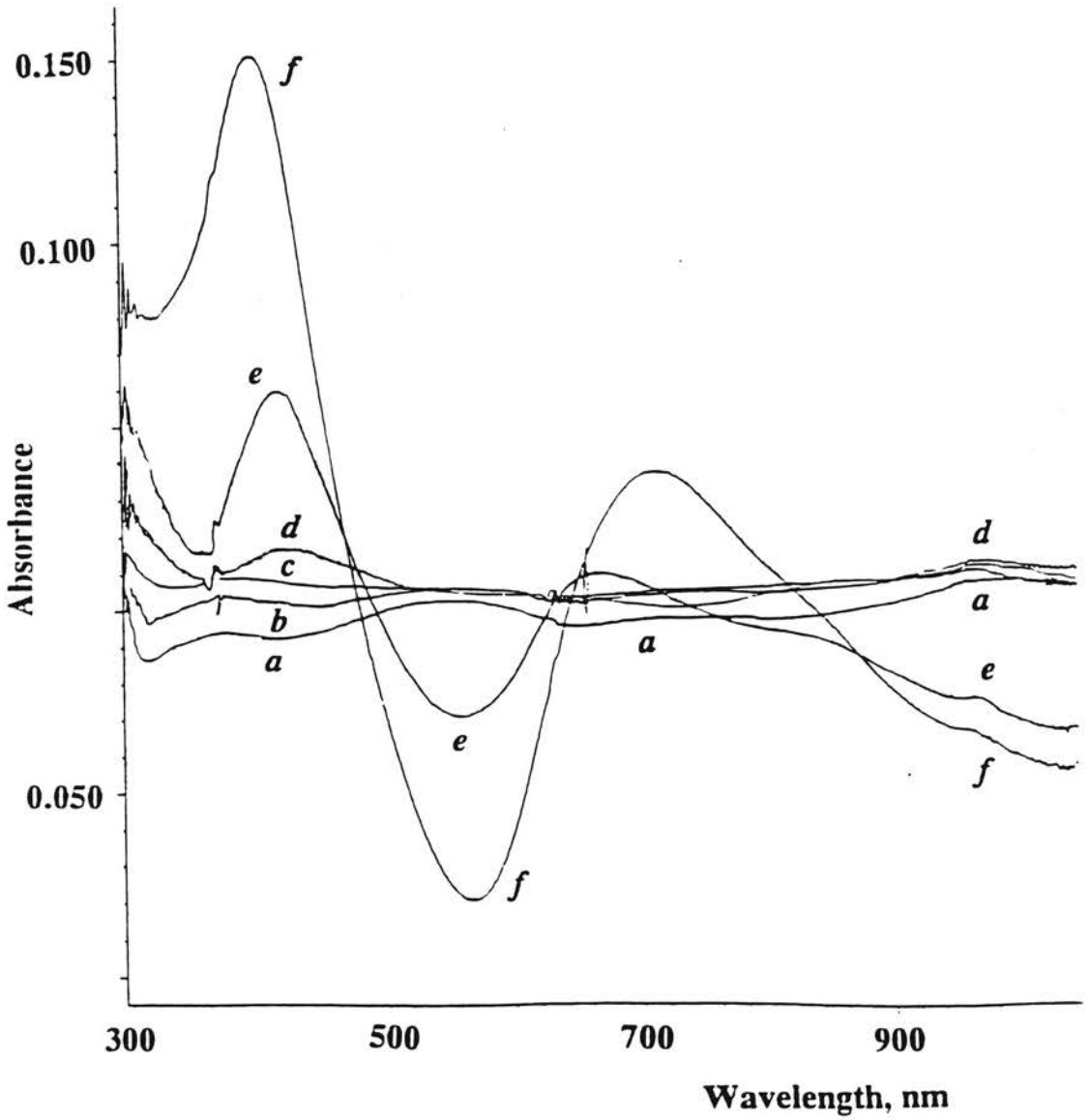

Figure 5.14. Difference spectra (with respect to open circuit conditions) of an electropolymerized film of ZnTAPc on an ITO surface immersed in 0.10 M $KClO_4$ and pH= 10.97. Applied potentials: (a): 1.000 V, (b): +0.800 V, (c): +0.500 V, (d): 0.000 V, (e): -0.500 V, and (f): -1.000 V.

Electrochemical Observations with Films Immersed in Aqueous Solutions of High pH. When electropolymerized films of CoTAPc and ZnTAPc on glassy carbon surfaces are immersed in aqueous solutions of 0.10 M $KClO_4$ of pH 8.00 or 9.66, and cyclic voltammograms are obtained, no difference was observed with the voltammograms obtained at a pH = 5.75 discussed earlier in this research. However, when the pH of the solution is increased above 10 (e.g., 10.60) no peaks were observed in the +1.000 V to -0.200 V potential window. Peaks are observed, however, if the window is extended up to -2.000 V. The CuTAPc complex is not significantly affected by the high pH solutions; both cathodic and anodic peaks are observed within the +1.000 V to -0.200 V potential window. In order to investigate the electrochemical behavior when films are kept immersed in aqueous solutions of relatively high pH, a series of test have been performed. The electrochemical behavior, as evidenced by cyclic and square wave voltammetry, was ascertained for films first immersed in 0.10 M $KClO_4$ of pH 5.75, then immersed overnight in 0.10 M $KClO_4$ of pH 10.90, and finally again overnight in solutions of pH 5.75, using the +1.000 to -2.000 V potential window. These films were the result of 10 cycles of electropolymerization. For CoTAPc, the freshly prepared films show at pH 5.75 only one oxidation peak ca. +0.100 V; this peak is probably due to $[Co(I)Pc]^- - e^- \longrightarrow [Co(II)Pc]$ (peak 11 in Fig. 4.9A). After overnight immersion in solutions of pH 10.90, the electrochemical behavior becomes less clear, but square wave voltammetry insinuates a weak and broad peak centered ca. -0.100 V, and at a scan rate of 200 $mV \cdot s^{-1}$ the corresponding reduction peak can be observed (probably this corresponds to $[Co(II)Pc] + e^- \longleftrightarrow [Co(I)Pc]^-$ (peaks 10 and 11 in Figure 4.9A). As the scan rate is increased the peak current increases proportionally, and the peak corresponding to $[Co(II)Pc] + e^- \dashrightarrow [Co(I)Pc]^-$ is evident. The significant change in the redox potential may be a result of some structural change of the thin film. After thoroughly washing the film with purified water and immersing overnight in a solution of pH 5.75,

the electrochemical behavior observed at pH 10.90 persists without return to the behavior originally observed at pH 5.75.

For the ZnTAPPc-based films, peaks 14, 15 and 16 (Figure 5.10) are originally observed at pH 5.75, but at pH 10.90 only peak 16 seems to persist. As observed with the CoPc-based films, after immersion in solutions of relatively high pH, the electrochemical behavior at pH 5.75 could not be recovered. The redox activity persisting at high pH seems to be mainly due to the $[Zn^{2+}, Pc^{3-}]^{-}/[Zn^{2+}, Pc^{4-}]^{2-}$ redox couple. Evidently, high pH solutions cause structural change in the film, and this is reflected in a change in the peak potential.

CHAPTER VI

ELECTROPOLYMERIZED COPPER, COBALT, AND ZINC(II)-TETRAAMINOPHTHALOCYANINE THIN FILMS: POTENTIAL RATE MODIFIERS OF LUMINOL CHEMILUMINESCENCE

INTRODUCTION

Chemiluminescence reactions have generated considerable interest in analytical chemistry becasue of their sensitivity to reaction conditions such as the presence of various metal ions and oxidants [104-115]. Many metal ions are known to modifiy the rate of chemiluminescence, and if reation conditions are adjusted, such reactions can be utilized in the analytical determination of the species causing the modification on the rate of chemiluminescence. These systems have a large concentration range for calibration, high sensitivity, and detection limits are in the ppb to ppt range [113]. One of the chief advantages of chemiluminescence applications is the simple instrumentation required. Different methods of immobilizing luminol or the rate modifier have recently been investigated. For example, immobilized luminol on an anion exchange resin has been used in the determination of sulfite and sulfur dioxide [116]. This method of immobilization has even been extended to a luminol and hexacyanoferrate(II) combination on an anion exchange resin used for the determination of iron(II) in blood samples [117].

The incorporation of immobilized metal phthalocyanine films in the design of chemiluminescence sensors for CO_2 (g) was motivated by the observation that some metal phthalocyanine complexes in solutions of high pH effectively increase the rate of luminol chemiluminescence in the absence of an added oxidant [29]. Immobilization methods of metal phthalocyanine by adsorption onto controlled pore glass (CPG) does

provide a signal, but the intensity is much less than when solutions of metal phthalocyanine are used. In addition, the complexes often leach from the CPG that places significant constraints on a detection system in terms of reproducibility, and its long-term use [118]. Therefore, and as part of the work described here, electropolymerized thin films of CuTAPc, CoTAPc, and ZnTAPc have been incorporated into a reactor cell to investigate the use of these thin films as potential rate modifiers of luminol chemiluminescence in the presence of carbon dioxide. Multilayered polymeric thin films, as expected, have been shown to give greater response signals than single monolayer thin films since they contain more sites available for interaction with the analyte. Immobilization of the complex onto a rotating disk facilitates a higher detection sensitivity. The rotation thoroughly mixes the reagents in the flow cell. These thin films, have therefore been tested as potenial rate modifiers in luminol chemiluminescence in the absence of added oxidant.

Some metal (II) complexes, in the presence of carbon dioxide, show significant changes in electrochemical behavior (e.g., in cyclic voltammetry) in terms of current density and reversiblilty of the system [119]. Consequently, it was of interest to investigate the electrochemical behavior of these films in the presence of carbon dioxide. Several possibilities exist for the interaction of carbon dioxide with metal tetraaminophthalocyanine. Carbon dioxide may interact: (1) with the central metal ion, or (2) with the phthalocyanine ring system. Some modified electrodes such as polyvinylpyridine membrane with cobalt phthalocyanine and derivatives of cobalt phthalocyanine, such as cobalt octabutoxyphthalocyanine, have been reported to help catalyze the reduction of carbon dioxde after the carbon dioxide has coordinated with the metal phthalocyanine [120-125].

EXPERIMENTAL SECTION

Instrumentation. The electrochemical instrumentation was described in Chapter 4. A three electrode cell using a glassy carbon electrode was employed as the working electrode when performing electrochemical experiments in the presence of carbon dioxide. The flowmeter to monitor the flowate of carbon dioxde was obtained from Alborg Corp (Monsey, New York). Figure 6.1 is a schematic diagram of the instrumentation utilized in the chemiluminescence studies [29]. The magnetic stirrer (MS) is used to rotate the disk that contains a small sitrring bar. As the pump (P) forces the solutions into the cell, the solutions are immediately mixed. The photomulitiplier tube (PMT) detects the light emission from the chemiluminescence reaction. The signal can be amplified via the auxiliary electronics (AE), and the digital oscilloscope serves as the readout device.

Worth mentioning is that a slight modification (Figure 6.2 A-D) of the flow cell and the rotating PTFE disk has been made to accommodate the modified surface. In this design, a glass slide (i.e., glass slide covered with ITO) modified with an M(II)TAPc film, is placed onto a disk which is positioned directly over the photomultiplier tube. A small magnetic stir bar is embedded within the disk. The disk is rotated (350 RPM) to thouroughly mix the solutions once they enter in the flow cell. The rotation of the disk is related to the voltage setting of the rheostat [126] that is connected to the magnetic stirrer (Figure 6.1A). The hydrodynamic flow of the solutions via the pump is not strong enough to effectively mix the solutions. The rotation of the disk causes convection and substantially increases the chemiluminescence, and the efficiency of the system. The flow cell is essentially a rotating reactor [126]. The solutions are pumped via peristaltic pump at a flow rate of 1.2 mL/min (Gilson Medical Electronics, Middleton, WI), and flow through the cell via the solution channels [(a) in Figure 6.2]. The diameter of the hole for the disk is 14 mm since the length of the modified glass slide is 13 mm. The PTFE

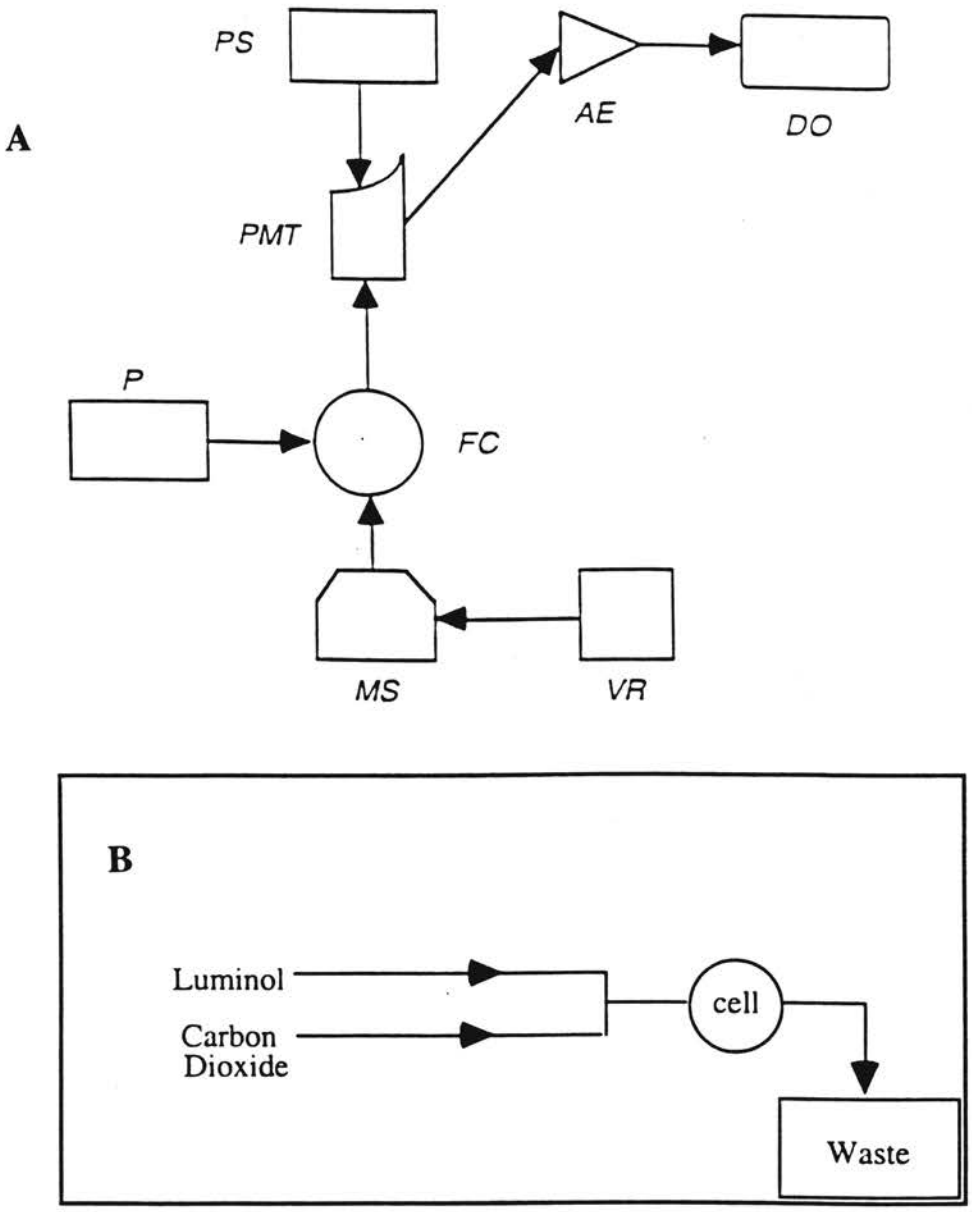

Figure 6.1 A. Instrumentation used for chemiluminescence studies. VR: Variable Rheostat; MS: Magnetic Stirrer; FC: Flow Cell; P: Peristaltic Pump; PMT: Photomultiplier Tube; PS: Power Supply; AE: Auxiliary Electronics; DO: Digital Oscilloscope. Figure 6.1 B. Schematic of flow system. Modified suface housed in the flow cell. Flow rate is 1.2 mL/min. Rotation of disk is 350 RPM.

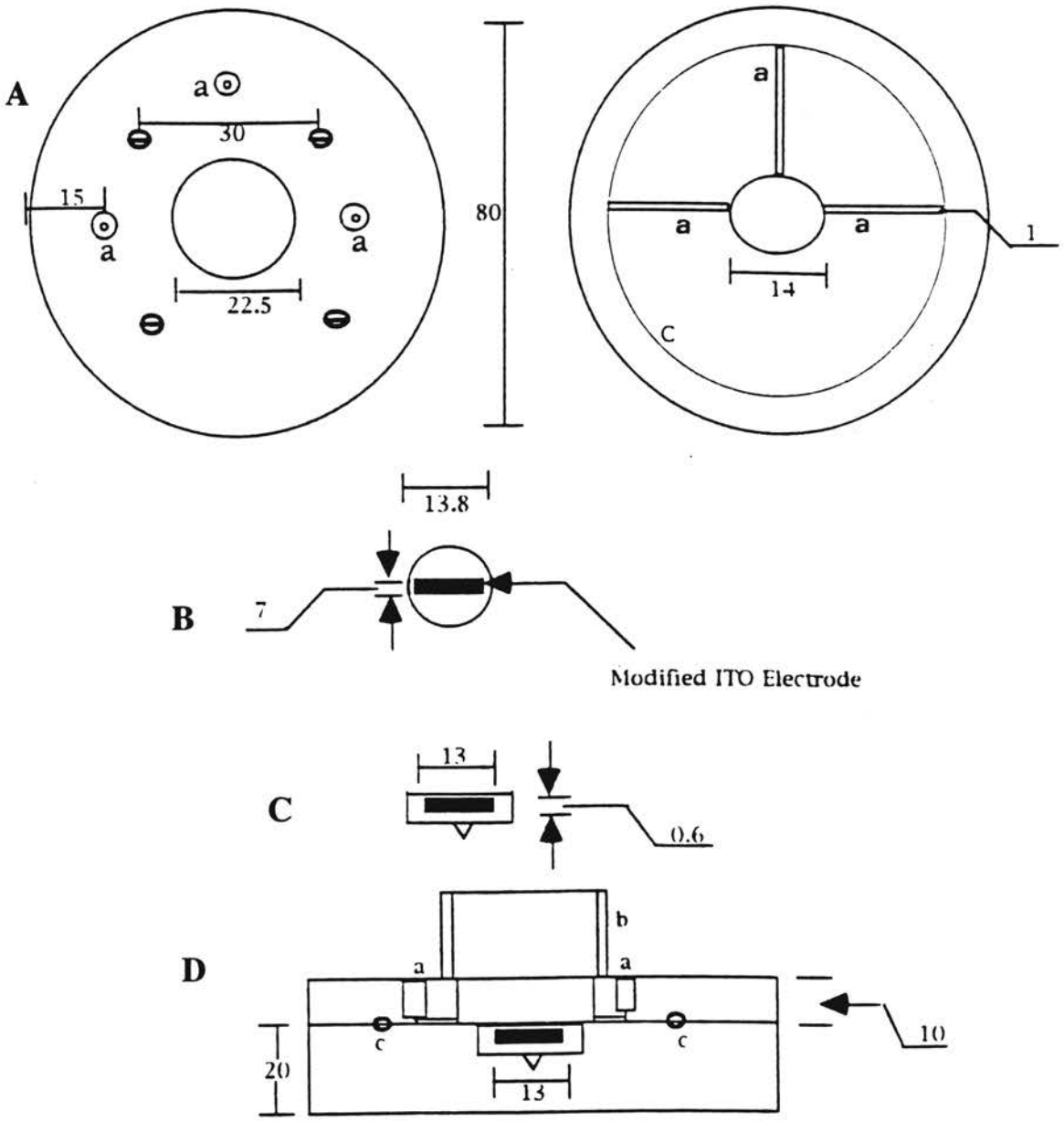

Figure 6.2. Diagram of flow cell containing the modifed surface. (A) Top view of the upper body of flow cell; (B) Bottom part of the cell, showing the inlet and outlet paths for solutions; (C) disk with needle that contains the modified surface; (D) Cross-section of flow cell showing the optical connector and disk with needle that contains the surface. Not drawn to scale. All measurements are in mm. (a) Channel for solution flow; (b) optical connector; (c) O-ring.

disk, 13.8 mm in diameter, was slightly modified by making an incision of 13 mm x 7 mm so that the modified glass slide could set securely within the disk. The depth of the incision is 0.7 mm. As a result, the disk is able to rotate freely without protruding into the cover slide. The disk is slightly smaller in diametrer that the hole for the disk so that it can rotate freely. Once the electropolymerizations were completed, the glass slide was rinsed with distilled water and allowed to dry, a small hand-held glass cutter was used to cut a 13 mm section which could be placed within the disk.

Reagents and Solutions. The solutions used in electropolymerizations were described in Chapter 3. Luminol was purchased from Aldrich (Milwaukee, WI). The concentration of all luminol solutions was 5.0×10^{-3} M. Potassium hydroxide used to adjust the pH of the luminol solutions to 13.2, was obtained from EM Science (Cherry Hill, NJ). The carbon dioxide gas in air (792 ppm) was obtained from Sooner Airgas (Shawnee, OK). The hydrogen peroxide concentration was 4.4×10^{-3} M and was obtained from J.T. Baker Chemical Company (Phillipsburg, N.J.).

For all electrochemical measurements, the maximum bubbling time of pure carbon dioxide (50 mL/min) was 1.5 minutes. After this time, carbon dioxide did not have an effect upon the thin film.

Procedure for Electropolymerization on ITO and Glassy Carbon Surfaces. The electrode preparation followed the same procedure as described in Chapter 4. Oxidative electropolymerizations of all complexes for chemiluminescence studies were performed at 200 $mV \cdot sec^{-1}$ using a potential window of 1.000 V to -0.200 V. The number of cycles completed was 49. It was not necessary to use a wider potential window for covering the surface. The number of cycles were, however, increased so that the thin films could be used for longer times in the continuous-flow system since surface coverage increases with the number of electropolymerization cycles. For electrochemical

experiments with carbon dioxide, the number of monolayers were approximately the same by adjusting the number of cycles of electropolymerization with respect to CuTAPc. This complex was chosen since it has a greater number of monolayers per electropolymerization cycle. It was not necessary to increase the number of cycles of electropolymerization beyond 5 to electrochemically investigate the interaction of carbon dioxide with modified electrode. Therefore, the number of cycles was kept to a minimum.

Procedure for Voltammetric Characterization. The experimental conditions for characterization of the thin films in the presence of carbon dioxide are the same as outlined in Chapter 5. All voltammograms corresponding to systems with solutions bubbled with pure carbon dioxide are compared to those systems with solutions bubbled with nitrogen gas.

RESULTS AND DISCUSSIONS

Interaction of Carbon Dioxide with CoTAPc, ZnTAPc, and CuTAPc. The electrochemical reduction of carbon dioxide to various products requires large overvoltages and may not be noticed within the potential limits dictated by the solvent, supporting electrolyte, and electrode material. When the glassy carbon electrode is not modified, and cyclic voltammetric measurements are taken in the presence of carbon dioxide, no peak giving evidence for carbon dioxide reduction is observed (Figure 6.3 A), even when the potential window is extended to -2.400 V. However, when CoTAPc is electropolymerized onto the glassy carbon surface, and characterized in a 0.10 M solution of TEAP in DMSO, containing pure carbon dioxide, significant changes are observed in the peak potentials, and in the number of peaks (Figure 6.3 B). These changes are with respect to Figure 5.8 (page 90-91). Peaks 8 and 9 are identified as previously ascribed to

the Co(III/II) redox couple. At the more negative potentials, the cathodic peaks are identified as pertaining to the following electrochemical reactions:

$$[Co^{2+}, Pc^{2-}]^{-} + e^{-} \text{ ----------> } [Co^{+}, Pc^{2-}]^{2-}$$

$$[Co^{+}, Pc^{2-}]^{2-} + e^{-} \text{ ----------> } [Co^{+}, Pc^{3-}]^{3-}$$

These have peak potentials of -0.500 V, and -1.350 V respectively. A fourth peak was identified with a peak potential of -1.950 V (Figure 6.3 B) This peak at -1.950 V is ascribed to $[Co^{+}, Pc^{3-}]$-------->$[Co^{+}, Pc^{4-}]$, and is related to the carbon dioxide reduction. Under a nitrogen atmosphere, and with the same potential window, the fourth peak is not present. These changes are attributed to the interaction of carbon dioxide with the CoTAPc thin film. This interaction seems to affect the coordination sphere of the complex since the carbon dioxide may participate in the reaction by axially coordinating the central metal ion. It has not been determined, however, if this interaction between central metal in the film and carbon dioxide corresponds a ratio of 1:1 or 1:2.

When cyclic voltammetry is performed at a constant scan rate, but with increased amounts of carbon dioxide, all peaks formally identified increase, except the peaks corresponding to $[Co^{3+}, Pc^{2-}] + e^{-}$ --------> $[Co^{2+}, Pc^{2-}]$ and $[Co^{2+}, Pc^{2-}] + e^{-}$ --------> $[Co^{+}, Pc^{2-}]$. Square wave voltammetry, under a nitrogen atmosphere, shows the peaks corresponding to the peaks in Figure 5.8 (page 90). However, in the presence of carbon dioxide, the peaks are displaced towards more positive potentials (Figure 6.4). As the amount of carbon dioxide is increased, the peaks corresponding to the above redox processes are decreased, and all other peaks are increased (Figure 6.5) These observations point to a mechanism in which carbon dioxide interacts with the central metal ion of an oxidation state of +1, and the Pc ligand has a charge of at least -3. Based on these observations, the mechanism shown in Figure 6.6 is proposed. When the cobalt metal ion is in the +1 oxidation state, the electron density surrounding the cobalt

ion is higher than when the cobalt is in the +2 oxidation state. Furthermore, the subsequent reduction of $[Co^{+}, Pc^{2-}] + e^{-}$ ------> $[Co^{+}, Pc^{3-}]$, and $[Co^{+}, Pc^{3-}] + e^{-}$ -----> $[Co^{+}, Pc^{4-}]$ increases the nucleophilicity of the CoTAPc. These factors contribute to the coordination of the electrophilic carbon of carbon dioxide to CoTAPc. The fact that other peaks, corresponding to the reduction of the ligand, increase with a greater concentration of carbon dioxide, insinuates that carbon dioxide is involved in a catalytic cycle when the ligand carries a charge -3.

In Chapters 3, and 4 it was shown that the central zinc metal ion does not ungergo a redox reaction. All redox processes are centered on the ligand. It is therefore expected that the electrochemical reaction involving ZnTAPc and carbon dioxide would proceed by a different process involving the ligand. The aza nitrogen of the Pc ring system is capable of coordinating with carbon dioxide [57]. Experiments conducted in the same manner as with CoTAPc indicate there is only a two-step proecss before carbon dioxide enters into a reaction with ZnTAPc. From square wave measurements, peaks corresponding to $[Zn^{2+}, Pc^{2-}] + e^{-}$ -------> $[Zn^{2+}, Pc^{3-}]$ decrease while peaks corresponding to $[Zn^{2+}, Pc^{3-}] + e^{-}$ -------> $[Zn^{2+}, Pc^{4-}]$, and $[Zn^{2+}, Pc^{4-}] + e^{-}$ --------> $[Zn^{2+}, Pc^{5-}]$ increase. This indicates that the energy requirements for ZnTAPc reduction of carbon dioxide are less than for CoTAPc, since it requires one step less for the electrochemical reduction of carbon dioxide. When thin films of CuTAPc are present, no catalytic activity is observed towards the reduction of carbon dioxide. In performing square wave measurements, all peaks corresponding to Cu(II/I), $Pc(2^{-}/3^{-})$, and $Pc(3^{-}/4^{-})$ decrease. Further work in this area has not been explored in this research. These results do, however, follow results reported by Meshitsuka, and co-workers that CoPc complexes show greater catalytic activity towards carbon dioxide reduction than CuPc complexes [128]. Moreover, the work performed by Premkuman and co-workers [129] indicates than ZnPc shows greater catalytic activity towards carbon dioxide reduction than CoPc.

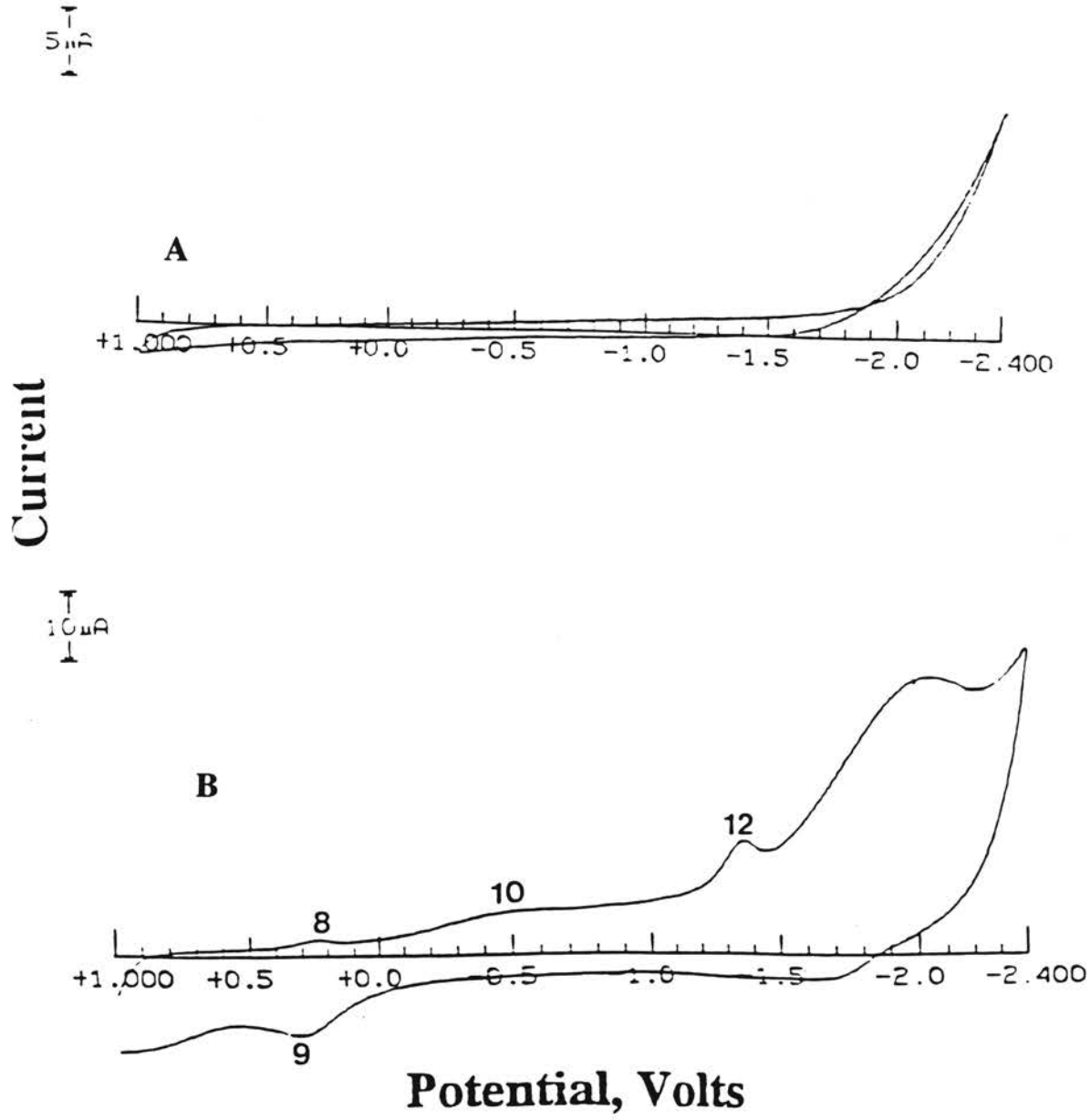

Figure 6.3 (A) Cyclic voltammogram of supporting electrolyte, 0.10 M TEAP in DMSO. (B) Same supporting electrolyte system as in (A); glassy carbon electrode modified with CoTAPc; the scan rate in both cases was 50 mV· sec-1. Fourth peak appears near -2.000 V. Bubbling time of pure carbon dioxide =30 seconds at 50 mL/min.

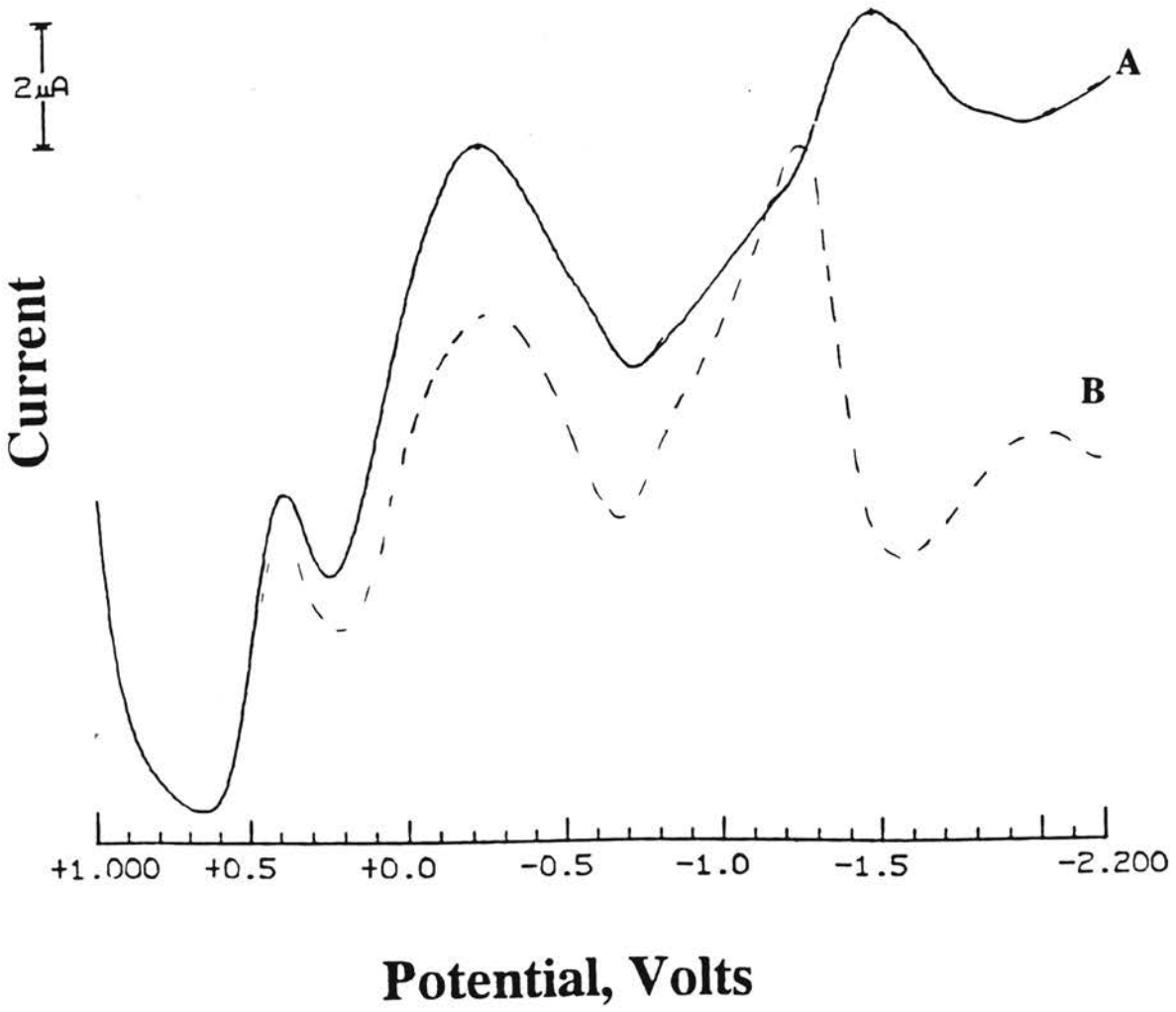

Figure 6.4. Square wave voltammetry. Supporting electrolyte: 0.10 M TEAP in DMSO. Scan rate: 60 mV·sec^{-1}. Glassy carbon electrode modidifed with CoTAPc. (A) under nitrogen atmosphere; (B) in the presence of solutions of pure carbon dioxide. Fourth peak appears near -2.000 V. Bubbling time of pure carbon dioxide= 30 seconds at 50 mL/min.

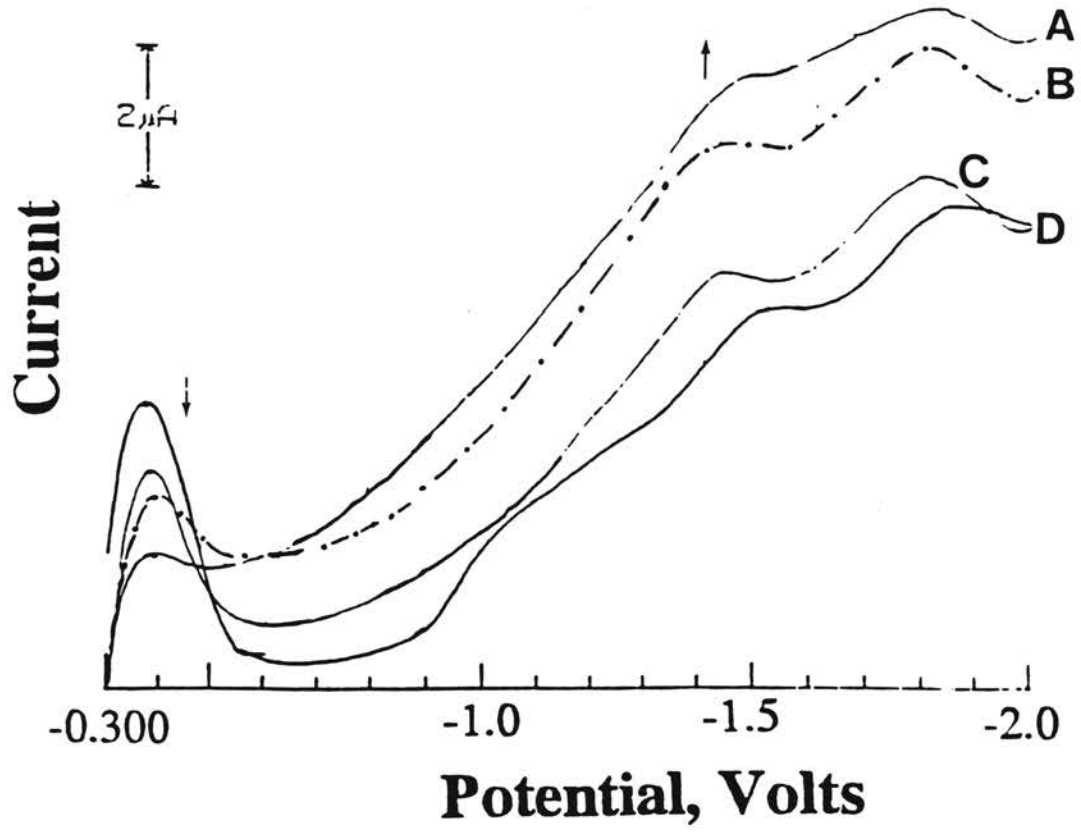

Figure 6.5. Square wave voltammetry. Supporting electrolyte: 0.10 M TEAP in DMSO. Scan rate: 60 mV·sec^{-1}. Glassy carbon electrode modidifed with CoTAPc. (A) under carbon dioxide atmosphere. Bubbling time of pure carbon dioxide in seconds: (a)120; (B) 90; (C) 60; (D) 30 seconds at 50 mL/min.

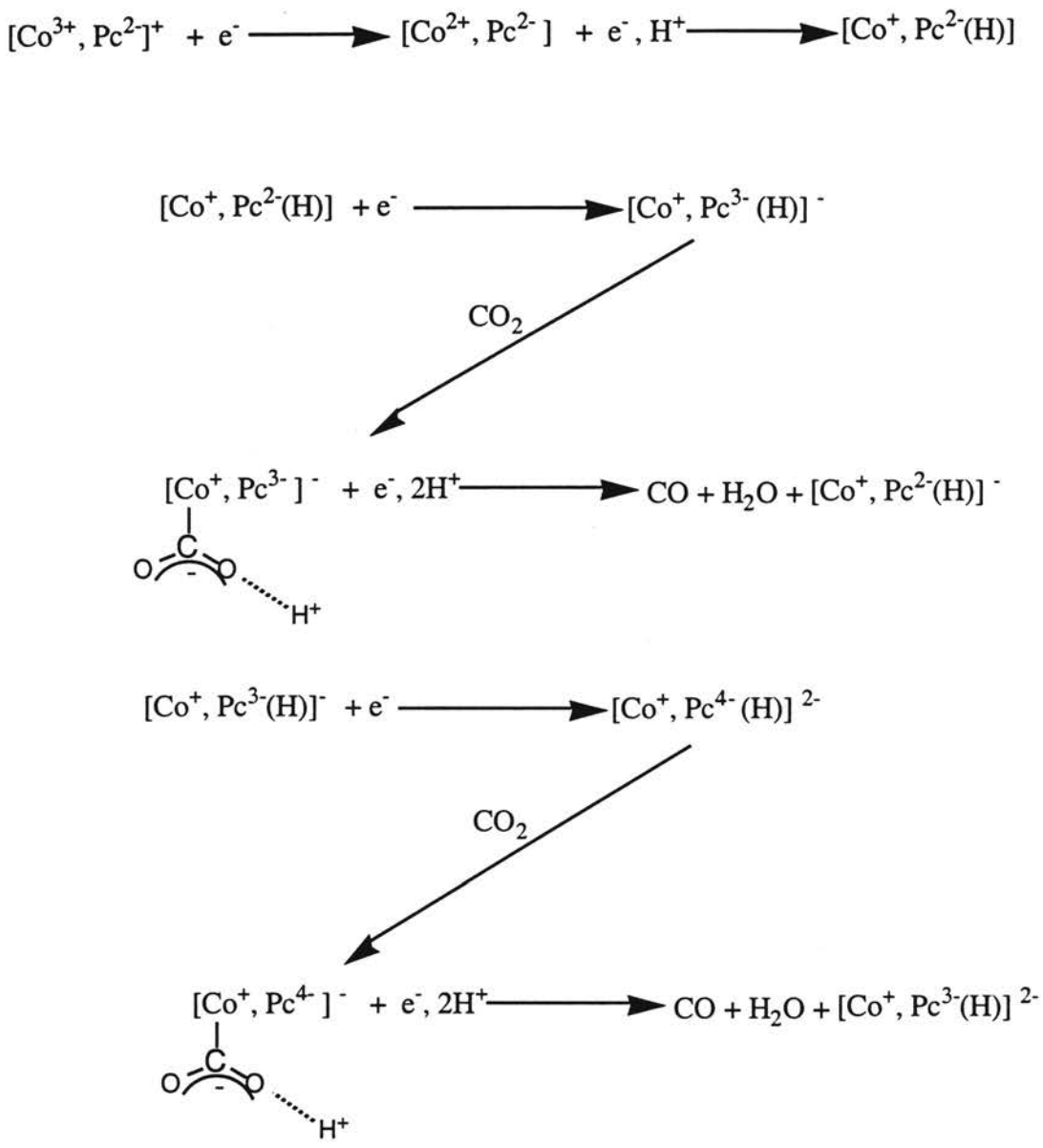

Figure 6.6. Proposed mechanism for the electrochemical reduction of carbon dioxide at a glassy carbon surface modified with CoTAPc.

Luminol Chemiluminescence in the Presence of H_2O_2 and Electropolymerized Films of CuTAPc, CoTAPc, and ZnTAPc. The mechanism for the luminol chemiluminescence in the presence and absence of added oxidant, modified by solutions of certain metal ion and metal complexes has been reported in several **publications.** When H_2O_2 is added to solutions of luminol and in the presence of electropolymerized films, an intense chemiluminescence emission is detected. These experiments, in the presence of H_2O_2, were performed first to verify that chemiluminescence does occur when using thin films of metal tetraaminophthalocyanine as opposed to using solutions of of metal phthalocyanines. After these intial experiments were performed, solutions of carbon dioxide in air were used without adding H_2O_2. The first injection of luminol and H_2O_2 with CuTAPc as the rate modifier, had a peak intensity of 981 mV. The subsequent injections were made afer the chemiluminescence emission decayed to a baseline value. The subsequent injections showed peak intensities of 767 mV, 741 mV, and 759 mV. Longer injection times result in a slight dilution of the luminol via the peroxide which causes the intensity of subsequent injections to be lower. When electropolymerized films of ZnTAPc are used as the rate modifier, the same type of observations were made in regards to the initial peak intensity and the decrease of subsequent peak intensities upon injection of peroxide into the luminol solution. The initial peak intensity was 868 mV, slightly lower than when CuTAPc was used as the rate modifier. However, the latter injections had peak intensities of 343 mV, and 343 mV. In the case of CoTAPc thin films, the peak intensities were 179 mv, 176 mV, and 172 mV. Significant differences in the number of accumulated monolayers between the three polymeric thin films is postulated as the reason that CuTAPc has larger peak intensities than both CoTAPc, and ZnTAPc. Polymeric thin films of CuTAPc are more compact than the other polymeric thin films, and have more monolayers.

Chemiluminescence in the Presence of Oxygen and Carbon Dioxide. When solutions of H_2O_2 were replaced with solutions bubbled with oxygen and carbon dioxide, chemiluminescence was observed when using all three polymeric thin films. Previous reports indicate that although oxygen is needed for chemiluminescence, its need is neglible when carbon dioxide is present [29]. The chemiluminescence when using solutions bubbled with carbon dioxide is nearly equal to or greater than when using solutions bubbled with oxygen. In all cases, the greatest chemiluminescence occurred when using CuTAPc thin films as the rate modifier. In comparing only thin films of ZnTAPc, and CoTAPc, the chemiluminescence was more intense when using thin films of ZnTAPc. The peak intensity when using thin films of ZnTAPc was almost 2 times greater than when using thin films of CoTAPc as the rate modifier. In view of these observation, it seems that the accumulated number of monolayers and film composition plays a significant role in chemiluminescence when carbon dioxide is present. Figure 6.7 is a typical chemiluminescence intensity-time profile utilizing thin films of CuTAPc, ZnTAPc, and CoTAPc as rate modifiers in the presence of carbon dioxide. As the figure shows, thin films of CuTAPcare 2.7 times more effective than films containing thin films of ZnTAPc, and 6 times more effective than thin films of CoTAPc. The foregoing seems to agree with the following observations: (1) The chemiluminescence intensity when bubbling carbon dioxide is always greater with CuTAPc films. (2) When using ZnTAPc films rather than CoTAPc films, the chemiluminescence is slightly larger even after correcting for the number of monolayers. The number of monolayers in the films vary, and the net result is a spatial distribution of metal centers which is different for the different films. The peak intensities of chemiluminescence in the presence of carbon dioxide are normalized with respect to the smallest chemiluminescence signal in the absence of carbon dioxide [i.e., peak intensities with carbon dioxide are normalized with respect to the peak intensity with CoTAPc thin film with solutions bubbled with oxygen]. These values suggest that thin films of CuTAPc are the best, then ZnTAPc, and

finally CoTAPc with respect to being the best rate modifier in luminol chemiluminescence in the presence of carbon dioxide. The electropolymerized films interact with carbon dioxide in high pH solutions to increase the electrophilicity of the carbon of carbon dioxide. This factor allows for the formation of intermediates involved in the carbon dioxide enhancement in the absence of any other added oxidant.

Figures of Merit. Once several injections have been made, and a steady signal is achieved, a calibration curve can be generated. Figure 6.8 is a typical calibration curve for carbon dioxide using the CuTAPc film as the rate modifier. The limit of detection, 10.7 ppm, was taken as the average of the ten blank readings plus 3(s.d.), where s.d. is the sample standard deviation of the blank readings. The signals due to the blank were substracted from the signals due to the standards. The regression equation of $Y=0.64429 + 0.92672\log(X)$ has a correlation coefficient of 0.991. The sensitivity of the measurement is taken as the slope of the calibration curve, and is 0.927 $mV \cdot ppm^{-1}$.

Mechanism of Luminol Chemiluminescence in the Presence of Carbon Dioxide. When carbon dioxide is added to solutions of luminol in high pH solution, and only if peroxide is present, the chemiluminescence intensity is increased. The enhancement of luminol chemiluminescence in the presence of carbon dioxide and in the absence of other added oxidant, is facilitated by the interaction of the rate modifier with carbon dioxide as illustrated in Figure 6.9. The mechanism for the overall reaction is shown in Figure 6.10. In a high pH solution (pH=13.2) the luminol exists as a dianion, **I**. The maximun intensity occurs when the pH is near 13. The dianion, **I,** can react with the carbon dioxide-MTAPc adduct in the presnce of HOO^- to form the superoxide radical and the luminol radical, **II.** The superoxide radical then reacts with the luminol radical, **II**, to form an endoperoxide, **III,** that is unstable. The endoperoxide generates the 3-aminophthalate, **IV,** in the excited state. The 3-aminophthalate has previously been

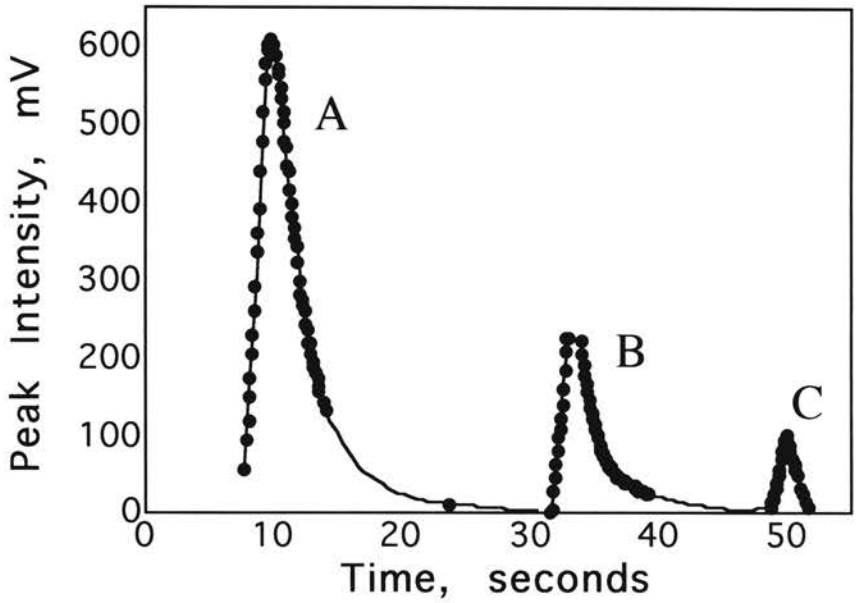

Figure 6.7. Chemiluminescence intensity-time profile in the presence of carbon dioxide; pH=13.2. Rate modifiers are: (A) CuTAPc, (B) ZnTAPc, and (C) CoTAPc Number of cycles of electropolymerization was 49. Carbon dioxide: 201 ppm.

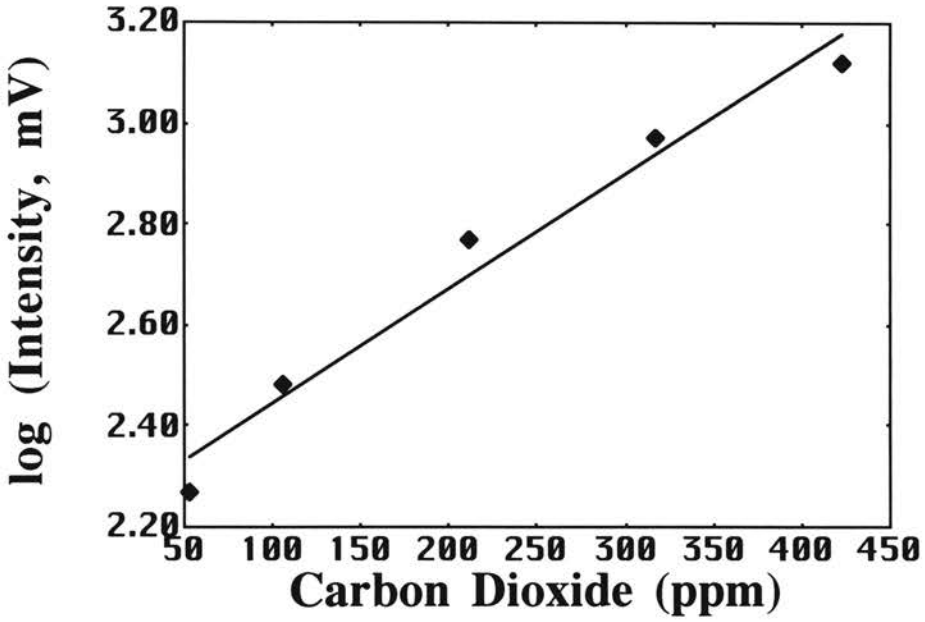

Figure 6.8. Typical calibration curve for carbon dioxide using CuTAPc film as rate modifier; pH=13.2; Linear range of curve extends to 422 ppm.

identified as the light emitting species [130-131]. The carbon of carbon dioxide undergoes a nucleophilic attack by the HOO^- anion. This forms peroxycarbonates, **VI**. The decomposition of these peroxycarbonates form radical species from **V**, and **VI** (Figure 6.11). The superoxide radical is formed from the dissociation of the HO_2 at high pH. The superoxide radical can also be formed via dissolved oxygen reacting with luminol radical, **II**. The carbonate radical can oxidize the luminol dianion into the luminol radical. When the conditions such as concentration of luminol, and rate modifier are adjusted, the chemiluminescence may be used as a method for carbon dioxide determination since the chemiluminescence is enhanced in the presence of carbon dioxide. The scan rate of electropolymerization, potential window, and supporting electrolyte/solvent system, all affect the composition of the films. These experimental conditions should therefore be optimized in tailoring the thin film for use as a rate modifier. The films are stable for at least one month.

Monolayer Coverage. [See Appendix for details]. The calculated number of monolayers for the different complexes show significant differences even though the central metal ions have nearly the same diameters. In view of this, the differences in the nominal coordination number of the complexes are considered as a reason for the differences in the number of calculated number of monolayers for the electropolymerized films when the number of electropolymerization cycles are the same. As mentioned earlier, ZnTAPc, and CoTAPc have larger coordination numbers than CuTAPc. During the electropolymerization process, solvent molecules (i.e., DMSO) coordinate with the central metal ion to fill the coordination sphere of the complex (e.g., $[CoTAPc]L_2$, where L=DMSO). If DMSO is included as part of the model for monolayer coverage, the effective volume of the MTAPc complex is larger. Therefore, the effective volume of ZnTAPc is smaller than CoTAPc. Hence, the concentration of ZnTAPc in a "well-compact" layer is larger than that of CoTAPc. For a given number of

electropolymerization cycles, the number of monolayers per electropolymerization cycle follow the series: CuTAPc> ZnTAPc> CoTAPc. Figure 6.12 shows how the number of monolayers vary with the number of electropolymerization cycles.

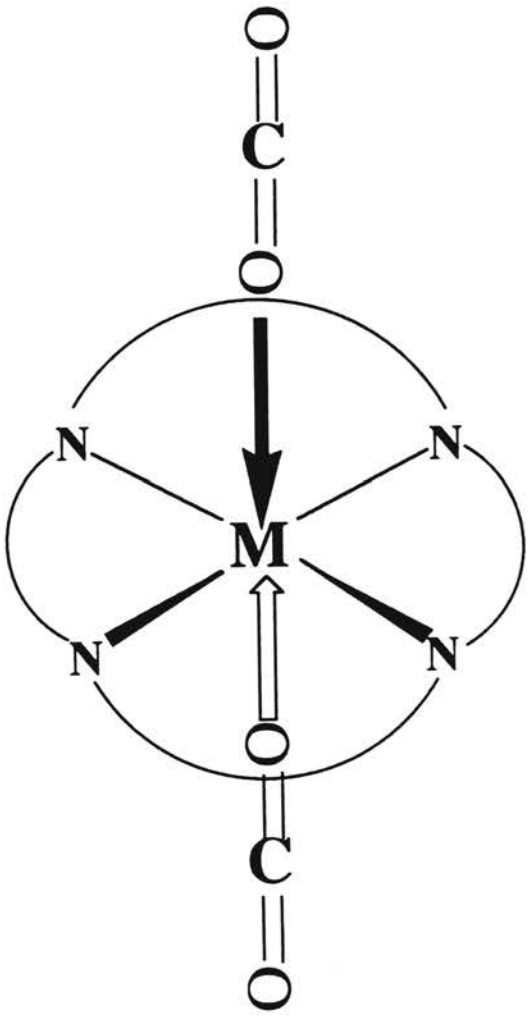

Figure 6.9. Interaction of carbon dioxide with MPc compounds in luminol chemiluminescence.

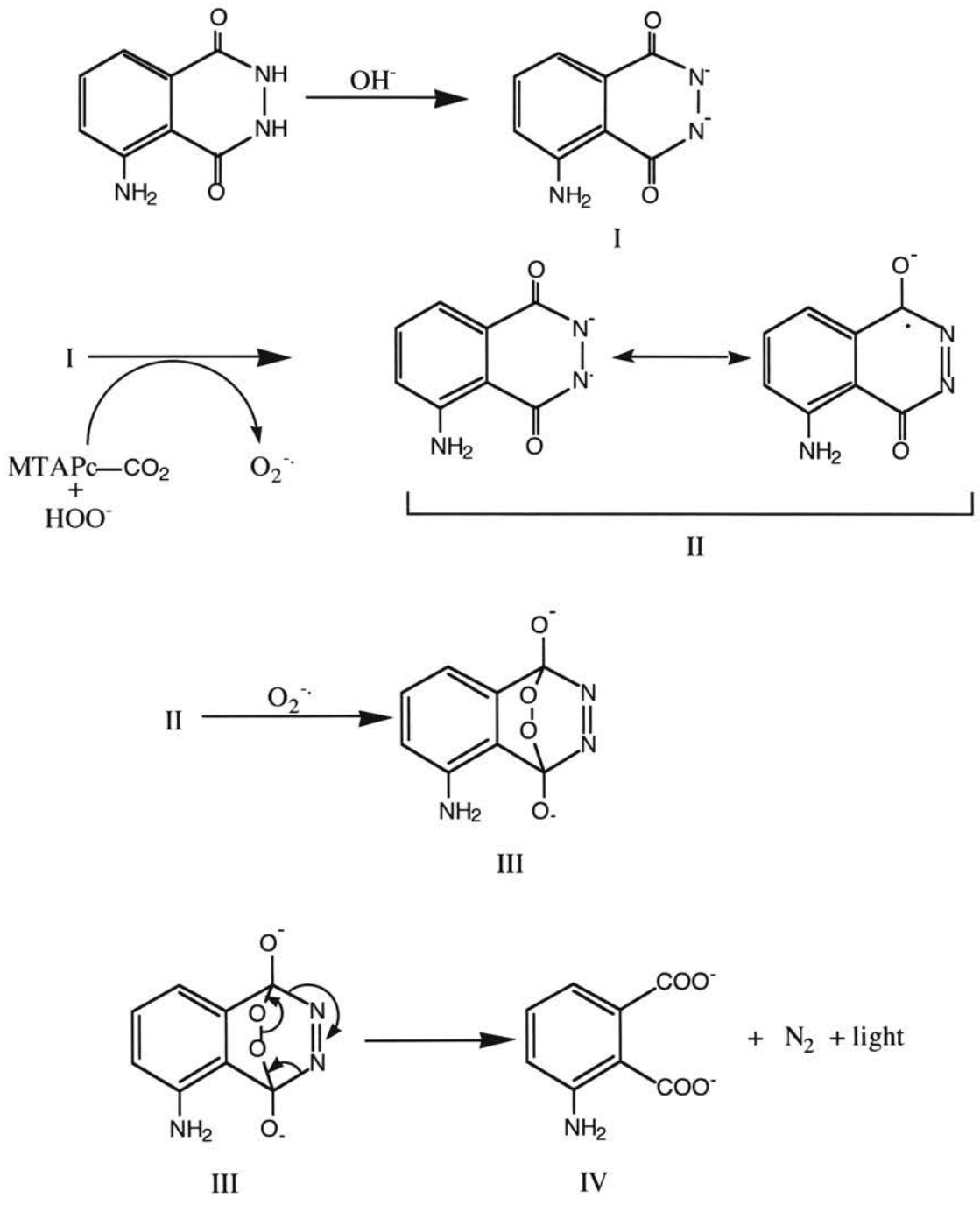

Figure 6.10. Mechanism of luminol chemiluminescence.

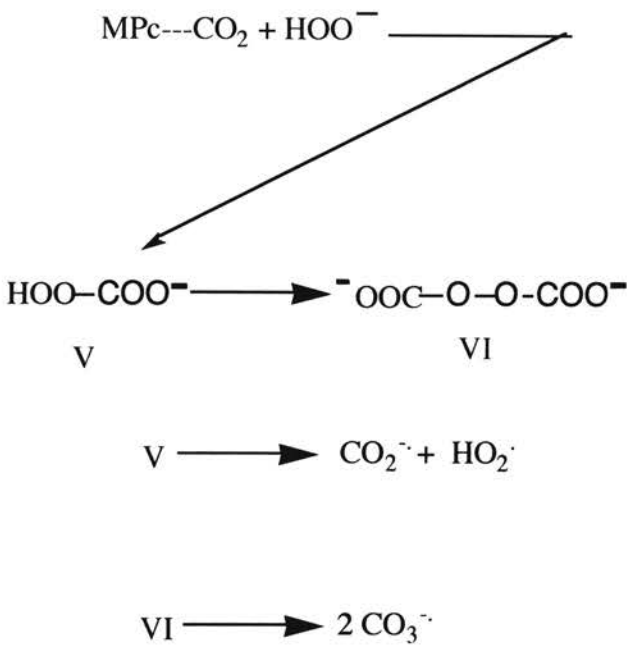

Figure 6.11. Species involved in luminol chemiluminescence in the presence of carbon dioxide.

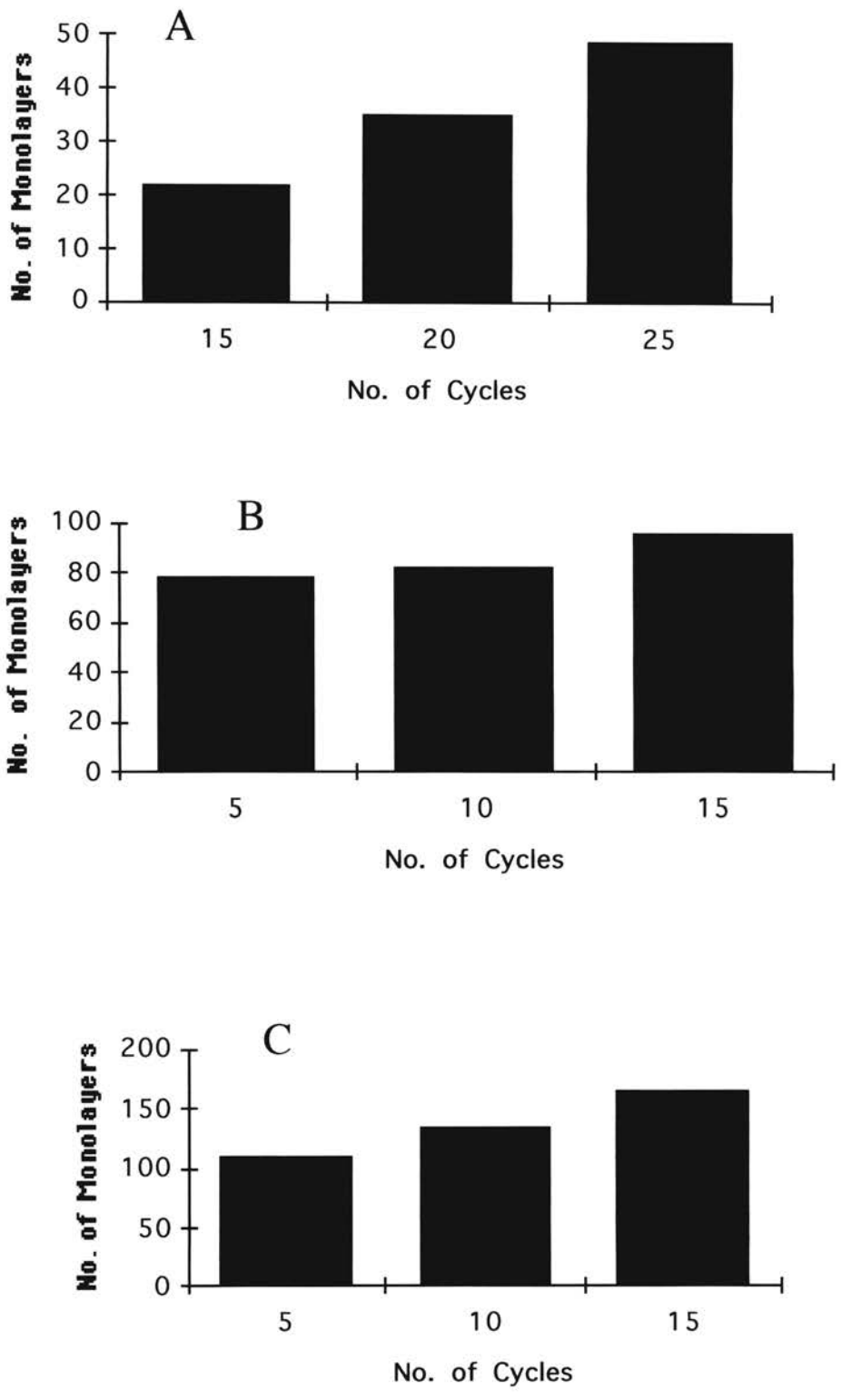

Figure 6.12. Bar graphs showing how the number of monolayers vary with cycles of electropolymerization for: (A) CoTAPc, (B) ZnTAPc, and (C) CuTAPc.

Conclusion. The electropolymerization of MTAPc complexes offer a unique method of immobilization. The immobilization of ZnTAPc, CoTAPc, and CuTAPc for use in a rotating reactor, coupled to a flow system was motivated by the fact that MPc complexes are among the best rate modifiers in luminol chemiluminescence. This research focused on the electropolymerization and the characterization of the resultant thin films by cyclic voltammetry, chronocoulometry, square wave voltammetry, and spectroelectrochemistry. Electropolymerization by cyclic voltammetry as opposed to constant potential depositions is more advantageous because there are certain energy requirements associated with propagating the electropolymerization that can be better achieved if a potential window is scanned. The electrochemical characterization of the thin films are related to the observed electrochemical processes occurring during the electropolymerization. It was also of interest to look at the electrochemical properties of the thin films when exposed to carbon dioxide and high pH solutions, and to see if the films would remain intact . After this, the films were used as rate modifiers in luminol chemiluminescence.

In using solutions of MPc complexes, ZnPc was identitifed as the best rate modifer, followed by CoPc, and finally CuPc. Since ZnPc, and CoPc were identified as the best rate modifiers, CuPc was used in this research for comparison purposes. The information obtained from using the thin films as rate modifiers are compared to using solutions of the rate modifier. Ultimately, this information is used in the selection of the film for analytical purposes.

In comparing electrochemical characteristics occurring in solution during electropolymerization and electrochemical characteristics of the thin film, some general conclusion can be made. During the electropolymerization of CuTAPc, peaks 1 and 3 are correlated as pertaining to the same process. The increase in the overpotential to sustain the electropolymerization process is reflected in the decrease of the MLCT band. In addition, the peak separation corresponding to the cyclic voltammetric characterization

point to quasireversisble electrochemistry with reduction favoring low surface coverage, and oxidation favoring high surface coverage.

In CoTAPc, the electropolymerization involves two metal ion redox processes. These processes are also evident in spectroelectrochemistry by the presence of two MLCT bands that increase with the applied potential. There is no evolution of peaks as described for the CuTAPc system. However, as the electropolymerization proceeds the charge transfer becomes sluggish. This is reflected in the cyclic voltammetric characterization thepeak separation increases as the thickness of the film increases. However, the peak separation is much smaller than the peak separation as described in the case of the CuTAPc film system.

In ZnTAPc, all electrochemical processes are centered on the ligand. This was verified by the lack of MLCT bands in the spectroelectrochemical studies. The charge transfer process becomes more sluggish as the thickness of the film increases. The reduction potentials of the different redox processes in solution are very similar to the observed reduction potentials of the different redox processes when the film is characterized by cyclic voltammetry and square wave voltammetry. After exposure of the films to high pH solutions, the films remain intact, although there is some structural change in the films. This is seen by a change in peak potentials for both the CoTAPc and ZnTAPc films. The films of CuTAPc did not show any significant change in peak potentials. This is attributed to the fact that the films of CuTAPc are more compact, and it would be more difficult to induce a change in the film.

In the luminol chemiluminescence studies involving carbon dioxide and solutions of the rate modifier, ZnPc is the best, followed by CoPc, and then CuPc. Initially it was expected that when using solid thin films, the aforementioned series would follow the same pattern. However, in using the films as rate modifiers, CuTAPc is the best, followed by ZnTAPc, and then CoTAPc. The thin films of CuTAPc are more compact, and have more monolayers than ZnTAPc, and CoTAPc. Surfaces that have many

monolayers help to give larger signals than surfaces that have only a single monolayer or several layers. Therefore, since CuTAPc films contain a greater number of monolayers, than CoTAPc films, and ZnTAPc films, the thin films of CuTAPc should provide a greater signal. These observations point to the fact that CuTAPc thin films should preferably be used in luminol chemiluminescence system since these thin films provide more monolayers and there are insignificant changes when the film is exposed to a high pH solution.

REFERENCES

1. Murray, R. *Acc. Chem. Res.*, **1980**, *13*, 135-141.

2. Hillman, A.R. *Electrochemical Science and Technology of Polymers,* Elsevier: Amsterdam, **1987**.

3. Hart, J.P.; Wring, S.A. *Analyst,* **1992**, *117*, 1215.

4. Kaneko, M.; Wohrle, O. *Adv. Polm. Sci*, **1988**, *84*, 140.

5. Tse, Y-H; Janda, P.; Lever, A.B.P. *Anal. Chem.*, **1992**, *66*, 384-390.

6. Wang, J. *Anal. Lett.* **1996**, *29*, 1575-1587.

7. Schachl, L.; Alemu, H.; Klacher, K.; Jezkova, J. *Anal. Lett.,* **1997**, *30*, 2655-2673.

8. Collins, G.; Rose-Pehrsson, S.L.; *Anal. Chem*, **1995**, *67*, 2224-2230.

9. Lane, R.F.; Hubbard, A.T. *J. Phys. Chem.*, **1973**, *77*, 1401.

10. Murray, R.; Lennox, J.C.; *J. Electroanal. Chem.*, **1977**, *78*, 395.

11. Green, J.M.; Faulkner, L.R.; *J. Am. Chem. Soc.*, **1983**, *105*, 2950.

12. Macor, K.A.; Spiro, T.G. *J. Am. Chem. Soc.,* **1983**, *105*, 5601.

13. Denisevich, P.; Abruna, H.D.; Leidner, C.R.; Meyer, T.J.; Murray, R.W. *Inorg. Chem.,* **1982**, *21*, 2153.

14. Calvert, J. M.; Schmehl, R.H.; Sullivan, P.B.; Facci, J.S.; Meyer, T.J.; Murray, R.W. *Inorg. Chem.*, **1983**, *22*, 2151-2162.

15. Kobayashi, T.; Yoneyama, H.; Tamura, H.; *J. Electroanal. Chem.*, **1984**, 419.

16. Mafatle, T.; Nyokong, T.; *Anal. Chim. Acta*, **1997**, *354*, 307-314.

17. Chebotareva, N., Nyokong, T. *Electrochim. Acta*, **1997**, *42*, 3519-3524.

18. Anson, F.C. Shigehana, K.; Oyama, N.; *J. Am. Chem. Soc.*; **1981**, *103*, 2552-2558.

19. Li, H.; Guarr, T.F.; *J. Electroanal. Chem*, **1991**, *297*, 169-183.

20. Aga, H.; Aramatta, A.; Hisaeda, Y. *J. Electroanal. Chem.*, **1997**, *437*, 111-118.

21. Li, H.; Guarr, T.F.; *J. Electroanal. Chem.* **1991**, *317*, 189-202.

22. Nekimken, H.L., *Thesis*, University of Wisconsin, **1981**.

23. Wang, J. *Anal. Lett.* **1996**, *29*, 1575.

24. Kang, T.; Xei, Z-Y.; Tang, H.; Shen, G.-L.; Yu, R.-Q. *Talanta*, **1997**, *45*, 291.

25. Abe, T.; Taguchi, F.; Yoshida, T.; Tokita, S; Schnurpfeil, G.; Wohrle, D.; Kaneko, M.; *Journal of Molecular Catalysis A: Chemical*, **1996**, *112*, 55.

26. Isaacs, M.; Aguirre, M.J.; Labbe-Toro, A.; Costamagna, J.; Paez, M.; Aagal, J.H.; *Electrochim. Acta*, **1988**, *43*, 1821.

27. Yoshida, T.; Kamato, K.; Tsukamoto, M.; Iida, T.; Schlettwein, D.; Wohrle, D.; Kaneko, M.; J. *Electroanal. Chem.*, **1995**, *385*, 209.

28. Park, C.; Yun, D.H.; Kim, S-T; Park, W.Y.; *Sensors and Actuators B*, **1996**, *30*, 23.

29. Lan, Z-H.; Mottola, H.A. *Analyst,* **1996**, *121*, 211.

30. MacDonald, A.; Can, K.W.; Nieman, T.A., *Anal. Chem.*, **1979**, *51*, 2077.

31. Burdo, T.G.; Seitz, W.R., *Anal. Chem.*, **1975**, *47*, 1639.

32. Seitz, W.R.; Neary, M.P., *Anal. Chem.*, **1974**, *46*, 188A.

33. Green, M.J.; Faulkner, L.R., *J. Am. Chem. Soc.*; **1983**, *105*, 2950.

34. Abruna, H.; Meyer, T.J.; Murray, R.W., *Inorg. Chem.*, **1979**, *11*, 3233.

35. Lenhard, J.R.; Murray, R.W., *J. Electroanal. Chem.*, **1977**, *78*, 195.

36. Bard, A.J., Faulkner, L.R. *Electrochemical Methods. Fundamentals and Applications,* Wiley: New York, **1980**.

37. Lyons, M.G. *Electroactive Polymer Electrochemistry*, Plenum Press, New York, N.Y. , **1994**.

38. Oyama, N.; Anson, F.C., *J. Electroanal.Chem.*, **1980**, *127*, 247.

39. Maksymiuk,L.; Doblhofer, K.; *Electrochim. Acta*, **1994**, *39*, 217.

40. Shaw, B.R.; Haight, G.P.; Faulkner, L.R., *J. Electroanal. Chem.*, **1982**, *140*, 147.

41. Yagi, M.; Mitsumoto, T.; Kaneko, M.; *J.Electroanal. Chem.*, **1997**, *437*, 219.

42. Shgehara, L.; Oyama, N; Anson, F.C.; *J. Am. Chem. Soc.* **1981**, *103*, 2552.

43. Nyasulu, F.W.W., Mottola, H.A.; *J. Electroanal. Chem*, **1988**, *239*, 175.

44. Ellis, C.D.; Murphy, W.R.; Meyer, T.J.; *J. Am. Chem. Soc.*, **1981**, *103*, 8480.

45. Ellis, C.D.; Murray, R.W..; Meyer, T.J.; Margerur, L.D., *Inorg. Chem.*, **1983**, *22*, 1283.

46. Bettelheim, A.; White, B.A.; Raybuck, S.A.; Murray, R.W., *Inorg. Chem.*, **1987**, *26*, 1009.

47. Diaz, A.F.; Kanazawa, K.K.; Gardini, G.P.; *J. Chem. Soc. Chem. Commun.*, **1979**, 635.

48. Genies, A.F.; Kanazawa, K.K.; Gardini, G.P. *J. Electroanal.Chem.*, **1983**, *149*, 101.

49. Cui, C.Q., Ong, L.H.; Tan, T.C.; Lee, J.Y., *J. Electroanal. Chem. Interfacial Electrochem.*, **1993**, *346*, 447.

50. Kang, T.F.; Shen, G-L.; R-Q;, *Anal. Lett.*, **1997**, *30*, 647.

51. Malitesta, C.; Palmisano, F.; Torsi, L.; Zambonin, P.G. *Anal. Chem.*, **1990**, *62*, 2735.

52. Bartlett, P.N.; Tebbutt, P.; Tyreee, C.H.; *Anal. Chem.*, **1992**, *64*, 138.

53. Sun,C.; Zhang, X.; Jiang, D.; Gao, Q.; Xu, H.; Sun, Y.; Shen, J.; J. *Electroanal. Chem*, **1996**, *411*, 73.

54. Moser, F.H.; Thomas, A.L.; *Phthalocyanine Compounds*, Reinhold Publishing: New York, **1963**.

55. Leznoff, C.C.; Lever, A.B.P., Eds., *Phthalocyanines: Properties and Applications* VCH: New York, **1989**, V. 1, 2, 3, 4.

56. Brewis, M.; Clarkson, G.J. , Humberstone, P.; Makhseed, S.; McKeown, N.B., *Chem, Eur. J.*, **1998**, *4*, 1633.

57. Berezin, B.D.; *Coordination Compounds of Porphyrins and Phthalocyanines*, Wiley: New York, **1981**.

58. Achar, B.N.; Fohlen, G.M.; Parker, J.A.; Keshavayya, L. *Polyhedron*, **1987**, *6*, 1463.

59. Eisenbraun, E.J.; Hall, H.; *J. Chem. Ed.* , **1978**, *55*, 806.

60. Mho, S.; Ortiz, B.; Park, S.; Ingersoll, D.; Doddapaneni, N.J., *J. Electrochem. Soc.*, **1995**, *142*, 1436.

61. Silverstein, R.M.; Bassher, G.C.; Morrill, T.C.; *Spectrometric Indentification of Organic Compounds*, John Wiley and Sons, Inc., New York, **1991**.

62. Melson, G.A., *Corrdination Chemistry of Macrocylic Compounds*, Plenum Press, New York, **1979**.

63. Lever, A.B.P; Hempstead, M.R.; Leznoff, C.C. Liu, W.; Melink, M.; Nevin, W.A.; Seymour, P., *Pure and Appl. Chem.*, **1986**, *58*, 1467.

64. Myers, J.F., Canham, G.W.; Lever, A.B.P., *Inorg. Chem.*, **1975**, *14*, 461.

65. Denisevich, P.; Abruna, H.D.; Leidner, C.R., Meyer, T.J., Murray, R.W., *Inorg. Chem.*, **1982**, *21*, 2153.

66. Van Benschoten, J.J.; Lewis, J.Y.; Heimneman, W.R.; Roston, D.A.; Kissinger, P.T., *J. Chem. Edu..*, **1983**, *60*, 772.

67. Doriomedoff, M.; Cristofini, F.H.; Surville, R.; Josefowicz, M.; Yu, L.T.; Buvet, J. *J. Chim. Phys.*, **1971**, 68, 1055.

68. Nyasulu, W.M.F.; Mottola, H.A., *J. Electroanal. Chem.*, **239**, *1988*, 175.

69. Lin, L. I-K.; *Biometrics*, **1992**, *48*, 599.

70. Neter, J.; Kutner, M.H.; Nachtsheim, C.J. Wasserman, W.; *Applied Linear Regression Models*, Irwin: New York, **1989**.

71. Ellis, C.D.; Margerum, L.D.; Murray, R.W.; Meyer, T. J., *Inorg. Chem.*, **1983**, *22*, 1283.

72. Mho, S.; Ortiz, B.; Park, S.; Ingersoll, D.; Doddapaneni, N.J. *Electrochem. Soc.*, **1995**, *142*, 1436.

73. Brett, C.M.A., Brett, A.M.O., *Electrochemistry Principles, Methods, and Applications*, Oxford University Press, New York: **1993**.

74. Nicholson, R.S., *Anal. Chem.* **1966**, *38*, 1406.

75. Christie, J.H.; Lauer, G.; Osteryoung, R.A.; Anson, F.C., *Anal. Chem..*, **1963**, *35*.

76. Christie, J.H.; Lauer, G.; Osteryoung, R.A.; *J. Electroanal. Chem.*, **1964**, *7*, 60.

77. Gulens, J.; Konrad, D.; Anson, F.C. *J. Electrochem. Soc.*, **1974**, *121*, 1421.

78. Holub, I.; Weber, *J. Electroanal. Chem. Interfacial Electrochem.* **1976**, *73*, 129.

79. Chambers, J. Q. *J. Electroanal. Chem. Interfacial Electrochem.*, **1981**, *130*, 381.

80. Oldham, K.B. *J. Electroanal. Chem. Interfacial Electrochem.*, **1983**, *145*, 9.

81. Daum, P.H.; McHalsky, M.L. *Anal. Chem.*, **1980**, *52*, 293.

82. Anson, F.C.; Osteryound, R.A. *J. Chem. Educ.*, **1983**, *60*, 293.

83. Anson, F.C. *Anal. Chem.*, **1966**, *38*, 54.

84. Anson, F.C. *Anal. Chem.*, **1966**, *38*, 1924.

85. Heineman, W.R. *Anal. Chem.*, **1978**, *50*, 390A.

86. Heineman, W. R.; Kuwana, T. *Acc. Chem. Res.*, **1976**, *9*, 241.

87. Brown, A.P.; Koval, C.; Anson, F.C. *J. Electroanal.Chem.*, **1986**, *72*, 379.

88. Ortiz, B. Park, S-M.; Doddapaneni, J. *J. Electrochem. Soc.*, **1966**, *143*, 1800.

89. Smyth, M.R.; Vos, J. G. *Wilson's and Wilson's Comprehensive Analytical Chemistry*, Elsevier Science Publishers, B.V. **1992**, *27*, p. 478.

90. Kuo, K-N. *Current Separations*, **1983**, *5*, 26.

91. He, P.; Faulkner, L.R. *Anal. Chem.*, **1982**, *54*, 1313A.

92. Redepenning, J.; Miller, B. R.; Burnham, S. *Anal. Chem..*, **1994**, *66*, 1560.

93. Moelwyn-Hughes, E. A. *Physical Chemistry*, 2nd ed.; Pergmon Press: Belfast, **1964**, p. 859.

94. Heineman, W. R. *Current Separations*, **1986**, *7*, 58.

95. Robertson, J. M. *J. Chem. Soc.* **1936**, 1195.

96. Moser, F. H.; Thomas, A. L. *Phthalocyanine Compounds*, ACS Monograph Series; Reinhold; New York, **1963**, p. 40.

97. Ortiz, B. Park, S-M.; Doddapaneni, J. *J. Electrochem. Soc.*, **1996**, *143*, 1047.

98. Schlettwein, D.; Yoshida, T. *J. Electroanal. Chem.*, **1998**, *441*, 139.

99. Laviron, E.*J. Electroanal. Chem..*, **1974**, *52*, 335.

100. Lyons, M. E. G. *Electroactive Polymer Electrochemistry*, Plenum, New York, 1994.

100. Lyons, M. E. G. *Electroactive Polymer Electrochemistry,* Plenum, New York, 1994, p. 18.

101. Reference 96.

102. Boucher, L. J. *Metal complexes of Phthalocyanines, in Coordination Chemistry of Macrocyclic compounds*, G.A. Melson, Ed., Plenum: New York, **1979**, Chapter 7.

103. Nevin, W.A.; Hempstead, M.R. Liu, W., Lenzoff, C.C. Lever, A. B. P. *Inorg. Chem.*, **1987**, *26*, 570-577.

104. Ingle, J. D.; Wolfe, F.; Marino, D. F. *Anal. Chem.* **1979**, *51*, 2051-2053.

105. Seitz, W.R.; Burdo, T.G. *Anal.Chem.* **1974**, *47*, 1639-1643.

106. Neary, M.P. ; Seitz, W.R. *Anal. Chem.* **1974**, *46*, 188A-200A

107. Svehla, G. *Wilson and Wilson's Comprehensive Analytical Chemistry*, Elsevier: New York, **1992**, *29*, p. 33.

108. Isaccson, V.; Wettermark, G. *Anal.Chim. Acta.* **1974**, *68*, 339-342.

109. Paul, D.B. *Talanta,* **1978**, *25*, 377-382.

110. Motano, L.A.; Ingle, J.D. *Anal. Chem,* **1979**, *51*, 926-930.

111. Hartkopf, A. *Anal. Lett.* **1974**, *7*, 79-84.

112. Montano, L.A.; Ingle, J.D. *Anal. Chem.* **1979**, *51*, 919-926.

113. Cormier, M.J.; Hercules, D.M.; Lee, J. *Chemiluminescence and Bioluminescence*, Plenum Press: New York, **1973**, p. 427.

114. Klopf, L.L.; Neiman, T.A. *Anal. Chem.* **1983**, *55*, 1080-1083.

115. Jones, P.; Williams, T.; Ebdon, L. *Anal. Chem. Acta.* **1989**, *27*, 157.

116. Qin, W.; Zhang, Z.J.; Zhang, C.J. *Fresenius J. Anal. Chem.* **1988**, *361*, 824-826.

117. Qin, W.; Zhang, Z.J.; Zhang, C.J. *Mikrochimica Acta,* **1988**, *129*, 97-101.

118. Lan, Z-H. *Thesis,* Oklahoma State University, **1996**, p. 75-77.

119. Collins, J.P.; Jouaiti, A.; Sauvage, J.P. *Inorg. Chem.* , **1988**, *27*, 1986-1990.

120 Abe, T.; Yoshida, T.; Tokita, S.; Taguchi, F.; Imaya, H.; Kaneklo, M. *J. Electroanal. Chem.* **1996**, *412*, 125-132.

122. Meshitsuka, S.; Ichikawa, M. ; Tamaru, K. *J. Chem. Soc. Chem. Commun.* **1974**, 158-159.

123. Hiratsuka, K.; Takahasi, H.; Toshima, S. *Chem. Lett.*, **1977**, 1137.

124. Lieber, C.M.; Lewis, N. S.; *J. Am. Chem. Soc.* **1984**, *106*, 5033.

125. Yoshida, T.; Kamato, L.; Tsukanoto. T.; Iida, T.; Schlettwein, D.; Kanekn, M. *J. Electroanal. Chem.* **1995**, *385*, 209.

126. Matsumoto, K.; Baeza Baeza, J.J.; Mottola, H.A. *Anal. Chem.* **1983**, *65*, 636.

127. Eggins, B.R. ; Irvine, T.S. Grimshaw, J. *J. Electroanal. Chem.* **1989**, *266*, 125.

128. Meshitsuka, S.; Ichikawa, M.; Tamura, K. *Chem. Commun.* **1974**, 158.

129. Premukumar, J.R.; Ramaraj, M. *Chem. Commun.* **1997**, 343.

130. Fridovich, I.; Hodgson, E.K. *Photochem and Photobio.*, **1973**, 18, 451.

131. Lind, J.; Merenyi G.; Eriksen, T.E. *J. Am. Chem. Soc.* **1983**, 105, 7655.

APPENDIX

Calculation of the Number of Monolayers for Electropolymerized Metal(II)-Tetraminophthalocyaine Thin Films. The calculation of the number of monolayers for these thin films is motivated by the fact that in order to effectively cover the electrode surface it is necessary to have multilayers on the electrode surface The CuTAPc complex is used to describe the calculations in this appendix. However, because of the different redox processes within the same potential, the number of monolayers were also calculated for both CoTAPc, and ZnTAPc. The number of monolayers for both CoTAPc, and ZnTAPc were calculated in the same manner as the CuTAPc complex.

In general, the calculations begin with an estimate of the electrode surface area, followed by a calculation of the volume of the MTAPc complex. Since the complex is planar, the height of the molecule was taken as the diameter of the central metal atom. The amount of material on the electrode suface was determined by cyclic voltammetric characterization of the film by integrating the area under the current-potential curve. The number of monolayers was then determined after calculating the volume of a monolayer, and the number of moles per monolayers.

Calculation of the Electrode Area. The diameter of the electrode surface used to calculate its area was measured under a Stero Star Zoom (1X to 6X) microscope model AO 580 with a ruler. The circular area of the glassy carbon surface was determined to be 0.0706 cm^2.

Calculation of the Area and Volume of the Cu(II)TAPc Complex. From the dimensions of the phthalocyanine molecule (obtained by X-ray diffraction, [95]), the area of the tetraaminephthalocyanine was obtained. The area for the base of the prism was determined to be 2.34×10^{-14} cm^2. The height of the molecule is given by the

diameter of the central metal ion of 2.60 Å for copper, 2.68 Å for zinc , and 2.50 Å for cobalt. Taking the height of the molecule into consideration, the volume of the molecule is 6.08×10^{-22} cm^3.

Integration of Peak Areas. The area under the characterization cyclic voltammogram was used calculate the number of the amount of material on the electrode surface. In all cases, the cyclic voltammogram corresponding to cycle 3 was used. The third was used to make sure that the peak currents did not change. Normally, after the thrid cycle it was evident that the peak currents did not change after cycling the potential several times. The amount of material immobilized on the electrode surface is proportional to the charge transferred during the electropolymerization process. This corresponds to the area under the current-potential curve. Integration of peak areas by a cut and weight approach was used to find the coverage on the electrode surface.

A small part of the area under the curve (e.g., the cathodic peak) was cut into a small trapezoid of known width (Volts), and height (Amps). The time interval was determined from dividing the width by the scan rate. The charge was then determined from the current and the time shown by equation A.1,

$$Q = (\text{current})(\text{time}) = i \times t \qquad (A.1)$$

This area was then weighed on a balance to obtain its corresponding weight. The weight was used to obtain a charge per weight ratio. The charge per weight ratio was used to determine the total charge, **Q,** passed during the cathodic process, after obtaining the total weight of the area under the current-potential curve. The amount of material on the electrode surface due to the anodic/cathodic process was then calculated from the following equation:

$$\Gamma = Q/nFA \qquad (A.2)$$

where **Q** is the charge, **n** is the number of electrons, **F** is the Faraday constant, and **A** is the area of the electrode surface. An application of using these equations is shown below, using as a model the CuTAPc complex. The product of the current and time is $(5.47 \times 10^{-6}A)[(0.037V/0.050V \cdot s^{-1})]$ or 4.04×10^{-6} C. The weight of this representative area is 0.0048 grams. Therefore, the charge/weight ratio is 8.41×10^{-4} C/gram. For convience, 5 cycles of electropolymerization were chosen as a for calculating the number of monolayers on the electrode surface. The cathodic peak had a total weight of 0.0631 grams. Therefore, the total charge represented by the cathodic current-potential curve was determined to be

$$(0.0631 \text{grams})(8.41 \times 10^{-4} \text{ C/gram}) \text{ or } 5.31 \times 10^{-5} \text{ C.}$$

Calculation of the Volume of Monolayer. The number of molecules on the electrode surface is equal the area of the electrode divided by the area of a single molecule of MTAPc, in this case: $0.0706 cm^2/2.34 \times 10^{-14} cm^2$ or 3.01×10^{12} molecules/monolayer. The volume of a monolayer is determined by taking into consideration the volume of the complex. If the 3.01×10^{12} is the number of molecules/monolayer, and $6.08 \times 10^{-22} cm^3$/molecule is the volume of the complex, then the volume of the monolayer becomes the product of the number of molecules/monolayer and the volume (cm^3/molecule) of the complex. This gives a total volume of 1.83×10^{-9} cm^3/monolayer.

Calculation of the Number of Moles per Monolayer. The number of moles per monolayer is (i.e., 3.01×10^{12} molecules/monolayer)(1 mole/N_a) or 5.00×10^{-12}

mole/monolayer, where $\mathbf{N_a}$ is Avogadros Number. If the area of each layer is 0.0706 cm^2 (the area of the electrode surface), then the number of moles/cm^2 in 1 monolayer is

$$(5.00X\ 10^{-12}\ \text{mole/monolayer})/(0.0706\ cm^2/\text{monolayer}) = 7.08\ X\ 10^{-11}\ \text{mol}\ /\ cm^2.$$

Then the amount of material on the electrode surface, via integration, is calculated using equation A.2. Substituting the appropriate values into equation A.2 gives, for CuTAPc:

$$5.31\ X\ 10^{-5}\ C/[(96500\ C\cdot mol^{-1})(1)(0.0706\ cm^2)] \text{ or } 7.79\ X\ 10^{-9}\ \text{mol}\ /\ cm^2.$$

Calculation of the Number of Monolayers. Finally, the number of monolayers is determined using the values obtained from equation A.2, and the number of moles per monolayer. Therefore, the number of monolayers in this case is:

$$(7.79\ X\ 10^{-9}\ \text{mol}\ /\ cm^2)\ /\ (7.08\ X\ 10^{-11}\text{mol}\ /\ cm^2) \text{ or } 110 \text{ monolayers.}$$

VITA

Kenneth Lionel Brown

Candidate for the Degree of

Doctor of Philosophy

Thesis: ELECTROPOLYMERIZATION OF COPPER, COBALT, AND ZINC(II)-TETRAAMINOPHTHALOCYANINE: POTENTIAL RATE MODIFIERS OF LUMINOL CHEMILUMINESCENCE IN THE PRESENCE OF CARBON DIOXIDE

Major Field: Chemistry

Biographical:

Education: Graduated from William H. Spencer High School, Columbus, Georgia, in June 1987; received Bachelor of Science in Chemistry from Oral Roberts University, Tulsa, Oklahoma in May 1993. Completed the Requirements for the Doctor of Philosophy degree in Chemistry at Oklahoma State University in July of 2000.

Experience: Employed as an analytical chemist for Lab One Analytical in Tulsa, Oklahoma from 1993 to 1994; employed as a research technician for Dowell Schlumberger Research and Engineering Technology, Tulsa, Oklahoma from 1994 to 1995; employed as a graduate teaching assistant for Oklahoma State University, from 1995 to 1999.

Professional Memberships: Phi Lambda Upsilon, President, 1997-1998.